SUPPLEMENTAL MATERIAL

Supplemental Methods

Animal studies
All animal studies were performed using the PPL license PA8E7CA4E in accordance with the United Kingdom Animals (Scientific Procedures) Act 1986 following ARRIVE guidelines. Protocols detailing experimental specifics were designed by us and were approved by the University of Manchester Ethics Committee and the relevant animal welfare officers. All mice and rats were housed in a pathogen-free facility at the University of Manchester with food and water provided *ad libitum* in a 12-hour light/dark cycle. C57BL/6 mice were purchased from Envigo (UK) while pregnant Sprague-Dawley rats were purchased from Charles River (UK). Humane endpoints were regarded as lethargy, poor gait, blood glucose >600mg/dL, dyspnea and bodyweight loss >10%, although no adverse effects were observed. Where data from animals are presented, each data point represents one animal. A total of 207 animals were used and cohort sizes were calculated using data from a preliminary study using >80% power, α=0.05. With the exception of strain, age and sex, no exclusion/inclusion criteria were set, and all animals are presented in the data. Animals were randomly allocated into groups using an online random group generator and investigators were blinded to experimental groups for data analysis. Confounders were not controlled.

H9C2, C2C12, and Human embryonic kidney 293A (HEK293A) cell lines
H9C2 rat myoblasts and C2C12 mouse myoblasts were obtained from the European Collection of Authenticated Cell Cultures (ECACC) (Sigma-Aldrich, 88092904; ATCC, CRL-1772), while HEK293A cells were acquired from Invitrogen (R70507). Cells were maintained in DMEM (Gibco, 11966) supplemented with 10% (v/v) heat inactivated fetal bovine serum (FBS), 100 µg/mL streptomycin, and 100 U/mL penicillin.

Human induced pluripotent stem cells-derived cardiomyocytes (hiPSC-CMs)
The hiPSC SEUR7 cells were established from human dermal fibroblasts using a CytoTune iPS Programming kit (Life Technologies) by Wellcome Trust Sanger Institute and made available via Public Health England through ECACC under a material transfer agreement. The hiPSCs were maintained and differentiated into cardiomyocytes as described previously.[49] Alternatively, hiPSC (DF19-9-11T.H, WiCell) derived from male foreskin fibroblasts were also used to differentiate to hiPSC-CMs. In short, hiPSCs were maintained in mTeSR Plus media (Stem Cell Technologies, 100-0276) on Geltrex-coated plates (Life Technologies, A1413302). Cardiomyocyte differentiation was achieved through incubation with 4 µM CHIR99021 (Millipore, 361559) and subsequently 5 µM IWP2 (Millipore, 681671), for 48 hours each, in RPMI1640 HEPES Glutamax medium (Life Technologies, 72400021) with B27 minus insulin supplement (Life Technologies, A1895601).

Neonatal rat cardiomyocytes (NRCMs)
Neonatal rat cardiomyocytes were isolated from 2/3-day-old male and female Sprague-Dawley rats in a manner described previously.[50] Briefly, excised hearts were dissected into small pieces and subjected to sequential cycles of enzymatic digestion, for 6 minutes per cycle, in 7ml of buffer [116 mM NaCl, 20 mM , 1 mM NaH_2PO_4, 6 mM glucose, 5 mM KCl, 0.8 mM $MgSO_4$, pH 7.4] containing 0.33 U/mL Collagenase A (Roche, 10103586001) and 100 mg/mL pancreatin (Sigma-Aldrich, P3292). NRCMs were cultured in medium [80% DMEM, 20% M199, 1% FBS, penicillin-streptomycin, fungizone, and 1 µM bromodeoxyuridine].

Human samples
The harvest, culture and treatment of human heart slice have been described previously.[24,26,49] Fresh human hearts were provided from a consented and deidentified donor through the Maryland Legacy Foundation (the USA transplantation network, Novabiosis). All procedures were approved by the Institutional Review Boards of the University of Louisville. The donor

was aged 37 years old with no cardiovascular disease. Cultured heart slices were treated with fatty acid-free BSA (0.5% w/v in culture medium) or BSA-conjugated palmitic acids and oleic acids (300 µM conjugated in 0.5% w/v BSA).

To perform RNA sequencing and liquid chromatography/mass-spectrometry analyses, snap frozen human heart left ventricular tissue purchased from Asterand (BioIVT, UK) was used. The normal myocardial tissue (as normal control) was obtained from consented donors without diabetes and cardiovascular diseases diagnosed (BMI<25). These donors died of intracerebral hemorrhage. Metabolic stress-associated heart failure (MS-HF) samples were obtained from consented donors, who displayed various cardiovascular complications 5-10 years after diagnosis of metabolic syndrome (hyperglycemia, hyperlipidemia, hypertension, BMI>30), including ischemic cardiomyopathy, atrial fibrillation, coronary artery disease, or congestive heart failure. These donors died of HF or cardiac arrest. Asterand obtained ethical approval and consent following the United Kingdom Human Tissue Authority regulations.

Heart	Age	Gender	Ethnicity	Comorbidities
Normal				
1	46	Female	Black or African American	Hypothyroidism
2	48	Male	White or Caucasian	N/A
3	58	Female	Native American or Alaskan Native	N/A
MS-HF				
1	71	Male	White or Caucasian	Diabetes mellitus
2	55	Male	White or Caucasian	Diabetes mellitus, hypercholesterolemia, hypertension, metabolic syndrome
3	53	Female	White or Caucasian	Diabetes mellitus, hypercholesterolemia
4	69	Male	White or Caucasian	hypertension, diabetes mellitus, hypercholesterolemia
5	59	Female	White or Caucasian	Diabetes mellitus, hypertension

On the other hand, to perform RNA sequencing and qPCR in HFpEF samples, human HFpEF hearts were obtained from the United Network for Organ Sharing (UNOS) through IIAM and Novabiosis, with next of kin informed consent. Human hearts were classified according to the following inclusion and exclusion criteria: Normal healthy donors: inclusion criteria: 1) aged 50 or above and, 2) ejection fraction>55%; exclusion criteria: 1) history of myocardial infarction, 2) pregnant women, 3) decompensated heart failure, 4) severe kidney disease, 5) asthma or severe chronic lung disease, 6) cardiac pacemaker or implantable defibrillator, 7) cerebral aneurysm clip, 8) neural stimulator, and 9) history of diabetes. HFpEF donors: inclusion criteria: 1) aged 50 or above, 2) ejection fraction>50%, 3) impaired relaxation (average E/E'>9), and 4) history of at least one of these conditions, chronic kidney disease, hypertension or diabetes; exclusion criteria: 1) history of myocardial infarction, 2) pregnant women, 3) decompensated heart failure, 4) asthma or severe chronic lung disease, 5) cerebral aneurysm clip, and 6) neural stimulator.

Heart	Age	Gender	Ethnicity	Comorbidities
Normal				
1	36	Male	Black or African American	N/A
2	54	Female	White or Caucasian	N/A
3	37	Male	Black or African American	N/A
4	44	Male	White	N/A
5	43	Male	White	N/A
6	38	Female	White	N/A
7	29	Male	White	N/A
8	44	Male	White	N/A

HFpEF				
1	53	Male	White	Hypertension, diabetes mellitus
2	61	Male	Caucasian	Hypertension, diabetes mellitus
3	56	Female	Hispanic	Hypertension, diabetes mellitus
4	66	Female	Caucasian	Hypertension, diabetes mellitus
5	68	Female	Caucasian	Hypertension, diabetes mellitus
6	52	Male	Caucasian	Hypertension
7	65	Female	Caucasian	Hypertension, diabetes mellitus
8	52	Male	Hispanic	Hypertension, diabetes mellitus, chronic kidney disease

Finally, all experimental procedures conducted on human samples were approved by the University of Manchester Research Ethics Committees and in agreement with the Declaration of Helsinki.

Adeno-associated virus 9 (AAV9) gene delivery
Cardiac-specific EDEM2 overexpression was achieved by using an AAV9 vector carrying *EDEM2* cDNA under the control of human cardiac troponin T (hTnT) promoter. The pSSV9 vector carrying *EDEM2* was generated by modifying the pSSV9-hTnT-*eGfp* vector. Briefly, the *eGfp* gene was replaced with *EDEM2-Myc-His* (pOTB7-*EDEM2* constructed into pcDNA3.1-*Myc-His*) using the SacII and NotI restriction enzymes. The viral packaging was performed as previously described.[51] EDEM2 overexpression was achieved by tail vein injection of AAV9-hTnT-*EDEM2* at a dosage of 1×10^{11} viral particles per mouse, while mice injected with AAV9-hTnT-*eGfp* served as control mice.

EDEM2 knockdown was achieved via AAV9-delivered U6 promoter-driven *shRNA* targeting mouse *Edem2*, with more efficiency of knockdown in the myocardium.[52] Tail vein injection of AAV9-U6-*shEdem2* (Boston Children's Hospital), generated using a validated plasmid for *shEdem2* (hairpin sequence: CCUCAUAGCCACUGGAUAAUUCUCGAGAAUUAUCCAGUG GCUAUGAGG) with puromycin resistance (VectorBuilder), at a dosage of 1×10^{12} viral particles was applied, while AAV9-(CMV)*eGfp* injection was as a control.

Cardiac-specific XBP1s overexpression was achieved by using an AAV9 vector carrying *XBP1s* cDNA under the control of human cardiac troponin T (hTnT) promoter. The pSSV9 vector carrying *XBP1s* was generated by modifying the pSSV9-hTnT-*eGfp* vector. Briefly, the *eGfp* gene was replaced with *Flag-XBP1s* (pCMV5-*XBP1s*) (Addgene, 63680) using BamHI and NotI restriction enzymes. The viral packaging was performed as previously described.[51] XBP1s overexpression was achieved by tail vein injection of AAV9-hTnT-*XBP1s* at a dosage of 1×10^{11} viral particles per mouse, while the mice injected with AAV9-hTnT-*eGfp* served as control mice.

XBP1s abrogation was achieved by AAV9-delivered H1 promoter-driven *shRNA* targeting mouse *Xbp1* (hairpin sequence: GUCUUAAAGGUGGUAGUAUACUUUCAAGAGAAGUAUA CUACCACCUUUAAGAUUUU, targeting both unspliced and spliced *Xbp1*). The vector carrying the shRNA was constructed by modifying the pDS-H1-(CMV)*eGfp* vector where the *shRNA* sequence was inserted using SalI and XhoI restriction enzymes. The viral packaging was performed as previously described.[51] XBP1 knockdown was achieved via tail vein injection of AAV9-H1-*shXbp1*-(CMV)*eGfp* at a dosage of 1×10^{12} viral particles per mouse, while AAV9-(CMV)*eGfp* injection was administered as a control.

To achieve both XBP1 knockdown and EDEM2 overexpression concurrently, AAV9-H1-*shXbp1*-(CMV)*eGfp* and AAV9-hTnT-*EDEM2* were simultaneously injected via the tail vein at a dosage of 1×10^{12} and 1×10^{11} viral particles per mouse, respectively.

3

Induction of HFpEF

C57BL/6 mice aged ~7-weeks-old were provided with either a standard chow diet (Envigo, 2018 Teklad Global 13 kcal% fat, 18 kcal% protein Rodent diet) or a 60% high-fat diet (HFD, 60 kcal% fat) (SDS, 824054) *ad libitum*. Additionally, mice were provided with either regular drinking water (HFD alone) or water containing Nω-nitro-l-arginine methyl ester (L-NAME) (Sigma-Aldrich, N5751) at a concentration of 0.5 g/L (pH 7.4) (two-hit method). The drinking water was changed every 2 days to maintain drug stability. This murine model of HFpEF is clinically relevant as the combined stress induced by HFD and L-NAME is known to induce many pathological features of the disease including metabolic dysfunction, diastolic dysfunction, endothelial dysfunction and hypertension.[25]

Administration of ALDA-1, SR-4995, and oxytocin

To apply for various treatments, the chemicals, Alda-1 (Sigma-Aldrich, 349438-38-6), SR-4995 (Sigma-Aldrich, SML2207), and oxytocin (Tocris Bioscience, 1910), were administered via intraperitoneal injection to 8-week-old AAV9-U6-*shEdem2* or AAV9-(CMV)*eGfp* injected mice at a dose of 3 mg/kg twice a week for 4 weeks along with HFD+L-NAME according to individual experimental design.

Metabolic profile measurements

For the glucose tolerance test (GTT), mice were fasted for 6 hours, followed by intraperitoneal 2 g/kg glucose injection. Blood was collected from the lateral tail vein and glucose levels were measured at 30-minute intervals over 2 hours using an Accu-Chek Aviva glucometer.

Blood pressure

Diastolic and systolic blood pressure measurements were performed on conscious mice using the CODA volume pressure sensor recording system (CODA, Kent Scientific). Ten acclimatization cycles were discarded before measurements were recorded. At least five successful readings were averaged per mouse.

Echocardiography

Mice were anesthetized with 2% isoflurane mixed with 100% oxygen at a rate of 1.5 L/min. Transthoracic two-dimensional M-mode and pulse wave Doppler ultrasound images were obtained using the Acuson Sequoia C256 system. LV chamber and wall dimensions, diastolic function parameters (IVRT, E/A) and systolic function parameters (FS%, EF%) were measured or calculated for each mouse, with IVRT being the primary outcome measure used to determine sample size

OCT embedding and sectioning of blocks

Freshly collected hearts were immediately embedded in OCT embedding matrix and stored at -80°C for histological analyses. Cryosections were cut to a thickness of 10 μm using the Leica CM3050S Cryostat microtome.

Hematoxylin and Eosin (H&E) staining

H&E staining on myocardial cryosections was conducted to determine the cardiomyocyte cross-sectional area. Cryosections were incubated in Harris' Hematoxylin (Sigma-Aldrich, HHS32) for 5 minutes and differentiated with acid alcohol (1% v/v hydrochloric acid, and 70% ethanol) for 10 seconds. Nuclei were counterstained with Eosin (Thermo Fisher , 6766007) for 1 minute. Samples were dehydrated in increasing concentrations of IMS (75%, 95%, 100%), cleared in xylene and mounted with xylene-based medium DePex mounting medium.

WGA staining

Wheat germ agglutinin (WGA) staining was also used to assess the cardiomyocyte cross-sectional area in heart sections. WGA-647 (10 μg/mL, Invitrogen, W32466) was applied to heart sections in a dark humid chamber at room temperature for 1 hour, following which they were washed with PBS prior to mounting with VECTASHIELD® Antifade Mounting Medium. After

imaging, 200 cardiomyocytes from each heart section were randomly selected to measure the area. The mean value of cross-sectional area from each heart were used for statistical analyses.

Dihydroethidium (DHE) staining

The superoxide (O_2^-) levels in heart tissue were evaluated using the oxidative fluorescence dye DHE (Thermo Fisher, D1168). Fresh heart tissue was embedded with OCT, followed by immediate sectioning. Heart sections were incubated with DHE diluted in PBS (10 μM) in a dark humidified chamber at 37°C for 30 minutes, mounted with coverslips and imaged immediately.

Oil Red O (ORO) staining of heart sections

To assess lipid droplets, heart sections were fixed in 10% (v/v) buffered neutral formalin for 5 minutes and incubated with ORO (Sigma-Aldrich, O0625) [0.375% (w/v) of ORO in isopropyl alcohol diluted in double distilled water] for 15 minutes. Sections were rinsed with running water prior to mounting with water soluble Immuno HistoMount mounting solution.

Transmission electron microscopy (TEM)

Lipid droplets were detected using TEM. Freshly excised heart tissue was fixed in fixative solution containing 2.5% (v/v) glutaraldehyde and 4% (v/v) formaldehyde in 0.1 M HEPES buffer (pH 7.2). Tissues were then post-fixed in 0.1 M cacodylate buffer (pH 7.2) with 1% (w/v) osmium tetroxide and 1.5% (w/v) potassium ferrocyanide for 1 hour, followed by 1% tannic acid in 0.1 M cacodylate buffer (pH 7.2) for 1 hour, and finally in 1% uranyl acetate for 1 hour. Samples were then dehydrated in ethanol and embedded in TAAB 812 resin and polymerized for 24 hours at 60°C. Sections were cut with a Reichert Ultracut Ultramicrotome. Images were taken with Gatan Orius SC1000 CCD camera and analyzed using Talos L120C transmission electron microscope at 100 kV accelerating voltage.

Real-time quantitative polymerase chain reaction (RT-qPCR)

Total RNA was extracted using Trizol and treated with DNAse (Invitrogen, AM1906) to eliminate genomic DNA contamination. The RNA was converted into complementary DNA (cDNA) using LUNAscript (New England Biolabs, E3010) following the manufacturer's instructions. The qPCR reaction was conducted on 30 ng cDNA using SYBR Select PCR master mix (Applied Biosystems, 4472908) and the appropriate primers (Major Resources Tables), followed by running on the StepOne Plus PCR system. The fold change was determined using the comparative threshold (Ct) method (△△CT method). The mRNA level of the target gene was normalized to housekeeping gene 18S.

RNA sequencing

Total RNA of human MS-HF hearts was extracted using Trizol and treated with DNAse. The quality and integrity of RNA were initially checked using a 2100 Bioanalyzer and the TruSeq Stranded mRNA assay (Illumina) as described previously.[49,50] Unmapped paired-reads of 59bp were interrogated using a quality control pipeline consisting of FastQC v0.11.3 (http://www.bioinformatics.babraham.ac.uk/projects/fastqc/) and FastQ Screen v0.14.0 (https://www.bioinformatics.babraham.ac.uk/projects/fastq_screen/). The reads were trimmed to remove any adapter or poor-quality sequence using Trimmomatic v0.39.[53] Reads were truncated at a sliding 4bp window, starting 5', with a mean quality <Q20, and removed if the final length was less than 35bp. Additional flags included: 'ILLUMINACLIP:./Truseq3-PE-2_Nextera-PE.fa:2:30:10 SLIDINGWINDOW:4:20 MINLEN:35'. The filtered reads were mapped to the human reference sequence analysis set (hg38/Dec. 2013/GRCh38) from the UCSC browser,[54] using STAR v2.7.7a.[55] The genome index was created using the comprehensive Gencode v41 gene annotation applying a flag suitable for the read length (sjdbOverhang 75).[56] During mapping the flags 'quantMode GeneCounts' was used to generate read counts into genes. Normalization and differential expression analysis was performed using DESeq2 v1.34.0 on R v4.1.2 (http://www.R-project.org/). Log fold change shrinkage was applied using the lfcShrink function along with the "ashr" algorithm. The *p*

values are calculated using the Wald test, while multiple testing correction of adjusted p values was performed by Benjamini Hochberg method, and adjusted p less than 0.1 ($p_{adj}<0.1$) was the default cutoff.[57] Thus, the genes with $p_{adj}<0.1$ were considered as genes with differential expression and applied for pathway analyses using Enrichr (https://maayanlab.cloud/Enrichr/).[58] Finally, the pathway enrichment dot plots were generated using RStudio software.

On the other hand, we also performed RNA sequencing on HFpEF samples. Total RNA of human HFpEF hearts was extracted using Trizol, followed by RNA Library Preparation and NovaSeq Sequencing (GENEWIZ UK Ltd.). RNA samples were quantified using Qubit 4.0 Fluorometer (Life Technologies, Carlsbad, CA, USA) and RNA integrity was checked with RNA Kit on Agilent 5300 Fragment Analyzer (Agilent Technologies, Palo Alto, CA, USA). RNA sequencing libraries were prepared using the NEBNext Ultra II RNA Library Prep Kit for Illumina following manufacturer's instructions (NEB, Ipswich, MA, USA). Briefly, mRNAs were first enriched with Oligo(dT) beads. Enriched mRNAs were fragmented for 15 minutes at 94°C. First strand and second strand cDNAs were subsequently synthesized. cDNA fragments were end repaired and adenylated at 3'ends, and universal adapters were ligated to cDNA fragments, followed by index addition and library enrichment by limited-cycle PCR. Sequencing libraries were validated using NGS Kit on the Agilent 5300 Fragment Analyzer (Agilent Technologies, Palo Alto, CA, USA), and quantified by using Qubit 4.0 Fluorometer (Invitrogen, Carlsbad, CA). The sequencing libraries were multiplexed and clustered onto a flowcell on the Illumina NovaSeq instrument according to manufacturer's instructions. The samples were sequenced using a 2x150bp Paired End (PE) configuration. Image analysis and base calling were conducted by the NovaSeq Control Software (NCS). Raw sequence data (.bcl files) generated from Illumina NovaSeq was converted into fastq files and de-multiplexed using Illumina bcl2fastq 2.20 software. Data was firstly run through Variance Partition, which uses a linear mixed model to partition the variance attributable to multiple variables in the data. It was suggested that age contributes to some variance and was added to the modelling by splitting age into two groups (< and >52). The following normalization and differential expression analyses were performed as described above.

Stimulation of fatty acids or treatment on cells
Palmitic acid (PA, 300 µM) and oleic acid (OA, 300 µM) was prepared in 0.5% fatty acid-free bovine serum albumin (BSA) for conjugation. The molar ratio used for PA:BSA and OA:BSA was 7:1 to mimic pathophysiologic states.[24,59] Cells were treated with fatty acids for various durations depending on experimental design and purpose in Results. The control groups received 0.5% (w/v) BSA treatment. MG132 (10 µM) was used to pre-treat cells to block protein degradation, 6 hours prior to the other stimulation.

Construction of plasmids
To evaluate the effect of ER-retained ATGL on lipid accumulation, *ATGL* cDNA was inserted into the pEF/Myc/ER-Crimson vector (Addgene, 38770) containing the KDEL peptide sequence (AAGGACGAGCTG) at the C-terminal. Briefly, *ATGL* cDNA was obtained by PCR amplified from ATGL-EGFP[11] using the primers 5'-GTCGACAT GTTTCCCCGCGAGAAG-3' and 5'-TGCGGCCGCCAGCCCCAGGGCCCCGATC-3'. The fragment, digested by SalI and NotI restriction enzymes, was subcloned into the pEF/Myc/ER-Crimson vector to generate pEF/Myc/ER-*ATGL*-KDEL.

To assess the effect of XBP1s on transcriptional regulation of *Edem2*, a luciferase reporter plasmid containing ~500bp upstream of the transcription start site (TSS) of mouse *Edem2* was generated. In short, PCR products amplified from mouse genomic DNA using the primers 5'-GGTACCTAGAGACTGAAGGGA-3' and 5'-CTCGAGCAGCTCATCCTCCGA-3' were subcloned into the pGL3-promoter luciferase vector (Promega, E1751) via KpnI and XhoI restriction sites. The original pGL3-promoter vector was used as a control.

Adenovirus production

To achieve EDEM2 or XBP1s overexpression *in vitro*, recombinant adenovirus expressing *EDEM2* (Ad-*EDEM2-Myc-His*) was generated by subcloning *EDEM2* cDNA (Source Biosciences, #IRAUp969A037D) or *XBP1s* cDNA (Addgene, pCMV5-*XBP1s*) in Gateway pENTR Vector 11 (Invitrogen, A10467), followed by recombination-based cloning using pAd/CMV/V5-DEST vector (Invitrogen, V49320). PacI linearized plasmids were transfected (Thermo Fisher, 11668019) in HEK293A cells (Invitrogen, R70507). Viral plague was obtained 7 days post transfection. Packaged adenoviruses were amplified in HEK293A cells. Next, adenoviruses were purified using cesium chloride (CsCl) gradient purification methods (through 1.45 g/ml and 1.33 g/ml CsCl solution) by centrifuging at 100,000g (rotor SW40 rotor, swing-bucket Beckman Optima) for 18 hours. Finally, the collected adenoviral particles were dialyzed using a dialysis tubing (Medicell, cellulose 14kDa, 28.7mm diameter) soaked in the chemical exchanging buffer (10 mM Tris base, 1 mM $MgCl_2$, 135 mM NaCl, 10% v/v glycerol) for 2 hours. Titration was then assessed by infection of HEK293A cells before administration in experimental cells.

Overexpression of genes

Infection of Ad-*EDEM2* at multiplicity of infection (MOI) of 25 for 48 hours before PA and OA treatment was performed. XBP1s overexpression was achieved by infection with Ad-*XBP1s* (adenovirus expressing *XBP1s*) - either from the Schiattarella group[2] or generated using pCMV5-*XBP1s* (Addgene, 63680). For ATGL overexpression, cells were transfected with 2 µg of purified plasmids [wild type ATGL (WT), mutant ATGL (S47A), mutant ATGL (N172K)] and ATGL-KDEL using Lipofectamine 2000 Reagent (Thermo Fisher, 11668-019).[11,60] Regarding SEC23A overexpression, 2 µg of human *SEC23A* cDNA containing plasmids (modified from Addgene, 66609, by removing GFP) was used for transfection in NRCMs or H9C2 using Lipofectamine 2000 Reagent and transfection in hiPSC-CMs using Lipofectamine Stem Reagent (Thermo Fisher, STEM00001).

siRNA knockdown of genes

EDEM2, XBP1s, ATGL, and SEC23A knockdown was achieved using Lipofectamine LTX & Plus Reagent (Thermo Fisher, 15338100) mediated transfection of Silencer Select Pre-Designed rat *siEdem2* (Invitrogen, s150033), rat *siXbp1* (s144590, which can target both unspliced and spliced *Xbp1*), rat *siAtgl* (s167783), and rat *siSec23a* (s132863), respectively, following the manufacturer's instructions. The control cells were transfected with a negative control *siRNA* (*siNeg*) (AGGUAGUGUAAUCGCCUUG). Cells transfected with 50 nM of *siRNA* were incubated for 48 hours at 37°C before further treatment.

Luciferase reporter assay

The luciferase reporter plasmids and Renilla plasmid were co-transfected using Lipofectamine 3000 (Thermo Fisher, L3000015) into NRCMs. Following XBP1s overexpression using Ad-*XBP1s*, luciferase activity was measured using Dual-Luciferase Reporter Assay System (Promega, E1910), and data was read on a GloMax Explorer Multimode Microplate Reader (Promega).

ChIP assay

Chromatin immunoprecipitation (ChIP) was performed using the SimpleChip Plus Enzymatic ChIP kit (Cell Signaling, 9004) as per manufacturer's instructions. Briefly, control (Ad-*LacZ*) and XBP1s-overexpressing (Ad-*XBP1s*) C2C12 cells were fixed with 1% v/v formaldehyde and harvested. Nuclear membrane was lysed by sonication. Fragmented chromatin was immunoprecipitated by an anti-XBP1s antibody (dilute as 1:20, Cell Signaling, 40435). qPCR was subsequently performed using the following primer sets designed from mouse *Edem2* (NC_000068.8) sequence. Data was normalized to input chromatin (mouse):
Set 1: 5'-CTAGATGGCGCCTGTAAAG-3' and 5'-GAGCATCTCGGGATTTC-3'
Set 2: 5'-GTGTGCTCCAAACTTGC-3' and 5'-GAATATGTTCTGGTCACC-3'

Liquid chromatography-Mass spectrometry (LC-MS)

To determine the alterations of protein profiles in human hearts, mice hearts, or cells, liquid chromatography/mass-spectrometry analyses were performed as described.[61] 40 μg of protein was transferred to a 130 μl AFA tube (Covaris®, 520045) with 50 μl of S-trap solubilization buffer [5% (w/v) SDS in 7.55 triethyl ammonium bicarbonate]. The sample was disrupted using AFA sonication in a Covaris® LE220+ for 1 minute, with 200 cycles per burst, a duty factor of 40%, and a peak incident power of 500 W. Protein reduction and alkylation of cysteine bonds was performed using 10 mM DTT (Fisher Scientific, BP172-5) and 15 mM IAM (Sigma-Aldrich, I1149). The supernatant was quantified using Millipore Direct Detect and trapped in S-trap columns using 1.2% phosphoric acid and S-Trap binding buffer [90% aqueous methanol containing a final concentration of 100 mM triethyl ammonium bicarbonate, pH 7.1]. The samples were digested, eluted, and desalted using Oligo R3 beads and subsequently vacuum concentrated using a Heto vacuum centrifuge according to the manufacturer's instructions. The dried peptides were subjected to Q Exactive mass spectrometer measurement. Quantitative abundances were normalized based on the total peptide amount per channel. The data processing workflow involved the use of precursor Quan, label-free Quan, and Sequest Percolator. Variable modifications included N-terminal-oxidation of methionine (M), -acetylation, -loss of M, and -loss of M plus acetylation. 'Carbamidomethylation of cysteine' was set as a fixed modification. The proteins were annotated according to Swissprot protein database with false discovery rates set to 1%. The differential expression results were analyzed using Proteome Discoverer, using Bonferonni correction. Proteins altered between two experimental groups in each cohort ($p_{adj}<0.05$) were presented in heatmap. On the other hand, raw abundances human and cell results were also applied for pathway analyses. To do so, among the total proteins identified, proteins with absolute Log_2 fold change greater than 0.5 and raw abundances count greater than 6 in total samples were selected and analyzed using Enrichr (https://maayanlab.cloud/Enrichr/) to determine and present the altered pathways between the experimental groups ($p_{adj}<0.05$) according to the database of GO cellular component, GO cellular biological process, Reactome, and KEGG.[58] Finally, the pathway enrichment dot plots were generated using RStudio software.

Mass spectrometry was also employed to explore the interactome of EDEM2 as described.[49] EDEM2 was overexpressed in NRCMs by infection with Ad-*EDEM2-Myc-His*. After 48 hours, cells were fixed with 0.4% (w/v) paraformaldehyde (PFA) in PBS for 10 minutes at room temperature. Protein was extracted using RIPA buffer [50 mM Tris-HCl, 150 mM NaCl, 0.1% (w/v) SDS, 0.5% (w/v) sodium deoxycholate, 1 mM EDTA, 1% (v/v) NP-40, 25 mM glycerophosphate, protease and phosphatase inhibitor cocktail (Merck, PPC1010)]. EDEM2 and its interactors were immunoprecipitated using the anti-His tag antibody (Genscript, A00186) crosslinked to Pierce protein G Agarose (Life Technologies, 20398), with approximately 2 mg of input protein being used. Immune complexes were eluted using 2xLaemmli sample buffer [125 mM Tris-HCl, 4% (w/v) SDS, 20% (v/v) glycerol, 0.01% (w/v) bromophenol blue, 10% (v/v) β-mercaptoethanol, pH 6.8]. Precipitated proteins were subjected to SDS-PAGE, and the whole bands were excised. Post acetonitrile dehydration, the gel pieces were reduced and alkylated with 10 mM dithiothreitol and 55 mM iodoacetamide, respectively. Additionally, in-gel digestion was performed overnight at 37°C with trypsin. The resulting peptides were analyzed by LC-MS using UltiMate® 3000 Rapid Separation LC system (RSLC, Dionex Corporation, Sunnyvale, CA) coupled to an Orbitrap Elite mass spectrometer. Peptide mixtures were separated using a gradient from 92% solvent A (0.1% formic acid in water) to 8% solvent B (0.1% formic acid in acetonitrile) for 45 minutes, using a 75 mm × 250 μm i.d. 1.7 mM BEH C18, analytical column (Waters). Peptides were selected for fragmentation automatically by data-dependent analysis. Protein identification was done using Mascot (Matrix Science, UK) by searching against a rat Swissprot proteome database. The data were further validated using Scaffold software (Proteome Software, Portland, OR). Interacting proteins of EDEM2 were identified as the proteins that exhibited no

binding in control but displayed the presence of at least one additional unique peptide with an 80% peptide probability in EDEM2-overexpressing cells.

Lipidomics assay

To assess lipid species profiling in human and mouse hearts, the mass spectrometry-based lipidomics assay was performed. Heart tissue (25 mg) was pulverized using the Covaris cryoPREP system. The pulverized tissue samples were then loaded into milliTUBEs for lipid extraction using ice old methanol and chloroform subsequently. 0.1 M ammonium formate was added to the samples to promote phase separation. After centrifuge, the subnatant was transferred to glass autosampler vials and was dried under a stream of nitrogen gas at 40°C. Mass spectrometry analysis was conducted using a SCIEX Exion LC system coupled with a SCIEX 7600 ZenoTOF Q-TOF mass spectrometer equipped with a TurboV Optiflow ion source and a 50 µm ESI probe. The system was controlled by SCIEX OS v3.0. Analytes were separated using Thermo Accucore C18 column (2.6 µm, 2.1 × 10 mm). The mass spectrometer was operated in positive mode, and the source conditions were as follows: ion spray voltage, 5500 V; curtain gas pressure, 50 psi; temperature, 400°C; ESI nebulizer gas pressure, 50 psi; heater gas pressure, 70 psi; and declustering potential, 280 V.

Data acquisition was performed in an information-dependent manner, involving 10 product ion scans over a mass range of 50-1600 Da, each with an accumulation time of 100 ms. Additionally, a TOF survey scan with an accumulation time of 250 ms was conducted. MS/MS analysis was only performed on ions with a mass-to-charge ratio (m/z) greater than 350 Da. The total cycle time for data acquisition was 1.3 seconds. Collision energy was determined using the formula CE (V) = 0.084 x m/z + 12, with a maximum value of 55 V. Isotopes within 4 Da were excluded from the scan. The acquired data were evaluated using PeakView 2.2 software and then imported into Progenesis Qi v3.0 for metabolomics analysis. In Progenesis Qi, the data were aligned, peaks were detected, and normalization to all compounds was applied. Furthermore, deconvolution was performed according to standard Progenesis workflows. Normalized peak intensity was used for analyses of fold change. Putative annotations were made by searching the accurate mass against the LipidMaps LMSD database with a mass tolerance of ± 0.005 Da.[62]

Protein lysates extraction and immunoblotting

Cell and tissue total protein lysates were produced utilizing Triton lysis buffer [137 mM NaCl, 20 mM Tris, 0.1% (w/v) SDS, 2 mM EDTA, 10% (v/v) glycerol, 1% (v/v) Triton-X, 25 mM glycerophosphate, protease and phosphatase inhibitor cocktail, pH 7.4]. Heart lysates from *ob/ob* mice were ready to use.[59] Protein concentration was determined using the Bradford assay (Bio-Rad, 500-0006) and immunoblotting was performed using 30 µg of protein lysate. Primary antibodies and both the anti-mouse and anti-rabbit HRP conjugated secondary antibodies were diluted in 5% (w/v) fat free milk in TBS-T (Major Resources Tables). Thermo Fisher ECL (34087) and Amersham ECL Prime (RPN2232) and Select (RPN2235) detection reagents were utilized to visualize protein bands via chemiluminescent imaging on Carestream BioMax XAR film (F5513-50EA, Kodak) in Hypercassette (Amersham BioSciences) or rarely by the ChemiDoc system (BioRad).

Co-immunoprecipitation

To investigate the association between EDEM2 and SEC23A, co-immunoprecipitation on Ad-*EDEM2-Myc-His* treated H9C2 cells was performed with Protein G agarose beads (Thermo Fisher, 20398) following the manufacturer's instructions. Briefly, the infected cells were fixed with 0.4% (w/v) PFA and protein was extracted using RIPA buffer. Approximately 2 mg of input protein was used to pull out EDEM2 using anti-His antibody. Immune complexes were eluted in Laemmli sample buffer. Precipitated proteins were subjected to SDS-PAGE and immunoblotting. On the other hand, to investigate the ubiquitinated ATGL in H9C2 cells or heart tissue, whole lysates were precipitated using anti-ATGL antibody. Immunoblotting was performed using anti-ubiquitin antibody.

ER isolation

The ER was isolated from heart tissue and cells using the ER enrichment kit (Novus Biologicals, NBP2-29482) following the manufacturer's instructions. In brief, 150 mg of heart tissue, containing 3 samples from the same experimental group (50 mg/each), was used as a pool sample to yield enough amount of the ER. The total ER fraction was collected for the following immunoblotting assessment.

ATGL activity assay

We used a simplified ATGL activity assay to measure ATGL activity as described,[63,64] with some modifications. Extracts from fresh tissue or H9C2 cells were obtained by sonication within a lysis buffer [50 mM Tris (7.4), 150 mM NaCl, 0.1% (v/v) Triton-X]. For each sample, 30-100 µg of whole extracts were incubated in 95 µl of the lysis buffer with an addition of 5 µl of 20 µM EnzChek lipase substrate (final concentration of the substrate was 1 µM in each reaction, Thermo Fisher, E33955) at 37°C for 60 minutes in the dark. The fluorescent reading was gained at excitation and emission wavelengths of 485 nm and 510 nm, respectively. The time-dependent fluorescence increase was linear after 20 minutes of the reaction. ATGL activity was presented as the relative value by normalization of initial rates to protein levels.

Diglycerides and triglycerides assay

The contents of triglycerides (TGs) and diglycerides (DGs) were measured in H9C2 cells ($1x10^6$ cells) according to experimental design. The assays were performed using Diglycerides Assay kit (abcam, ab242293) and Triglycerides Assay kit (abcam, ab65336), respectively, following the manufacturer's instructions.

ATP assay

Cellular ATP concentration was calculated using the Luminescent ATP Detection Assay kit (abcam, ab113849) following the manufacturer's instructions. Briefly, $3x10^4$ H9C2 were seeded and treated with 5 µg/ml brefeldin A (BFA, Tocris Bioscience, 1231), 50 µM IXA4 (Cayman Chemical, 36788), or 5 µM Etomoxir (Selleck, S8244) prior to PA and OA treatment depending on the experimental design.

Lipid droplet isolation

Lipid droplets were isolated from $5x10^7$ H9C2 cells per sample using the Lipid Droplet Isolation kit (abcam, ab242290) following the manufacturer's instructions. Protein amount was normalized to cell number.

Immunofluorescent staining

Cellular co-localization staining was performed on NRCMs, H9C2 cells or hiPSC-CM following stimulation with PA and OA for various time durations. Cells were fixed with 4% (w/v) PFA or cold methanol at room temperature for 15 minutes. Subsequently, the fixed cells were permeabilized with 0.1% (w/v) sodium citrate and 0.1% (v/v) Triton-X or Tween-20 in PBS on ice for 10 minutes. After being blocked with 1% (w/v) BSA in PBS, the coverslips were incubated with primary antibodies diluted in 1% (w/v) BSA in PBS overnight. Incubation with fluorescent-conjugated secondary antibodies (Major Resources Tables) in 1% (w/v) BSA in PBS was applied for 2 hours at room temperature. The coverslips were then washed with PBS and mounted with VECTASHIELD® Antifade Mounting Medium with DAPI (Vector Laboratories, H-1000).

BODIPY staining of cells

Cellular lipid droplets in H9C2 cells were visualized using BODIPY staining following fatty acid treatment. Alive cells were incubated with BODIPY™ 493/503 (Thermo Fisher, D3922) for 30 minutes and subsequently fixed with 4% (w/v) PFA for 15 minutes at room temperature. The coverslips were mounted with VECTASHIELD® Antifade Mounting Medium with DAPI.

ORO staining of cells

Following respective treatments in hiPSC-CMs and NRCMs, the coverslips were fixed with 10% formalin for 45 minutes and subsequently incubated with ORO solution [0.15% (w/v) ORO in isopropyl alcohol diluted in double distilled water] for 5 minutes. Hematoxylin was applied for 1 minute to stain nuclei prior to mounting with a permanent aqueous ImmunoHistoMount mounting solution (Sigma-Aldrich, I1161).

Imaging of histology

ORO stained cryosections were imaged on a 3D-Histech Pannoramic-250 microscope slide-scanner using a Zeiss 20x/0.80 Plan Apochromat objective. Snapshots of the scanned slides were taken using the Case Viewer software (3D-Histech) with individual magnification. Lipid droplet area percentage was calculated using QuPath v0.4.3. Fluorescent-labelled slides for WGA, DHE, BODIPY, and co-localization staining were imaged using a Zeiss Axioimager D2 upright microscope with Zeiss LD Plan-Neofluar objectives (x40, x63, x100) and captured using a Coolsnap HQ2 camera (Photometrics) through Micromanager software v1.4.23. Specific band pass filter sets for DAPI, FITC, and Texas Red were used to prevent bleeding from one channel to the next. Images were then further processed and analyzed using Image J software.

Statistical analyses

Data are presented as bar/dot plots showing mean ± SEM. Where sample sizes were ≥5, the Shapiro-Wilk test was conducted to determine whether data was normally distributed. Normally distributed data sets were analyzed using ordinary One-way or Two-way ANOVA followed by appropriate post-hoc tests, whereas comparisons between only two groups were performed using Student's t test. The non-parametric equivalents were utilized for skewed data and data sets where sample sizes were <5. Statistical analysis was performed using the GraphPad Prism 10 software and p values <0.05 were considered statistically significant. The sample size corresponds to biological replicates and is specified for each experiment within the figure legend.

Study limitations

The main limitation of the 2-hit HFpEF model is that it only represents a proportion of HFpEF patients who present with both hypertensive and metabolic stress. Additionally, the HFD provides 60% of calories from fat which may not represent the high fat diet consumed by all HFpEF patients. Therefore, whether targeting XBP1s-EDEM2 signaling could be beneficial in the treatment of all HFpEF patients requires further study. Another limitation is the inclusion of only male mice so whether our findings could be recapitulated in females needs investigation.

Major Resources Tables

Immunoblotting Antibodies

All immunoblotting antibodies are diluted as shown in 5% fat free milk (w/v) in TBS-T.

ANTIBODIES	DILUTION	SOURCE	IDENTIFIER
EDEM2	1:1000	Proteintech	11241-1-AP
EDEM2	1:1000	Sigma-Aldrich	E9906
CD36	1:500	Proteintech	18836-1-AP
CPT1B	1:1000	Proteintech	22170-1-AP
ATGL	1:1000	Santa Cruz Biotechnology	sc-365278
ATGL	1:1000	Abcam	ab207799
DGAT2	1:1000	Antibodies.com	A89902
Cleaved caspase 9	1:500	Cell Signaling Technology	9505
PLIN2	1:1000	Abcam	ab108323
Cytochrome C	1:1000	Cell Signaling Technology	11940
SEC23A	1:1000	Cell Signaling Technology	8162
XBP1s	1:1000	Proteintech	24868-1-AP
XBP1	1:1000	Abcam	Ab37152
ATF4	1:1000	Proteintech	10835
ATF6	1:1000	Abcam	ab37149
Ubiquitin	1:1000	Proteintech	10201-2-AP
G beta (Gβ)	1:1000	Santa Cruz Biotechnology	sc-166123
Beta-Actin (β-Actin)	1:1000	Proteintech	66009-1-lg
Calnexin	1:1000	Proteintech	10427-2-AP
Alpha-Tubulin	1:1000	Sigma-Aldrich	T5168
His-Tag	1:500	Genscript	A00186
HRP-linked anti-mouse	1:1000	Cell Signaling Technology	7076
HRP-linked anti-rabbit	1:1000	Cell Signaling Technology	7074
HRP-linked anti-mouse	1:2000	Proteintech	RGAM001
HRP-linked anti-rabbit	1:2000	Proteintech	RGAR001

Immunofluorescence Antibodies

All immunofluorescence antibodies are diluted as shown in 1% (v/v) BSA in PBS.

ANTIBODIES	DILUTION	SOURCE	IDENTIFIER
ATGL	1:50	Proteintech	55190-1-AP
EDEM2	1:50	Proteintech	11241-1-AP
PDI	1:50	Proteintech	66422-1-lg
CANX	1:50	Proteintech	66903-1-lg

	1:50	Santa Cruz	sc-365158
ERGIC53	1:50	Santa Cruz Biotechnology	sc-365158
Anti-mouse AlexaFluor 488	1:1000	Jackson ImmunoResearch	715-546-151
Anti-mouse AlexaFluor 594	1:1000	Jackson ImmunoResearch	715-586-151
Anti-rabbit AlexaFluor 488	1:1000	Jackson ImmunoResearch	711-545-152
Anti-rabbit AlexaFluor594	1:1000	Jackson ImmunoResearch	711-585-152

Animal Use

SPECIES	STRAIN	SOURCE
Mouse	C57BL/6J	Envigo
Rat	Sprague-Dawley	Charles River

Cultured Cells

PRODUCT	SOURCE	IDENTIFIER
H9C2	Sigma-Aldrich	88092904
C2C12	ATCC	CRL-1772
HEK293A	Invitrogen	R70507
NRCMs	Primary Cells	N/A
hiPSC-CM	Primary Cells	N/A

qPCR Primers

PRODUCT	SOURCE	IDENTIFIER
EDEM2 (Hu)	Qiagen	QT00056224
XBP1 (Hu)	Qiagen	QT00068383
EDEM1 (Hu)	Qiagen	QT00033012
CANX (Hu)	Qiagen	QT00092995
DNAJB9 (Hu)	Qiagen	QT00002716
PDIA3 (Hu)	Qiagen	QT00048776
HERPUD1 (Hu)	Qiagen	QT00026418
SYVN1 (Hu)	Qiagen	QT01669983
VIMP (Hu)	Qiagen	QT00008169
DERL1 (Hu)	Qiagen	QT00033096
EIF2A3 (Hu)	Qiagen	QT00066003
PGK1 (Hu)	Qiagen	QT00013776
Edem2 (Ms)	Qiagen	QT00160587
Dgat2 (Ms)	Qiagen	QT00134477
Cd36 (Ms)	Qiagen	QT01058253
Pnpla2 (Ms)	Qiagen	QT00111846
Lipe (Ms)	Qiagen	QT00169057

Cpt1b (Ms)	Qiagen	QT00172564
Acadl (Ms)	Qiagen	QT00101248
Cat (Ms)	Qiagen	QT01058106
Acox1 (Ms)	Qiagen	QT00174342
Col1a2 (Ms)	Qiagen	QT02325736
Col3a1 (Ms)	Qiagen	QT00297094
Nppb (Ms)	Qiagen	QT00107541
18s (Ms)	Qiagen	QT02448075

Other Major Resources

PRODUCT	SOURCE	IDENTIFIER
CytoTune iPS Programming Kit	Life Technologies	A13780
mTeSR Plus	Stem Cell Technologies	100-0276
RPMI HEPES GLutamax	Life Technologies	72400021
CHIR99021	Millipore	361559
IWP2	Millipore	681671
B27 Minus Insulin Supplement	Life Technologies	A1895601
DMEM	Gibco	11966-025
M199	Gibco	31150-
Collagenase A	Roche	10103586001
BRDU	Sigma-Aldrich	B5002
Pancreatin	Sigma-Aldrich	P3292
L-Name	Sigma-Aldrich	N5751
Alda-1	Sigma-Aldrich	349438-38-6
SR-4995	Sigma-Aldrich	SML2207
Oxytocin	Tocris Bioscience	1910
Brefeldin	Tocris Bioscience	1231
MG132	Selleckchem	S2619
Lipofectamine 2000	Thermo Fisher Scientific	11668019
Lipofectamine 3000	Thermo Fisher Scientific	L3000015
Lipofectamine LTX & Plus Reagent	Thermo Fisher Scientific	15338100
Lipofectamine Stem Reagent	Thermo Fisher Scientific	STEM00001
IXA4	Cayman Chemical	36788
IAM	Sigma-Aldrich	I1149
DTT	Fisher Scientific	BP172-5
Etomoxir	Selleck	S8244
Lipid Droplet Isolation Kit	Abcam	ab242290
Triglyceride Assay Kit	Abcam	ab65336
Diglyceride Assay Kit	Abcam	ab242293
ATP Assay Kit	Abcam	ab113849
Oil Red O	Sigma-Aldrich	O0625

DHE	Thermo Fisher Scientific	D1168
BODIPY™	Thermo Fisher Scientific	D3922
VECTASHIELD® Antifade Mounting Medium with DAPI	Vector Laboratories	H-1000
ImmunoHistoMount	Sigma-Aldrich	I1161
Protein G agarose	Thermo Fisher Scientific	20398
TRizol reagent	Ambion	15596018
DNA-free Kit	Ambion	AM1906
LunaScript	New England Biolabs	E3010L
Power SYBR Green PCR master mix	Applied Biosystems	4367659
Wheat germ agglutinin (WGA)	Thermo Fisher Scientific	W32466
Chromatin IP kit	Cell Signaling Technology	9004
Dual-Luciferase reporter assay	Promega	E1910
EnzChek lipase substrate	Thermo Fisher Scientific	E33955
ER enrichment kit	Novus Biologicals	NBP2-29482
ECL Select Western Blotting detection reagent	Amersham	RPN2235
ECL Prime Western Blotting detection reagent	Amersham	RPN2236
SuperSignal West Pico PLUS Luminol/Enhancer	Thermo Fisher Scientific	1863094
Carestream BioMax XAR film	Kodak	F5513-50EA

Supplemental Table 1

GENE NAME	Mean Normal	Mean MS-HF	Log$_2$ Fold Change	$p_{adj.}$
PDE4DIPP1	27.30048263	0.1	-9.516573059	2.88E-05
THRSP	95.1441955	2.076318396	-5.622989665	5.00E-06
SAA1	26.74308439	1.27138854	-4.239885833	0.00416325
ADIPOQ	71.89047626	1.763277435	-4.02421263	6.06E-05
CIDEC	46.94029281	0.952029825	-3.929419908	0.000340753
TFRC	1897.041785	260.005401	-2.687993756	0.000149159
PLIN1	97.50820488	16.30441819	-2.613403778	0.000178584
LGALS12	14.56439586	0.836168296	-2.567925321	0.065652861
NPPA	638.3801066	59.98847122	-2.423564071	0.042469311
SERPINB9P1	77.24086969	8.279077168	-2.420483647	0.021284269
UTS2R	25.14679939	1.805881347	-2.386347489	0.024189806
F2RL3	55.34572278	20.55174107	-2.372629862	0.059699044
COLQ	111.4590098	21.41209297	-2.153408805	0.005245332
IDH3A	663.8526027	152.4868528	-1.996271993	0.038052138
DLAT	1377.016696	350.1995712	-1.93063916	0.017047658
TF	35.85355089	8.327492472	-1.907486364	0.036229724
ACO2	4717.927782	977.5380951	-1.836772752	0.04684107
TGFA	39.28603702	7.130368237	-1.833765974	0.043141559
ALAS1	1823.950244	476.0572005	-1.773120407	0.005431578
SBK3	29.3813099	7.951247799	-1.741662559	0.076922384
TUBA4A	2083.14755	573.7170986	-1.682991985	0.010679537
FHOD3	1954.291787	497.625797	-1.642309556	0.065624252
TUBB4B	7528.397394	2031.785494	-1.579642251	0.017764092
PDK4	13998.50151	3341.709399	-1.578420505	0.077468491
CPVL	1245.800032	307.8829228	-1.578048506	0.045687506
UQCRFS1	4999.763023	1464.144511	-1.56214578	0.005245332
ETFDH	3309.743097	969.4771791	-1.548294356	0.024195482
POF1B	92.9669965	23.20997941	-1.537912363	0.060271391
ALDOC	2880.485107	814.6358402	-1.533099594	0.021789893
PDSS1	74.08947397	19.32508813	-1.511651772	0.043847556
CITED2	1533.671289	457.3525167	-1.4774057	0.004887994
GFM2	481.6269978	149.4131521	-1.454984522	0.056479414
C6	1291.071381	436.7972952	-1.454619453	0.04688464
TOMM40L	311.291208	107.0951609	-1.43524785	0.009623939
AIMP2	212.6891664	57.23295653	-1.430948893	0.064874934
XBP1	1577.354281	548.5819447	-1.413867474	0.000622307
LPCAT3	63.87913869	22.01575816	-1.403833781	0.083478317
FKBP5	2306.064249	763.7782663	-1.396462202	0.026037685
PRMT5	162.45921	52.80621489	-1.378359827	0.023839382
SLC39A14	2470.25944	872.4685232	-1.357687996	0.045687506
HSPA5	7563.531896	2560.992601	-1.351587041	0.045703638
DNAJC11	379.2399096	120.2408882	-1.350136675	0.066572791
CASQ2	20190.86249	5992.410743	-1.339972082	0.047144934
TUBB6	2100.178507	689.8983034	-1.334085194	0.022981713
SLC5A1	3782.71389	918.4358437	-1.331467509	0.092192046

Supplemental Table 1

GENE NAME	Mean Normal	Mean MS-HF	Log$_2$ Fold Change	$p_{adj.}$
SGCD	2012.741319	627.6880369	-1.330890305	0.084473386
PGAM1	649.9408767	223.5632392	-1.321079981	0.005714804
IMMT	3698.313399	1336.541198	-1.318417814	0.004501146
LINC00881	1427.031974	479.5031799	-1.314390328	0.008760177
CD274	215.2250109	77.25624978	-1.311418283	0.018664752
FTCDNL1	33.72840604	11.25739442	-1.310904792	0.063566319
PINK1	989.9049791	342.9725534	-1.296249365	0.045950623
DLST	2243.002613	816.1830014	-1.294978848	0.005431578
TRAP1	491.6506318	160.9131262	-1.289985972	0.066572791
TMLHE	216.7533397	77.12549501	-1.285756982	0.057685966
DNAJA3	1149.35417	420.9707828	-1.283513797	0.004887994
ATP5F1B	32958.28597	11831.50637	-1.282390183	0.011535564
ENOX1	166.3068189	54.31139302	-1.277617292	0.032837328
RAB15	784.4244364	263.345677	-1.275680948	0.029687972
SERPINA5	67.67212388	21.21072434	-1.263370382	0.097659603
DLD	5039.798701	1783.033514	-1.24573422	0.022981713
DNAJA4	1782.845475	697.3672418	-1.240206941	0.015252073
PPIF	2081.734985	698.5006717	-1.239877809	0.030689582
DUS2	88.46030755	29.73360309	-1.233686429	0.020515351
PPIL1	1312.313225	450.8958359	-1.233466554	0.063649431
ALDH4A1	571.6647283	186.8151313	-1.216504469	0.048893751
SRL	8292.212477	2524.76044	-1.201564001	0.067485423
PFKP	1997.713144	747.4863502	-1.188068552	0.022227779
MDH2	8588.195149	3336.87721	-1.185165697	0.008481482
ALDOA	393.2394903	130.5330313	-1.184298519	0.057842855
FITM2	2241.657982	755.9754436	-1.175421378	0.084792299
CCT2	1486.669298	593.7114104	-1.173229495	0.010784727
PDK2	873.5900015	301.4262626	-1.167322329	0.069571283
ATP1A1	1035.747972	355.3414041	-1.166904665	0.084109489
MRPL33	2421.048942	936.916262	-1.160271321	0.017047658
LAPTM4B	3165.452753	1304.152159	-1.156791923	0.047902342
WIPI1	544.7606245	224.1178749	-1.150693113	0.034967285
PGK1	5007.04129	2074.467233	-1.14893111	0.00147137
TPI1	9483.951629	3894.965167	-1.141853523	0.002595867
CALU	4912.447878	2086.315028	-1.127835189	0.002273825
SLC25A19	76.50733687	28.47857819	-1.126962678	0.071690301
COPS4	864.1827892	346.6518838	-1.118181718	0.039881883
MTND6P4	204.8764498	80.04298991	-1.10496582	0.048333582
CES2	1238.323863	478.0179869	-1.104294859	0.081436243
SDHC	728.6278925	289.7497248	-1.104039718	0.022531502
PHB1	1129.406326	419.5005323	-1.086554926	0.056308192
ATP5F1A	25227.30215	8558.850384	-1.082709637	0.084109489
UQCRC2	7759.781733	2900.728549	-1.08156109	0.065624252
DBNDD2	200.4660926	70.67915568	-1.079490056	0.071384606
NDUFA10	3479.588353	1418.90373	-1.062102494	0.030501266
BNIP3	2714.891779	987.1589589	-1.049689941	0.064951596

Supplemental Table 1

GENE NAME	Mean Normal	Mean MS-HF	Log$_2$ Fold Change	$p_{adj.}$
VLDLR	1089.635379	432.8274843	-1.048208874	0.069571283
PEX11A	165.9457024	72.44596656	-1.038936578	0.066098423
ABHD2	951.9656626	407.9105511	-1.035431393	0.01737933
TUBG1	650.7603635	274.6261033	-1.034733201	0.048893751
CYC1	7482.178057	3011.372905	-1.022514151	0.043847556
B3GALNT1	762.5058897	306.7767198	-1.015874461	0.084473386
CS	6715.408315	2603.996487	-0.999331783	0.066759787
MPP1	525.139182	234.1340315	-0.9979011	0.024783935
GART	494.8202432	229.3245554	-0.99717203	0.023839382
HSPA8	14932.83563	5558.374674	-0.995895901	0.099742194
MRPL37	1406.576832	645.393201	-0.993280081	0.004887994
MCM4	313.2682921	139.4633072	-0.991913606	0.077455643
MRPS18B	1869.663304	806.4927322	-0.988337029	0.030647608
NTMT1	326.0940038	137.4363841	-0.982967682	0.049030407
ATP5PB	6751.251892	2616.192138	-0.971810769	0.091243977
NUDT4	3289.460604	1375.85369	-0.96884687	0.065652861
PPP5C	1003.236473	457.5124428	-0.966095999	0.035362716
SDHB	4719.670954	1821.038295	-0.963705344	0.084473386
SMYD2	3896.90203	1670.633696	-0.957014114	0.081180571
MRPL13	644.7332852	289.5828889	-0.955445359	0.040464422
CENPV	140.9736007	58.27635727	-0.953712874	0.056802646
HYOU1	709.4342261	277.9223413	-0.946171977	0.099015002
PIGT	2293.237303	1105.780273	-0.941310088	0.00416325
COX10	720.1054037	278.0994611	-0.93863864	0.090478602
PGM1	3028.768728	1341.645067	-0.935145604	0.047144934
TBRG4	996.2542949	421.5959473	-0.927911803	0.065624252
UQCRH	7306.667492	3140.921259	-0.92376312	0.07048396
ACAA1	921.7445632	407.4049967	-0.919635881	0.063354739
GDE1	1303.474309	589.6217284	-0.914989951	0.069571283
ARAF	863.4107521	407.0392115	-0.906265953	0.030689582
PANK1	272.1413792	122.0940567	-0.901120737	0.070773412
POLD2	1632.987706	790.8758051	-0.898428517	0.024195482
BOLA3	375.5596856	169.6455976	-0.898374563	0.045687506
M6PR	516.2373428	225.9315997	-0.893770477	0.099015002
PRDX2	3248.838175	1330.118388	-0.887643466	0.099015002
PIGS	590.4852594	280.8825329	-0.886843369	0.032095321
MRPL44	447.8257031	205.6651891	-0.880860605	0.097506448
WFS1	1208.301991	569.4637744	-0.872297939	0.085234279
SLC25A20	1121.478129	545.2008885	-0.871433335	0.084792299
PSPH	134.5964348	63.44097456	-0.868395887	0.099015002
PARP1	1914.097032	941.6844307	-0.862261651	0.056308192
DARS2	182.4441998	85.15654713	-0.862141775	0.099015002
RUVBL1	434.4264546	200.6144638	-0.861487626	0.04434757
PSMD8	4216.753783	1925.364908	-0.857573427	0.073061504
UGP2	4043.39443	2018.436477	-0.852036164	0.04255453
STOML2	1695.462521	835.3924923	-0.850943245	0.030689582

Supplemental Table 1

GENE NAME	Mean Normal	Mean MS-HF	Log$_2$ Fold Change	$p_{adj.}$
ATP5MC1	4720.061959	2041.974952	-0.847204203	0.095358911
PDSS2	264.452708	131.3154123	-0.844976574	0.079200633
NDUFV1	6339.753929	2815.608334	-0.84055105	0.082514307
SLC31A1	293.3848797	143.5947919	-0.838875018	0.055727246
TMEM126A	852.4392112	400.6657825	-0.829833176	0.066525538
HINT3	630.9476879	302.1632591	-0.829035574	0.099015002
ACO1	1111.006281	544.4104468	-0.809905501	0.073061504
STARD7	3801.723228	1785.533985	-0.806209118	0.085804468
ACAD8	420.0850146	202.6858777	-0.799404566	0.063649431
NOP9	203.4907352	101.7029127	-0.79383464	0.073061504
CHST7	421.0946358	218.9982286	-0.79288219	0.033145664
GRHPR	1958.782137	949.5542283	-0.791901337	0.064951596
SMPD1	913.9949717	435.0422251	-0.786629629	0.084792299
ABCF1	651.7369913	339.2609864	-0.78616007	0.052686095
P4HB	2918.32028	1482.321086	-0.776746029	0.056397109
TSPAN9	2215.880167	1180.912055	-0.772454794	0.043847556
SLC25A3	15191.6041	7198.11196	-0.767365059	0.096391668
ABCD3	1027.282646	500.8320124	-0.764977328	0.078820354
MAD2L1BP	286.6579894	150.2474383	-0.764098005	0.081180571
HDHD5	696.9319961	361.4959949	-0.760088186	0.069571283
PSMD1	1618.879538	826.3808428	-0.752090361	0.084792299
SCAMP3	775.3347875	403.1921925	-0.751069675	0.07048396
IARS1	826.4850324	435.4476904	-0.749942555	0.099556132
METTL2A	245.6030682	126.7563801	-0.749920894	0.059501727
FARS2	279.170368	142.8514075	-0.733187871	0.095358911
SCO1	494.5684712	264.3998154	-0.731843213	0.084473386
MRPS16	911.5025964	480.7344298	-0.729665998	0.070773412
PDXDC1	895.64971	494.091557	-0.72683188	0.073061504
LARP4	579.9567002	310.0521294	-0.723758134	0.070800926
DCUN1D5	365.9162435	198.9215881	-0.723166081	0.082514307
NAA15	634.875273	336.6130251	-0.71331632	0.096139747
STIP1	1754.772515	990.9978551	-0.709617286	0.056247173
ABHD5	624.4280183	330.1641392	-0.695160569	0.080876583
CD99L2	1385.382646	752.6596445	-0.680508223	0.099735479
GMPPB	167.8973484	91.66430519	-0.677556061	0.084942786
MIOS	370.9792698	204.2190896	-0.676402464	0.08492604
PSMD2	2334.061655	1298.944961	-0.670235181	0.085804468
AKIRIN1	883.0701991	487.2341915	-0.667682595	0.097506448
P4HA2	518.9118467	298.173129	-0.661226486	0.059501727
ATP6AP1	1148.31795	669.0727342	-0.653295107	0.043847556
PPP2R5A	1572.434143	904.7725653	-0.652719079	0.09371826
RNH1	1936.056501	1121.31958	-0.648667164	0.060004463
DDOST	1632.808209	911.386078	-0.633974262	0.097282814
SF3B5	1148.358791	689.7279783	-0.628057427	0.03941928
CCT3	2188.703361	1247.658259	-0.621551729	0.09237101
TMEM147	1063.022176	630.2447396	-0.621489505	0.071025606

Supplemental Table 1

GENE NAME	Mean Normal	Mean MS-HF	Log$_2$ Fold Change	$p_{adj.}$
GORASP1	610.7409693	356.605795	-0.614116839	0.091243977
MMGT1	516.8914958	301.6030981	-0.612982401	0.084612148
TMX2	897.2744911	527.466472	-0.608411717	0.099015002
WDR1	2957.693968	1784.781478	-0.601756909	0.080790655
GSPT1	1457.7119	889.351259	-0.562134627	0.099015002
RPL29P11	14.77248542	0.582683755	-0.252295349	0.004887994
SORD2P	4.046568896	0.312847702	-0.135282529	0.073061504
EIF1AY	0.1	83.79246164	0.023608055	0.00416325
TTTY14	0.1	17.66341387	0.023704949	0.030991774
ZFY	0.1	12.89929484	0.030236565	0.035447926
UTY	0.266920267	16.00765197	0.030754409	0.043847556
TXLNGY	0.437778914	22.59320339	0.038583658	0.019834358
KDM5D	0.1	46.32606931	0.040036945	0.001512005
FOSB	11.35666595	73.9246548	0.058960392	0.057842855
TRIM67	0.1	2.165733417	0.059681653	0.056479414
FATE1	1.004128601	11.53173307	0.102428488	0.099015002
RN7SKP195	0.437778914	7.374050633	0.115342502	0.039881883
RUFY3	293.2158332	473.5857253	0.567086417	0.085234279
SH3YL1	87.48377759	157.3917631	0.668093638	0.099541607
RIMKLB	234.3326168	415.0235421	0.711111213	0.030647608
ZNF141	124.0362735	234.1076936	0.718967535	0.08023968
RALGDS	57.06157016	114.4922659	0.739056331	0.094688754
DTX3	275.6985923	522.795845	0.755852639	0.047144934
MTURN	415.5430724	776.2667739	0.760193782	0.033874666
FAM117A	114.6768216	243.9532929	0.762502185	0.098681108
TNFSF12	330.1861338	646.4631901	0.762589063	0.082514307
RUNX1T1	191.29854	394.227903	0.766197861	0.095447662
ABHD14B	222.3933236	442.7057453	0.768828899	0.085234279
UTRN	812.6439867	1580.576386	0.794118787	0.073061504
DGKH	128.1522781	251.8251691	0.797420649	0.055205613
ODF2L	136.1583306	273.6178585	0.805790885	0.081772284
FRG1CP	136.4163377	289.1074127	0.819738226	0.091243977
MTSS1	236.7642062	491.5011845	0.840864132	0.063649431
UACA	851.4749649	1679.911062	0.842504238	0.042469311
NLRP1	111.6707571	232.4869287	0.864052409	0.081436243
STIM2	119.5972295	254.6165999	0.872737498	0.094840527
TRANK1	54.98264586	121.3930492	0.876308737	0.073061504
EML4	92.39914401	202.0314048	0.877043451	0.094840527
RIPK2-DT	61.693039	132.003241	0.88877195	0.055727246
ZNF624	22.1780395	51.287408	0.891617831	0.084612148
PTPRB	619.9553342	1291.647329	0.894146695	0.048045653
PTH1R	125.9664735	294.9267281	0.907649054	0.090617855
DNAH1	27.47585841	61.29955	0.912777312	0.064874934
SHFL	104.406783	248.8284125	0.9156212	0.096987631
SPECC1	79.52263555	181.0518148	0.922998904	0.09371826
RAPGEF3	291.905109	635.8710507	0.923148023	0.071025606

Supplemental Table 1

GENE NAME	Mean Normal	Mean MS-HF	Log$_2$ Fold Change	$p_{adj.}$
RIPOR3	114.8374036	279.4749406	0.934522947	0.094840527
PCDH17	60.97103853	137.5209022	0.939276072	0.096987631
ADAM33	96.56916343	221.5057343	0.947781438	0.084109489
MEGF6	49.82728313	117.0259046	0.950005376	0.066098423
EBF2	187.704059	461.4764646	0.958907612	0.094709077
ZNF83	215.3270762	460.3551205	0.962202428	0.047144934
ST8SIA6	182.0161304	432.830335	0.966550136	0.081436243
INMT	534.8716565	1268.537214	0.972930093	0.099762668
KCNMB4	99.39448121	217.8531353	0.974930186	0.032837328
N4BP2L1	91.79623408	218.4695544	0.976268387	0.088547364
ARHGAP25	81.55204949	197.4882093	0.989307072	0.097282814
CAMK2N1	295.6555596	715.5025882	0.997916615	0.065391499
ITGB3BP	49.93537912	120.4853709	0.999947241	0.090478602
FMO2	751.8221298	1727.48391	1.009727098	0.084612148
TSPAN15	132.9569811	325.643267	1.017314617	0.07048396
LDB2	468.860808	1090.286067	1.018373984	0.070598212
LSR	78.12584978	184.0941643	1.021874714	0.056397109
PREX2	170.17445	399.8006734	1.026919039	0.077455643
IRF1	164.3083149	396.4256351	1.039552409	0.056479414
RNF157	39.59621326	107.8499438	1.043085664	0.07562747
CACNA2D4	12.46212042	33.12164931	1.047576324	0.095358911
SAMD9L	97.64251083	266.3404114	1.05182542	0.066572791
ST8SIA4	84.18800232	202.601003	1.057137422	0.082514307
EGFLAM	137.9036142	358.7670443	1.058791276	0.062562716
NFASC	100.8670581	251.3971159	1.06106584	0.04434757
BMP4	144.4338205	357.3255499	1.069384476	0.063354739
EFHD1	295.0920181	708.1746394	1.071862694	0.071295415
APBB2	270.6987309	621.0064196	1.072645011	0.013232997
UBA7	122.0415503	295.6577485	1.074835772	0.047144934
TMEM273	187.9775298	463.7503815	1.075823242	0.04688464
RFX3	39.49602971	98.14485421	1.076199294	0.032837328
KIAA1671	173.0811915	420.1541688	1.081269769	0.042469311
DBP	50.94727698	125.6782075	1.084401606	0.048333582
KIF17	74.47208889	196.2781682	1.092566872	0.060205807
CYP4X1	40.65908563	104.4399611	1.093868665	0.06825084
LRRC37A3	15.49583554	39.70320871	1.094658899	0.056308192
TBX2	215.3503791	586.8308116	1.098394866	0.063649431
PLCE1	139.0198988	346.5381853	1.103298917	0.032761734
EBF3	190.3269493	460.3315814	1.103306216	0.057842855
PLCB1	89.35940772	220.840073	1.105803547	0.078910824
MYO15B	178.8337072	463.549426	1.108456666	0.031448766
ZNF790-AS1	26.40075807	66.58351543	1.109986661	0.036881699
LHX6	76.71020515	194.7164048	1.110139166	0.093404119
GCNT1	30.25537157	82.56921321	1.112534456	0.085234279
PARP14	282.2950243	692.1708202	1.114437958	0.047144934
SULT1C4	89.78382284	220.3171179	1.116657983	0.071380642

Supplemental Table 1

GENE NAME	Mean Normal	Mean MS-HF	Log$_2$ Fold Change	$p_{adj.}$
PAPLN	20.4568175	65.0947434	1.121731658	0.097282814
LINC00639	22.5505301	59.36444528	1.1223624	0.079108353
CYYR1	583.7804086	1428.088734	1.122864037	0.056397109
SP110	128.0105522	322.9026161	1.129697565	0.042805856
LBX2-AS1	24.92828538	67.88464953	1.130685079	0.071025606
CCDC88C	57.21848479	148.0057541	1.132668966	0.069571283
ANKRD65	37.5928981	111.0972935	1.136950729	0.079200633
GATA3	37.38336458	94.58342665	1.137203085	0.049070772
AQP1	2435.03419	6229.639595	1.137706409	0.034967285
FMO3	46.51457468	140.0977547	1.138292338	0.0700001
BTN2A2	33.83005342	93.05981495	1.140427416	0.096102607
N4BP2L2-IT2	17.76032883	50.39125281	1.14528159	0.065341975
PRTG	25.25288175	66.0133748	1.146760896	0.063649431
MTMR9LP	33.25224499	88.60234586	1.156457044	0.056397109
CASP10	104.0696897	264.8433031	1.158350114	0.029687972
LINC00924	31.35706532	72.85097666	1.16084894	0.075293451
NRGN	84.81886792	232.6633086	1.16172283	0.053930831
HERC5	35.32469494	99.8978399	1.161770076	0.047144934
BATF2	18.49185624	55.37322683	1.167192496	0.07562747
C14ORF132	31.33886082	90.40056575	1.168587294	0.078647436
HIGD1B	103.6617407	289.4501351	1.174299655	0.036881699
RNF152	142.6055957	372.1288571	1.179711415	0.02438467
LTC4S	31.69553902	87.20672941	1.18474571	0.083478317
OAS2	137.7065924	362.5034589	1.184820784	0.04255453
ITIH5	292.1156164	891.7571793	1.189388563	0.091243977
IFNAR2	12.1885044	36.13823229	1.190981697	0.064874934
LINC02587	56.76396477	153.685668	1.192036317	0.093143511
ODF3B	91.25695868	309.8984653	1.198371771	0.079108353
ADH1B	1404.076648	3451.080947	1.199458817	0.004887994
ANKRD29	62.9774075	170.6917348	1.200628647	0.048140756
INKA1	31.69470766	85.7978651	1.201418366	0.058383512
SEMA6A	125.9580754	320.9930002	1.204370949	0.031448766
PDE5A	118.0922924	314.1619819	1.208119231	0.065624252
SPATA13	166.1208326	418.0417451	1.210411592	0.019446787
CYSLTR2	110.3701016	409.2389877	1.213561582	0.071805095
NDUFA4L2	1256.206231	3162.760312	1.21963385	0.014000643
NLRC5	64.34355702	189.5742561	1.225859467	0.045687506
LINC00342	40.85143645	112.8784688	1.233058402	0.024195482
PNISR-AS1	17.25162074	48.99162657	1.23458157	0.053539591
IFIT3	150.0532017	417.1188883	1.240156323	0.045950623
SVEP1	173.0184274	487.7626421	1.241996402	0.044397464
ISYNA1	227.9431921	596.3074735	1.244488079	0.017047658
DACH1	58.58526323	158.0658588	1.246692146	0.057842855
KLF3-AS1	11.97621606	41.04179044	1.249196714	0.076406089
COX4I2	129.3898369	339.7828614	1.258219304	0.030689582
SNAI1	18.11580206	52.08440535	1.259163047	0.065624252

Supplemental Table 1

GENE NAME	Mean Normal	Mean MS-HF	Log$_2$ Fold Change	$p_{adj.}$
SOX7	129.4127007	359.4116026	1.260091754	0.073061504
ANKRD36C	10.36774918	31.63702564	1.263252966	0.04742159
BTN3A3	92.47928938	268.2892071	1.278212517	0.04402192
FAM111A	97.47891922	260.184246	1.279700211	0.009270321
NXPH3	42.89379412	135.4505915	1.281151055	0.089854095
MME	63.48067743	176.9967253	1.282475211	0.09237101
FXYD6	162.1453935	443.6262959	1.286973291	0.036881699
RAMP2	617.6569147	1706.158169	1.293489594	0.029859577
TMEM178A	22.61764654	80.10577541	1.296903146	0.036881699
KCNS3	57.68420031	162.3428428	1.302201576	0.046555663
SSUH2	18.84074565	61.16603206	1.310853785	0.065624252
HCG27	8.658826447	28.05527195	1.313271256	0.051613946
LFNG	50.48127741	142.7455963	1.313586999	0.054331552
IL15	25.06849286	68.18635212	1.316978072	0.030501266
HCP5	124.1932175	364.3115769	1.325885722	0.030689582
ANO1	102.7406607	286.8369095	1.328097028	0.038776196
NR2F2-AS1	8.908575052	32.07037936	1.328222856	0.062143604
PSMB9	148.0706196	437.1856782	1.330553842	0.033145664
DIO2	183.4844398	508.4922394	1.336148755	0.073061504
CYP4F12	19.94818846	59.53895134	1.338548419	0.017047658
CD74	2901.285189	11225.33936	1.349388215	0.063354739
MX2	113.2221268	327.7989971	1.354019364	0.013894872
ADAMTS10	49.20658569	142.1171307	1.35414942	0.04639176
MYO10	90.11194109	253.5917071	1.355243007	0.005245332
RYR3	6.064337956	22.45221384	1.360905211	0.071384606
BTN3A2	177.572035	508.5929847	1.362974612	0.008475632
PLEKHH2	15.52145428	47.94628106	1.364170842	0.079699437
NRN1	228.19331	648.7228314	1.367975886	0.039447618
ABCA9	343.0059459	989.4554021	1.368172415	0.013768087
OAS1	53.34239865	173.0450278	1.369432201	0.054331552
THBS4-AS1	22.26963102	66.15390697	1.37054159	0.048496356
LINC02981	8.391018915	26.33837267	1.371828646	0.063354739
HLA-F	196.0048444	589.5703369	1.372906755	0.030501266
P2RX3	27.9601212	91.94430241	1.37441582	0.076567232
SLC16A4-AS1	23.290998	68.64888646	1.382225635	0.024207997
DHX58	37.53887548	128.894514	1.388020914	0.043847556
TMC4	16.64464503	52.28535362	1.395850323	0.036080322
FOXS1	25.4068671	106.1039386	1.399857496	0.069571283
HERC2P2	183.7694678	568.9697477	1.401021443	0.035447926
TSPAN7	192.5338781	561.9492778	1.401024551	0.043847556
TNFSF10	353.4174261	1049.224155	1.403965444	0.024195482
CXCL2	66.06655966	224.221648	1.411638703	0.085234279
IFI44	131.1684095	380.2375366	1.413556675	0.024619399
HLA-DPB1	407.2204784	1231.009601	1.418352007	0.024195482
HLA-L	8.964565841	29.47630055	1.42535399	0.068537798

Supplemental Table 1

GENE NAME	Mean Normal	Mean MS-HF	Log$_2$ Fold Change	$p_{adj.}$
CXCL14	49.24348297	195.1668837	1.430811894	0.059207184
LPAR6	269.4322123	798.2103904	1.435747456	0.023382023
ACCS	27.86555907	102.9517425	1.441654387	0.024195482
DSCAML1	6.08962725	25.96226352	1.447399797	0.059699044
CPE	472.5422237	1531.668889	1.455042558	0.065523062
RGS5	5186.516817	19338.16698	1.458645851	0.071295415
LETR1	23.81432938	79.51573515	1.461083351	0.048235267
PRELID2	32.49168872	101.8534182	1.464492061	0.004887994
WEE2-AS1	8.852739837	27.98606712	1.465706766	0.049030407
GRASLND	3.968668592	15.96759428	1.46638546	0.084792299
REEP2	46.2429776	144.6959137	1.470167915	0.034298897
PZP	9.102823197	32.03232282	1.47113896	0.052494244
BTN3A1	92.42186395	335.8531611	1.472133335	0.032483039
ABCA10	79.99066678	249.1798255	1.473178818	0.043141559
NOTCH3	360.1481249	1206.970866	1.478091248	0.00820866
OAS3	134.9814683	431.3254201	1.478432436	0.014000643
GBP2	297.9007485	888.3109371	1.484955425	0.004887994
ARHGEF28	24.62708949	80.00219841	1.496634224	0.010283302
RGS16	27.5511096	84.36321094	1.498609589	0.079371913
CMPK2	54.31755572	167.7170119	1.500643053	0.015620339
ATP1B2	56.12280587	195.6026092	1.513132464	0.016300841
BAALC	24.65303913	74.98517998	1.51478392	0.085234279
CLEC2D	40.29682977	127.1574684	1.51802607	0.00416325
STUM	21.03206357	72.79980328	1.520125485	0.004887994
LY75	4.827233241	18.75577131	1.520293102	0.077455643
SLITRK4	13.8490262	43.52206079	1.521658558	0.084109489
LOXHD1	3.444915965	14.70451151	1.527874682	0.09237101
FABP5P9	5.204902899	21.51676643	1.532423499	0.084612148
CASC15	8.954837875	34.67915266	1.560270487	0.036003618
CDH24	18.19725676	61.31643894	1.564035305	0.064532913
C11ORF80	8.195617264	31.13759704	1.565378433	0.057842855
PSMB8-AS1	25.20050283	80.63712121	1.567216556	0.032095321
C1QTNF3	5.924268043	23.97118348	1.568862011	0.070773412
COL11A2	13.62226262	48.73121949	1.570517043	0.043847556
CA4	184.7801991	599.5362054	1.578665597	0.057842855
SNTB1	57.7074584	195.529583	1.591510879	0.030689582
IRAG2	13.88141087	48.78273246	1.59731884	0.039958292
YPEL4	5.103868493	21.33680343	1.600589321	0.036080322
HLA-DMB	48.36455548	176.5946549	1.603428545	0.027906834
KLKB1	13.30811226	56.30160457	1.621268458	0.056308192
GBP1	102.1248642	341.9169364	1.629293737	0.017449445
ISM1	18.79112708	63.54623055	1.632218269	0.060042843
LINC00910	6.440864899	28.89447496	1.645152415	0.017047658
MX1	141.1444321	493.1462494	1.64902247	0.001032011
C5ORF38	8.103726127	48.1359466	1.656487187	0.063649431
GBP1P1	16.44313147	61.35084649	1.65783545	0.045687506

Supplemental Table 1

GENE NAME	Mean Normal	Mean MS-HF	Log$_2$ Fold Change	$p_{adj.}$
HSH2D	1.984712243	11.49078585	1.668968221	0.091944819
LINC01359	3.291911469	15.86137782	1.677664459	0.081436243
FOXL1	8.992372547	36.25870853	1.680346416	0.014897157
GBP4	203.5926212	694.4624232	1.684945258	0.001608573
UPB1	10.14001318	44.53491671	1.685773397	0.017047658
SV2B	21.93192563	84.66410321	1.690431885	0.036080322
OR2S1P	3.291620549	7.86003141	1.694839058	0.085234279
GABBR2	12.32945188	46.30553791	1.704903612	0.060775733
ISG15	127.7305869	488.0696175	1.707056001	0.004887994
OTULIN-DT	2.863775534	14.40906991	1.722780063	0.082514307
RSAD2	49.05431617	241.3322199	1.728867173	0.042805856
ADGRB3-DT	12.29449076	46.29647893	1.756485148	0.006178436
TBX2-AS1	14.44637149	65.20252311	1.774704629	0.030647608
MPIG6B	4.546912206	22.0210782	1.774937833	0.049030407
TRIM72	8.566045883	30.84068612	1.78588203	0.077487311
CARMN	75.78734766	286.2666023	1.792913032	1.27E-05
ARHGAP28	10.38536627	41.69619906	1.797562748	0.005643304
NEK5	5.451640368	24.76079704	1.804194468	0.015828057
GVINP1	22.53446163	87.06824925	1.852544209	0.004887994
TRBC2	9.517851567	40.24735535	1.865062891	0.001091323
HLA-DQA1	59.31357924	382.5979284	1.871881244	0.032837328
TFPI2	16.04471326	63.44940579	1.875231768	0.063649431
CXCL1	8.06575313	34.49178337	1.911764224	0.030991774
SLC26A4	5.36556762	20.83703424	1.936576153	0.039881883
SFTPD-AS1	3.858683049	16.96686298	1.954087004	0.061077887
NHLRC4	3.38104462	16.46550675	1.968760011	0.069571283
IFI44L	134.6564748	681.8390783	1.969804291	0.00820866
SGIP1	33.05082142	151.5855871	1.971782069	0.005245332
PRRG3	11.09430828	44.57090788	1.977092411	0.010283302
CCDC188	1.723857656	10.18043918	1.988128188	0.071025606
TDGF1	4.276765791	21.68042584	1.998093699	0.060004463
CD247	6.003176435	25.19848769	2.015691406	0.030501266
STRIT1	7.781093971	31.88824047	2.030772573	0.071025606
TRBC1	2.566941449	13.39227387	2.078007772	0.047144934
CD69	1.231010259	16.43417039	2.104361741	0.053320609
KCNA3	3.596933935	17.16717164	2.106544795	0.040424026
IL34	14.80736786	66.47855914	2.109688006	0.013232997
EPSTI1	38.47710952	177.1511963	2.129692538	0.000454675
BISPR	6.179235277	30.62589844	2.149866077	0.009852628
LRRC77P	24.01184376	131.3544005	2.168139175	0.017047658
STEAP1B-AS1	1.672314097	11.46165268	2.218619556	0.056397109
CXCL10	1.779526954	27.8587869	2.301693971	0.071053125
HLA-DOB	0.54036256	8.277810122	2.313881985	0.082514307
DEFB1	0.517613809	10.656997	2.344804381	0.082514307
HLA-DQB1	76.68362795	550.2596839	2.348878726	0.000622307

Supplemental Table 1

GENE NAME	Mean Normal	Mean MS-HF	Log$_2$ Fold Change	$p_{adj.}$
PLCG2	3.756422142	24.31229288	2.415757321	0.004887994
SLC6A1	8.518682819	62.96882999	2.442640993	0.00416325
KCNA5	23.82225375	106.025718	2.47996752	0.030501266
SLED1	1.689540392	9.284493326	2.604342288	0.066572791
LINC00517	0.672636259	10.4614293	2.623766063	0.061077887
ESM1	0.342363141	14.47519483	2.635564608	0.064874934
SLC1A7	1.430568153	29.18518041	2.646167317	0.017047658
CD79A	0.478951145	7.311227832	2.660118142	0.08023968
SELE	19.1441452	144.3732939	2.670220849	0.022531502
TNF	2.307636996	15.19069543	2.678973752	0.034967285
ACE	33.87437117	216.1607268	2.695911195	0.00018995
OLR1	0.54045518	9.69998215	2.697126845	0.080903273
FZD10-AS1	2.180509127	21.05502757	2.770628154	0.007744334
IDO1	1.405829699	32.32355593	2.822120725	0.00416325
ST8SIA6-AS1	1.723857656	15.69823055	2.867186878	0.010518032
IRX2	8.322845695	61.01175325	2.881881576	0.001091323
EGR3	9.848549403	67.55415086	2.914367248	0.016200664
RNU5B-1	3.709836693	23.37768261	3.010159942	0.024783935
OASL	2.892355307	29.06570249	3.024489292	0.000454675
C1QTNF9	15.25662573	145.2154224	3.136767602	0.000178584
SFRP2	0.458798231	10.41831431	3.164425434	0.043847556
IL6	10.6448174	78.33685025	3.334006151	0.00887128
IRX1	1.739039089	17.17091992	3.339468733	0.013370976
H1-4	2.784648611	16.70417317	3.440504788	0.030742923
CXCL11	1.056190651	12.75586475	3.521500022	0.017672803
CXCL9	5.259860243	73.19247861	3.625282462	0.000851051
NPIPB15	2.166149529	66.98831529	3.651884578	7.53E-05
GZMH	1.129900896	24.3615542	4.556876542	0.000178584
DDX3Y	0.492556204	46.63305371	6.667011606	0.00820866
USP9Y	0.569162943	49.83610998	6.943139869	0.00416325
RPS4Y1	0.395695188	96.53654956	9.45945841	0.00133451

Supplemental Table 1: RNA sequencing analyses of the gene profiles in human hearts.
RNA sequencing on human hearts from patients diagnosed with metabolic syndrome along with various cardiovascular complications such as ischemic cardiomyopathy, atrial fibrillation, coronary artery disease or congestive HF. Of 56,000 analyzed transcripts, 488 genes were differentially expressed in the metabolic stress-associated hearts compared to normal hearts, selected with an adjusted p_{adj} value less than 0.1 (n=3 human normal hearts, 5 human MS-HF hearts).

Supplemental Table 2

	Chow		HFD+L-NAME	
4 weeks	**AAV9-(CMV)*Gfp***	**AAV9-*shEdem2***	**AAV9-(CMV)*Gfp***	**AAV9-*shEdem2***
FS (%)	37.79±0.28	36.82±0.45	42.01±1.81	34.06±0.96*
EF (%)	75.92±0.32	74.76±0.54	80.27±1.85	71.19±1.23*
dLVID (mm)	3.91±0.14	3.90±0.03	4.00±0.09	3.92±0.09
sLVID (mm)	2.43±0.09	2.46±0.03	2.32±0.09	2.59±0.09
dIVS (mm)	0.83±0.04	0.80±0.05	0.75±0.04	0.76±0.03
sIVS (mm)	1.11±0.05	1.08±0.06	1.06±0.04	1.01±0.04
dPW (mm)	0.69±0.05	0.75±0.04	0.76±0.03	0.80±0.01
sPW (mm)	0.95±0.05	1.01±0.05	1.06±0.04	1.01±0.02
IVRT (ms)	8.40±0.24	8.80±0.37	12.33±0.33†	15.38±0.53†*
E/A	1.35±0.10	1.25±0.04	1.60±0.09	1.79±0.18
dBP (mmHg)	78.80±4.20	86.90±8.90	137.13±6.48†	131.29±7.04†
sBP (mmHg)	116.40±18.00	116.60±10.80	170.87±8.03†	163.19±6.36†
HR (bpm)	493.00±4.81	513.60±15.63	426.60±26.58	420.70±16.68
8 weeks	**AAV9-(CMV)*Gfp***	**AAV9-*shEdem2***	**AAV9-(CMV)*Gfp***	**AAV9-*shEdem2***
FS (%)	38.34±1.03	38.94±0.22	37.05±0.89	27.23±1.33†*
EF (%)	76.48±1.16	77.23±0.25	75.00±1.07	61.15±2.11†*
dLVID (mm)	3.94±0.10	3.93±0.08	4.13±0.08	4.11±0.07
sLVID (mm)	2.43±0.06	2.40±0.05	2.60±0.06	2.99±0.06†*
dIVS (mm)	0.79±0.06	0.82±0.02	0.80±0.03	0.76±0.02
sIVS (mm)	1.11±0.08	1.04±0.03	1.07±0.03	0.96±0.02
dPW (mm)	0.68±0.06	0.70±0.03	0.75±0.02	0.78±0.02
sPW (mm)	0.98±0.09	0.96±0.07	0.94±0.04	0.98±0.03
IVRT (ms)	8.80±0.58	9.40±0.60	14.20±0.37†	19.00±1.04†*
E/A	1.42±0.07	1.42±0.07	1.60±0.13	2.21±0.10*
dBP (mmHg)	67.20±3.40	45.20±1.40	122.87±9.39†	106.52±9.01†
sBP (mmHg)	94.40±3.40	75.20±2.20	150.33±9.93†	138.04±8.70†
HR (bpm)	444.60±20.99	475.40±9.08	408.60±11.02	392.20±17.05
HW (mg)/TL (mm)	5.92±0.40	7.01±0.25	7.92±0.10†	8.85±0.2†*
LW (mg)/TL (mm)	7.00±0.45	7.43±0.36	9.34±0.21†	13.49±0.79†*

Supplemental Table 2. Echocardiographic assessments of the mice with EDEM2 knockdown after 8 weeks of HFD+L-NAME stress

Fractional shortening (FS%), ejection fraction (EF%), end-diastolic left ventricular internal diameter (dLVID), end-systolic left ventricular internal diameter (sLVID), end-diastolic interventricular septum thickness (dIVS), end-systolic interventricular septum thickness (sIVS), end-diastolic left ventricular posterior wall thickness (dPW), end-systolic left ventricular posterior wall thickness (sPW), isovolumic relaxation time (IVRT), diastolic blood pressure (dBP), systolic blood pressure (sBP), heart rate (HR), ratio of heart weight to tibia length (HW/TL), and ratio of lung weight to tibia length (LW/TL). †*p*<0.05 vs chow diet; **p*<0.05 vs AAV9-(CMV)*Gfp* injection followed by stress (n=5, 5, 7, 9 mice in each group, respectively). Data are presented as mean ± S.E.M. *p* values were calculated using a Two-way ANOVA with Šidák post-hoc tests.

Supplemental Table 3

4 weeks post-treatment	HFD+L-NAME							
	AAV9-(CMV)*Gfp*				AAV9-*shEdem2*			
	Untreated	Alda-1	SR-4995	Oxytocin	Untreated	Alda-1	SR-4995	Oxytocin
FS (%)	38.33±1.27	47.70±0.93	42.15±0.48	43.44±1.87	19.05±4.28*	35.54±2.33†	23.53±1.39	35.63±1.12†
EF (%)	76.48±1.47	85.67±0.78	80.63±0.49	81.79±1.74	46.09±8.03*	72.91±0.2.89†	55.20±2.40	73.28±1.37†
dLVID (mm)	3.98±0.09	3.98±0.02	4.16±0.04	4.09±0.08	4.75±0.11*	4.15±0.17†	4.57±0.06	4.11±0.07†
sLVID (mm)	2.46±0.10	2.08±0.05	2.41±0.03	2.31±0.09	3.85±0.28*	2.69±0.19†	3.51±0.07	2.64±0.06†
dIVS (mm)	0.77±0.03	0.78±0.03	0.81±0.01	0.80±0.03	0.74±0.01	0.73±0.03	0.73±0.02	0.75±0.00
sIVS (mm)	1.08±0.03	1.01±0.05	0.98±0.02	0.97±0.02	0.90±0.04	0.96±0.05	0.99±0.05	1.03±0.01
dPW (mm)	0.78±0.01	0.69±0.01†	0.75±0.01	0.67±0.02†	0.84±0.03	0.67±0.03†	0.80±0.05	0.71±0.03†
sPW (mm)	0.99±0.03	0.99±0.03	1.05±0.04	0.97±0.03	1.05±0.04	0.93±0.03	0.97±0.02	1.01±0.09
IVRT (ms)	14.67±0.33	11.33±0.33†	14.67±0.33	11.67±0.33†	19.33±0.67*	12.50±0.65†	21.00±1.00	12.33±0.88†
E/A	1.76±0.09	1.32±0.08†	1.74±0.02	1.37±0.03†	2.15±0.23	1.43±0.03†	2.36±0.40	1.33±0.02†
HR (bpm)	400.70±5.21	447.67±8.74	410.33±5.49	424.67±17.81	413.00±9.87	431.5±22.88	387.00±6.25	402.30±16.22

Supplemental Table 3. Echocardiographic assessments on EDEM2 knockdown mice following drugs treatment
Fractional shortening (FS%), ejection fraction (EF%), end-diastolic left ventricular internal diameter (dLVID), end-systolic left ventricular internal diameter (sLVID), end-diastolic interventricular septum thickness (dIVS), end-systolic interventricular septum thickness (sIVS), end-diastolic left ventricular posterior wall thickness (dPW), end-systolic left ventricular posterior wall thickness (sPW), isovolumic relaxation time (IVRT), and heart rate (HR). *$p<0.05$ vs AAV9-*Gfp* injection untreated group; $^\dagger p<0.05$ vs untreated group (n=3-4 mice). Data are presented as mean ± S.E.M. *p* values were calculated using a Two-way ANOVA with Šidák post-hoc tests.

Supplemental Table 4

|	Chow		HFD+L-NAME	
4 weeks	**AAV9-*Gfp***	**AAV9-*EDEM2***	**AAV9-*Gfp***	**AAV9-*EDEM2***
FS (%)	44.44±2.81	38.29±2.19	37.55±1.76	36.22±1.12
EF (%)	82.31±2.71	76.15±2.36	75.30±2.05	73.74±1.37
dLVID (mm)	4.44±0.14	4.49±0.11	4.16±0.10	4.14±0.05
sLVID (mm)	2.47±0.18	2.78±0.15	2.60±0.09	2.64±0.06
dIVS (mm)	0.72±0.01	0.76±0.02	0.71±0.02	0.76±0.03
sIVS (mm)	1.01±0.04	0.98±0.03	1.01±0.03	0.98±0.03
dPW (mm)	0.66±0.02	0.66±0.02	0.75±0.02†	0.78±0.02
sPW (mm)	0.88±0.04	0.85±0.02	1.01±0.03	1.02±0.03
IVRT (ms)	10.0±0.84	9.40±0.51	14.00±1.03†	15.07±0.96
E/A	1.52±0.06	1.44±0.10	1.65±0.08	1.70±0.10
HR (bpm)	428±19.43	409.8±9.29	442.3±17.68	421.6±13.24
8 weeks	**AAV9-*Gfp***	**AAV9-*EDEM2***	**AAV9-*Gfp***	**AAV9-*EDEM2***
FS (%)	35.16±1.50	38.05±1.68	36.87±2.06	37.73±0.73
EF (%)	72.57±1.88	76.02±1.93	74.35±2.45	75.72±0.88
dLVID (mm)	4.36±0.10	4.30±0.07	4.01±0.12	4.03±0.06
sLVID (mm)	2.83±0.11	2.66±0.05	2.54±0.14	2.51±0.05
dIVS (mm)	0.73±0.03	0.68±0.04	0.75±0.02	0.74±0.03
sIVS (mm)	1.01±0.01	0.94±0.05	1.06±0.04	0.98±0.02
dPW (mm)	0.65±0.02	0.64±0.02	0.84±0.04†	0.71±0.02*
sPW (mm)	0.91±0.02	0.88±0.03	1.11±0.06†	0.93±0.03*
IVRT (ms)	8.80±0.66	8.40±0.51	16.29±1.17†	10.71±0.53*
E/A	1.45±0.04	1.41±0.11	1.82±0.11	1.38±0.07*
HR (bpm)	444.80±6.41	444.80±14.76	438.90±17.15	452.7±14.26
HW (mg)/TL (mm)	5.23±0.05	6.18±0.18	8.18±0.34†	6.38±0.07
LW (mg)/TL (mm)	6.83±0.34	7.50±0.38	9.23±0.32†	7.32±0.38
12 weeks	**AAV9-*Gfp***	**AAV9-*EDEM2***	**AAV9-*Gfp***	**AAV9-*EDEM2***
FS (%)	39.55±1.39	43.28±1.87	38.74±1.19	39.69±1.04
EF (%)	77.77±1.54	81.52±1.83	76.85±1.40	77.83±1.21
dLVID (mm)	4.21±0.08	4.18±0.10	4.07±0.05	4.13±0.05
sLVID (mm)	2.55±0.08	2.38±0.14	2.49±0.03	2.49±0.06
dIVS (mm)	0.81±0.06	0.67±0.03	0.81±0.03	0.74±0.02
sIVS (mm)	0.97±0.04	0.99±0.04	1.04±0.04	0.99±0.04
dPW (mm)	0.68±0.02	0.66±0.02	0.89±0.03†	0.74±0.02*

|				
sPW (mm)	0.90±0.04	0.93±0.04	1.24±0.07†	1.0±0.02*
IVRT (ms)	8.40±0.24	8.00±0.32	16.43±0.65†	11.54±0.50*
E/A	1.47±0.09	1.42±0.04	2.03±0.09†	1.51±0.06*
dBP (mmHg)	71.00±5.35	77.73±1.00	147.20±12.06†	132.33±7.91†
sBP (mmHg)	103.93±5.62	107.90±3.31	176.65±11.80†	168.90±4.63†
HR (bpm)	488.4±17.63	467.8±22.23	499.1±11.43	460.0±5.07
HW (mg)/TL (mm)	7.07±0.16	7.25±0.21	8.98±0.20†	7.64±0.18
LW (mg)/TL (mm)	7.61±0.20	8.48±0.15	12.38±0.34†	8.50±0.24

Supplemental Table 4. Echocardiographic assessments on the mice with cardiac EDEM2 overexpression following HFD+L-NAME stress
Fractional shortening (FS%), ejection fraction (EF%), end-diastolic left ventricular internal diameter (dLVID), end-systolic left ventricular internal diameter (sLVID), end-diastolic interventricular septum thickness (dIVS), end-systolic interventricular septum thickness (sIVS), end-diastolic left ventricular posterior wall thickness (dPW), end-systolic left ventricular posterior wall thickness (sPW), isovolumic relaxation time (IVRT), diastolic blood pressure (dBP), systolic blood pressure (sBP), heart rate (HR), ratio of heart weight to tibia length (HW/TL), and ratio of lung weight to tibia length (LW/TL). $^†p<0.05$ vs chow diet; *$p<0.05$ vs AAV9-*Gfp* injection followed by stress (n=5, 5, 7, 14 mice in each group, respectively). Data are presented as mean ± S.E.M. *p* values were calculated using a Two-way ANOVA with Šidák post-hoc tests.

Supplemental Table 5

	Chow		HFD+L-NAME		
4 weeks	**AAV9-(CMV)***Gfp*	**AAV9-***shXbp1*	**AAV9-(CMV)***Gfp*	**AAV9-***shXbp1*	**AAV9-***shXbp1+Edem2*
FS (%)	41.66±1.63	40.30±1.94	42.06±2.94	34.44±2.52[†*]	41.33±2.67[#]
EF (%)	80.10±1.66	78.68±2.11	80.43±2.93	71.74±2.90[†*]	79.70±2.81[#]
dLVID (mm)	4.05±0.06	3.98±0.04	4.02±0.0.22	4.04±0.04	3.99±0.06
sLVID (mm)	2.36±0.05	2.38±0.10	2.33±0.24	2.65±0.10*	2.34±0.14[#]
dIVS (mm)	0.69±0.01	0.71±0.04	0.77±0.05[†]	0.84±0.07[†]	0.75±0.03[#]
sIVS (mm)	0.87±0.04	0.93±0.03	1.06±0.06[†]	1.06±0.04[†]	0.96±0.05[#]
dPW (mm)	0.61±0.02	0.61±0.02	0.73±0.02[†]	0.79±0.03[†]	0.71±0.03[#]
sPW (mm)	0.92±0.04	0.95±0.04	1.14±0.09[†]	1.07±0.07[†]	0.94±0.06[#]
IVRT (ms)	9.25±0.96	9.33±0.58	13.80±0.84[†]	16.83±1.47[†*]	12.83±1.17[#]
E/A	1.25±0.07	1.36±0.03	1.81±0.11[†]	1.99±0.15[†]	1.41±0.20[#]
HR (bpm)	447.00±18.51	423.33±5.86	423.40±15.90	430.67±28.19	414.83±17.97
8 weeks	**AAV9-(CMV)***Gfp*	**AAV9-***shXbp1*	**AAV9-(CMV)***Gfp*	**AAV9-***shXbp1*	**AAV9-***shXbp1+Edem2*
FS (%)	42.74±2.59	41.07±2.06	39.85±3.09	33.45±1.52[†*]	41.27±3.00[#]
EF (%)	81.14±2.60	79.48±2.12	78.10±3.40	70.48±2.04[†*]	79.61±3.21[#]
dLVID (mm)	3.96±0.23	4.07±0.05	4.13±0.20	4.70±0.20[†*]	4.14±0.10[#]
sLVID (mm)	2.27±0.23	2.40±0.09	2.49±0.20	3.13±0.21[†*]	2.43±0.14[#]
dIVS (mm)	0.80±0.03	0.76±0.03	0.84±0.02	0.90±0.05[†]	0.78±0.04[#]
sIVS (mm)	1.00±0.03	0.93±0.03	1.06±0.07	1.21±0.14[†]	1.01±0.05[#]
dPW (mm)	0.60±0.031	0.60±0.01	0.80±0.06[†]	0.91±0.03[†*]	0.70±0.02[#]
sPW (mm)	0.98±0.07	0.90±0.06	1.09±0.13[†]	1.13±0.05[†]	1.02±0.06
IVRT (ms)	9.00±0.82	9.33±0.58	15.20±1.30[†]	19.33±1.75[†*]	12.67±1.21[#]
E/A	1.37±0.24	1.34±0.09	1.81±0.24[†]	2.05±0.16[†]	1.49±0.09[#]
HR (bpm)	460.25±26.90	422.67±10.07	457.20±26.63	450.00±32.63	438.83±32.64
HW (mg)/TL (mm)	6.57±0.08	6.80±0.38	8.15±0.18[†]	9.41±0.23[†*]	6.81±0.16[#]
LW (mg)/TL (mm)	7.68±0.27	7.18±0.40	9.32±0.25[†]	10.81±0.12[†*]	7.67±0.26[#]

Supplemental Table 5. Echocardiographic assessments on mice with XBP1s knockdown in the presence and absence of cardiac EDEM2 overexpression after feeding of HFD+L-NAME
Fractional shortening (FS%), ejection fraction (EF%), end-diastolic left ventricular internal diameter (dLVID), end-systolic left ventricular internal diameter (sLVID), end-diastolic interventricular septum thickness (dIVS), end-systolic interventricular septum thickness (sIVS), end-diastolic left ventricular posterior wall thickness (dPW), end-systolic left ventricular posterior wall thickness (sPW), isovolumic relaxation time (IVRT), heart rate (HR), ratio of heart weight to tibia length (HW/TL), and ratio of lung weight to tibia length (LW/TL). [†]$p<0.05$ vs chow diet; *$p<0.05$ vs AAV9-(CMV)*Gfp* injection followed by stress; [#]$p<0.05$ vs AAV9-*shXbp1* (n=4, 3, 5, 6, 6 mice in each group, respectively). Data are presented as mean ± S.E.M. *p* values were calculated using a Two-way ANOVA with Šidák post-hoc tests.

Supplemental Table 6

	Chow		HFD+L-NAME	
4 weeks	**AAV9-*Gfp***	**AAV9-*XBP1s***	**AAV9-*Gfp***	**AAV9-*XBP1s***
FS (%)	44.61±1.64	44.36±1.81	40.51±3.77	39.11±4.21
EF (%)	82.97±1.51	82.73±1.67	78.74±3.94	77.14±4.49
dLVID (mm)	3.96±0.14	4.01±0.10	4.16±0.24	4.11±0.37
sLVID (mm)	2.20±0.13	2.23±0.10	2.48±0.27	2.51±0.31
dIVS (mm)	0.73±0.03	0.72±0.05	0.78±0.04	0.76±0.05
sIVS (mm)	0.91±0.07	0.99±0.05	1.04±0.07†	1.00±0.07
dPW (mm)	0.59±0.04	0.61±0.03	0.73±0.02†	0.76±0.03
sPW (mm)	0.88±0.10	0.96±0.05	1.05±0.09†	1.11±0.11
IVRT (ms)	9.60±0.55	9.25±0.96	15.00±0.89†	14.20±1.48
E/A	1.41±0.20	1.24±0.09	1.86±0.13†	1.75±0.32
HR (bpm)	433.80±25.45	487.75±13.57	447.33±33.06	455.00±36.49
8 weeks	**AAV9-*Gfp***	**AAV9-*XBP1s***	**AAV9-*Gfp***	**AAV9-*XBP1s***
FS (%)	41.74±3.95	41.66±2.20	37.33±0.89	42.63±3.31
EF (%)	80.01±4.06	80.08±2.18	75.20±4.11	80.95±3.24
dLVID (mm)	4.08±0.28	4.18±0.13	4.18±0.33	4.03±0.29
sLVID (mm)	2.38±0.28	2.44±0.16	2.62±0.19	2.31±0.23*
dIVS (mm)	0.80±0.04	0.78±0.03	0.81±0.05	0.72±0.08*
sIVS (mm)	0.98±0.06	1.05±0.05	1.06±0.10	0.96±0.11
dPW (mm)	0.62±0.03	0.62±0.03	0.86±0.04†	0.66±0.08*
sPW (mm)	1.00±0.07	1.00±0.07	1.19±0.07†	0.92±0.08*
IVRT (ms)	10.20±0.84	9.50±0.58	16.17±0.75†	11.25±1.17*
E/A	1.45±0.24	1.32±0.06	1.93±0.19†	1.35±0.09*
HR (bpm)	447.40±30.94	434.25±27.73	466.00±33.11	462.13±26.43
HW (mg)/TL (mm)	5.85±0.30	6.47±0.08	7.84±0.37†	7.10±0.30
LW (mg)/TL (mm)	7.68±0.11	7.71±0.05	9.96±1.07†	7.65±0.16*

Supplemental Table 6. Echocardiographic assessments of the mice with cardiac XBP1s overexpression following HFD+L-NAME stress
Fractional shortening (FS%), ejection fraction (EF%), end-diastolic left ventricular internal diameter (dLVID), end-systolic left ventricular internal diameter (sLVID), end-diastolic interventricular septum thickness (dIVS), end-systolic interventricular septum thickness (sIVS), end-diastolic left ventricular posterior wall thickness (dPW), end-systolic left ventricular posterior wall thickness (sPW), isovolumic relaxation time (IVRT), heart rate (HR), ratio of heart weight to tibia length (HW/TL), and ratio of lung weight to tibia length (LW/TL). †$p<0.05$ vs chow diet; *$p<0.05$ vs AAV9-*Gfp* injection followed by stress (n=5, 5, 6, 8 mice in each group, respectively). Data are presented as mean ± S.E.M. *p* values were calculated using a Two-way ANOVA with Šidák post-hoc tests.

A

B

C

GO cellular component pathway enrichment dotplot

D

GO biological process pathway enrichment dotplot

E

Reactome pathway enrichment dotplot

F

KEGG pathway enrichment dotplot

G

GO cellular component pathway enrichment dotplot

H

GO biological process pathway enrichment dotplot
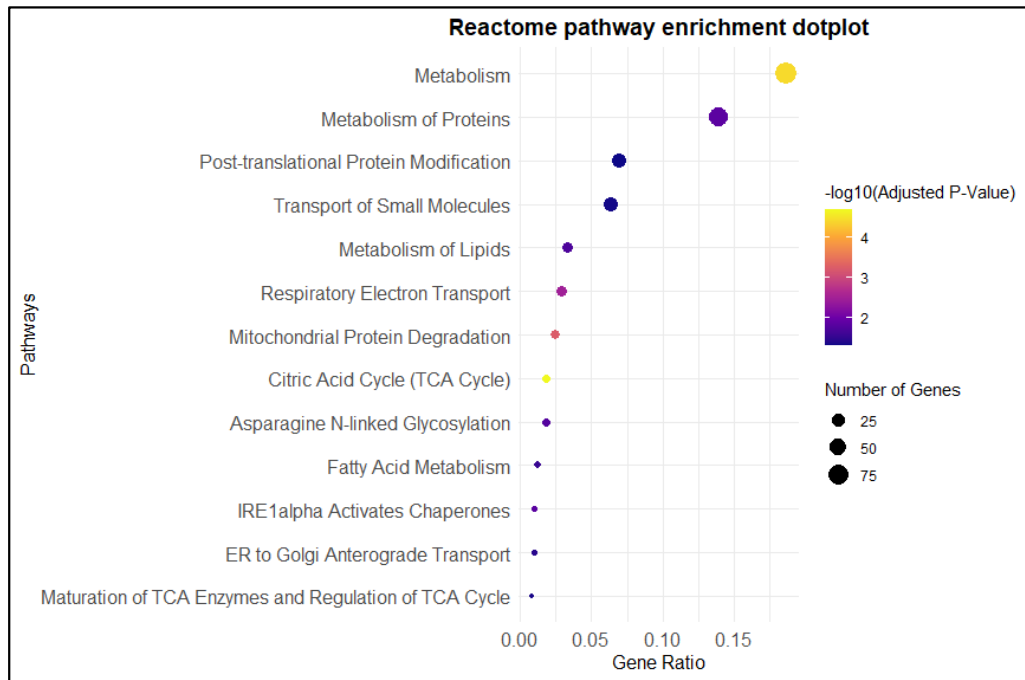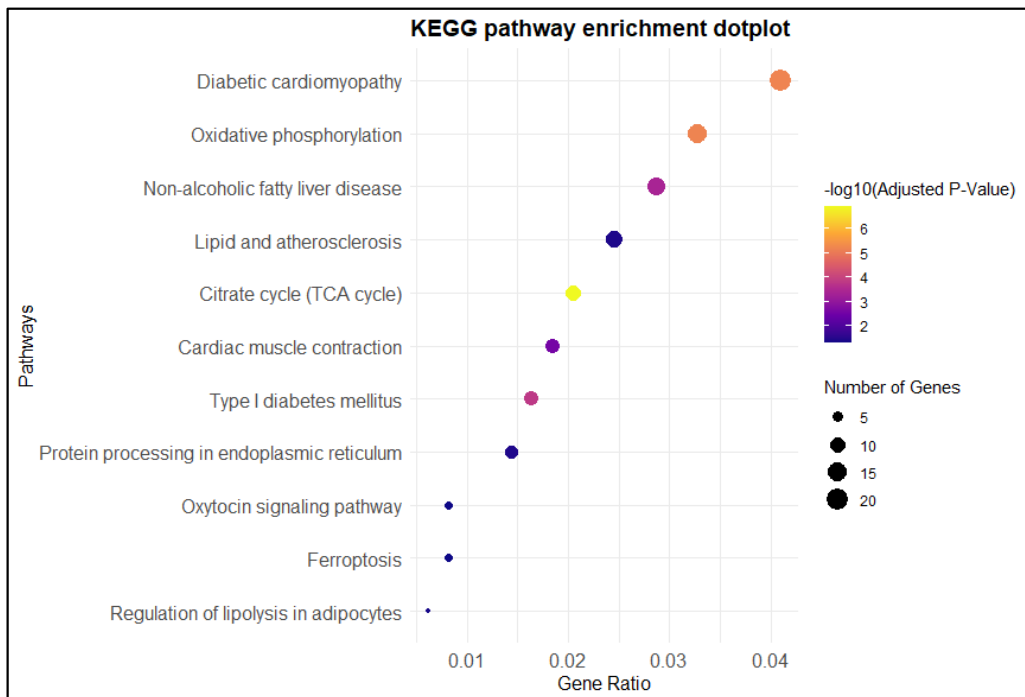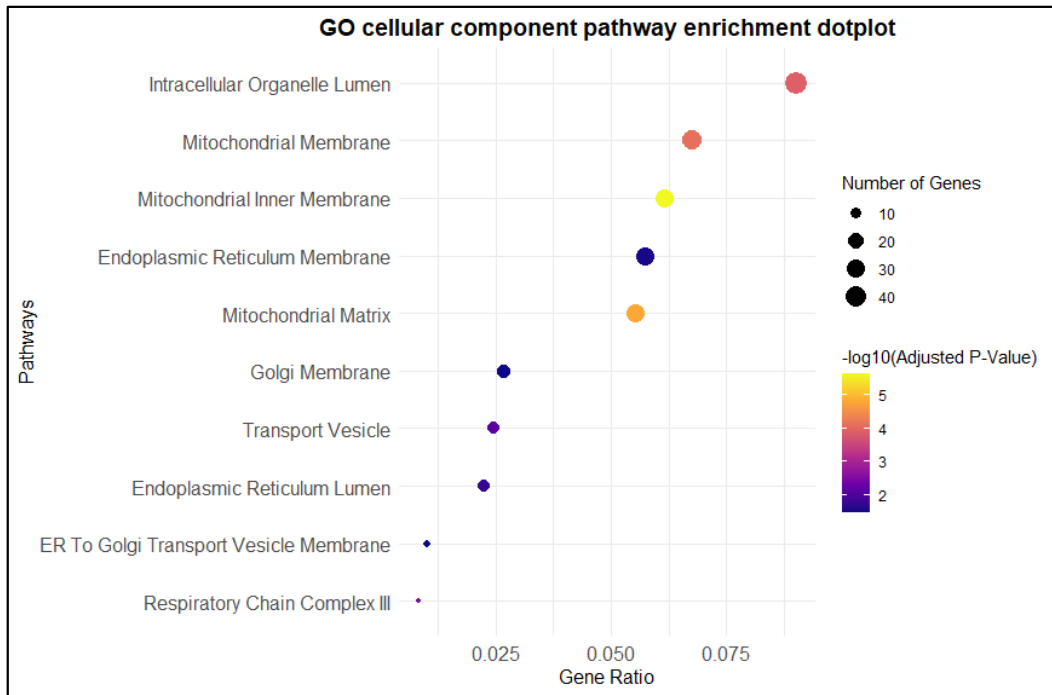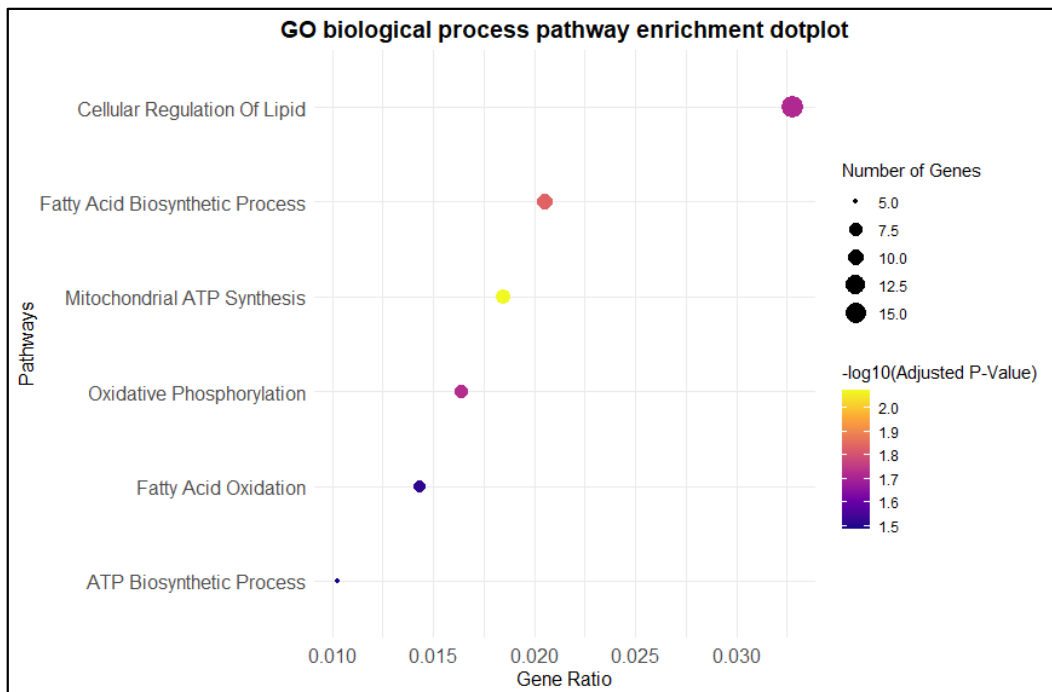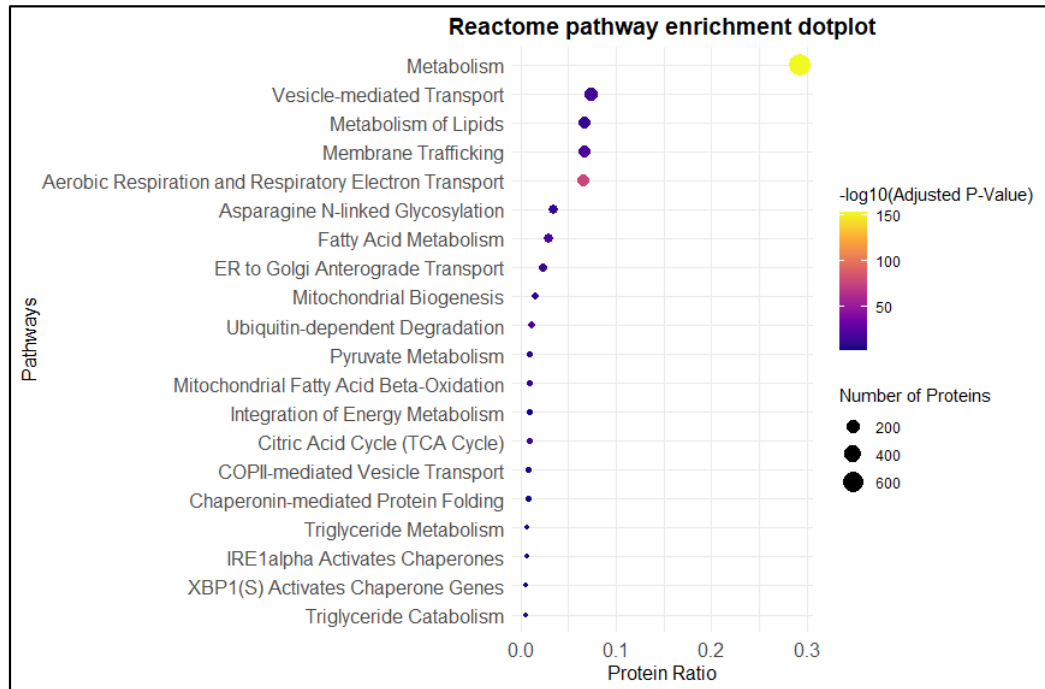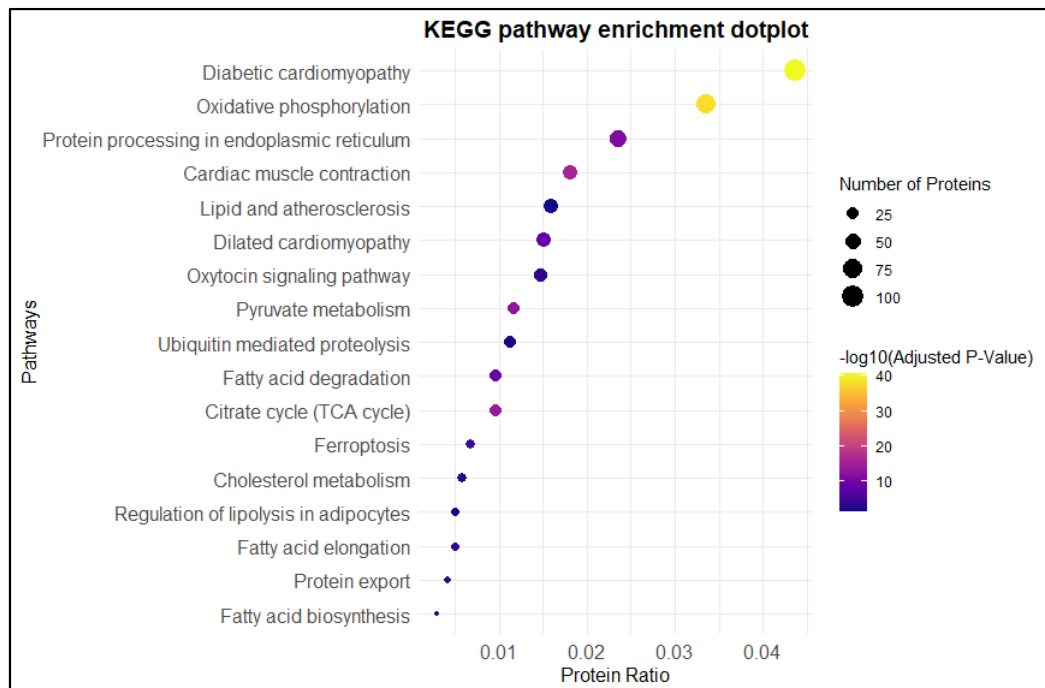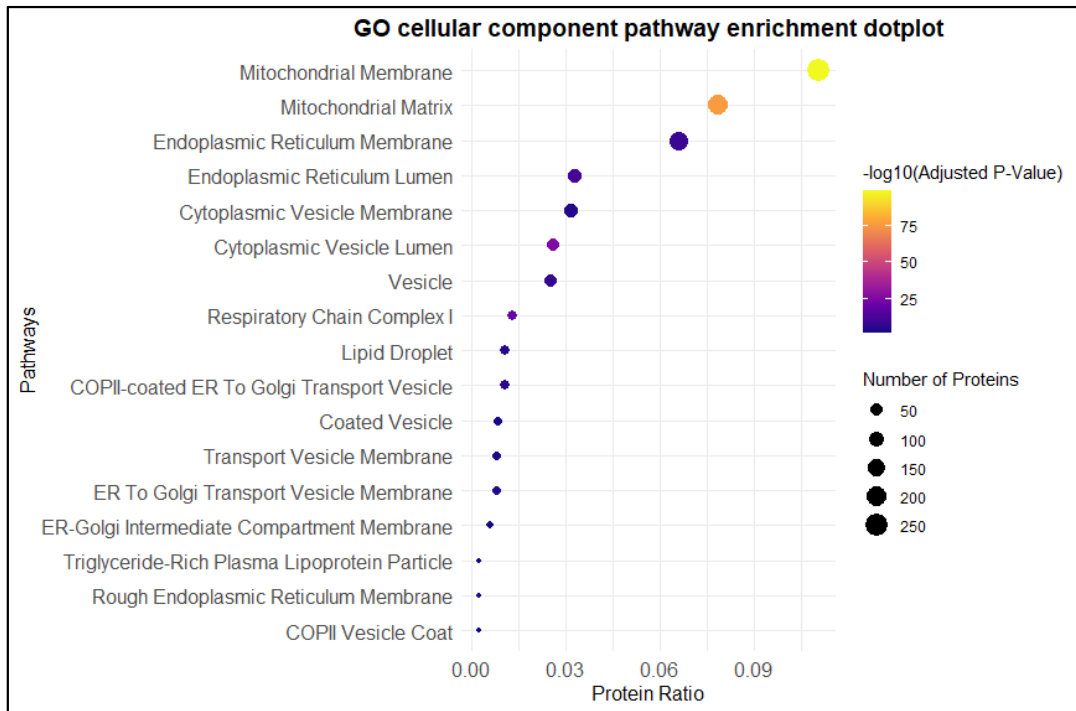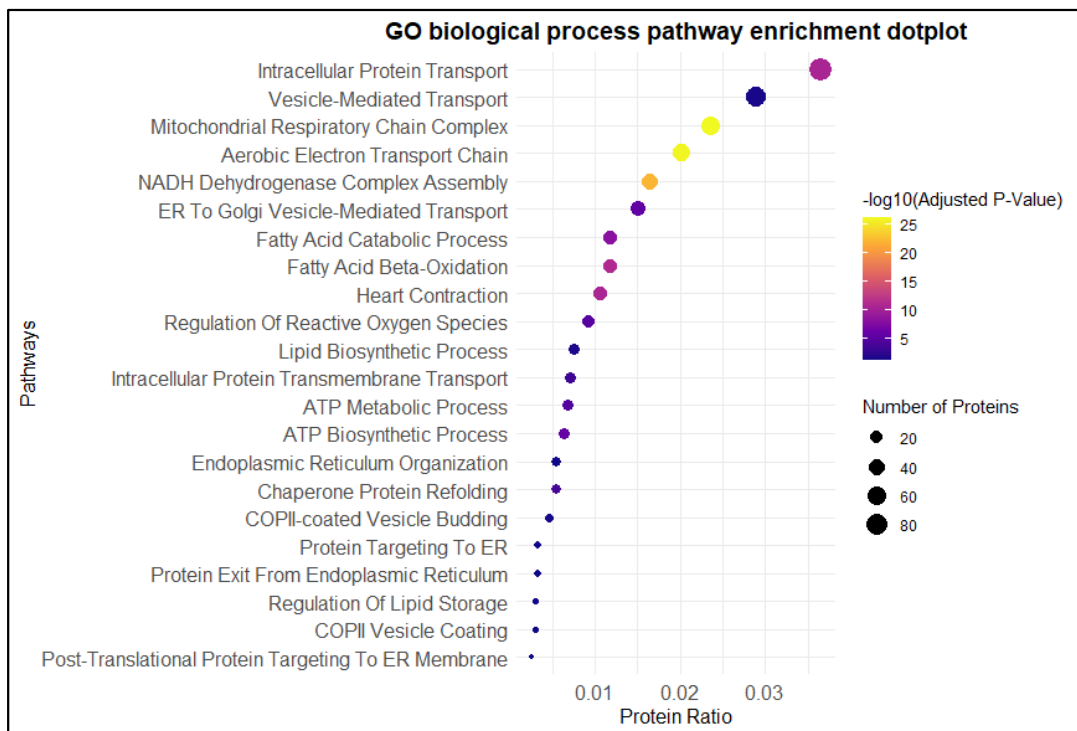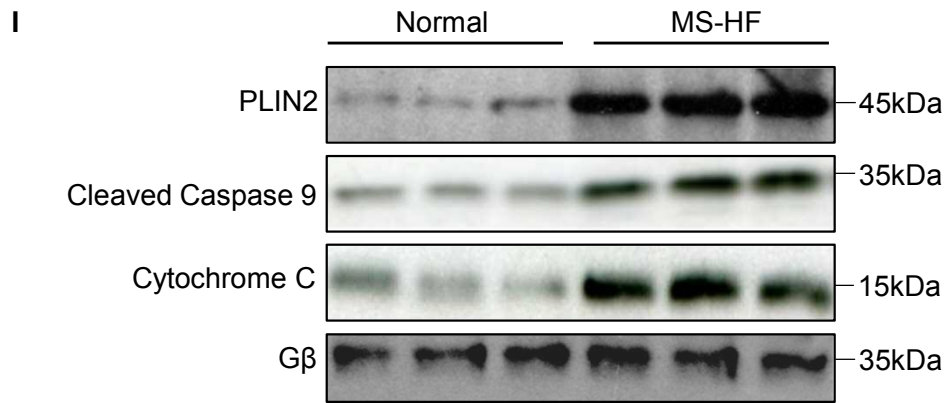
Supplemental Figure 1. Pathways for lipid homeostasis altered in the human heart under metabolic stress

RNA sequencing pathway enrichment analyses of **A**, Reactome, **B**, KEGG, **C**, GO cellular component, and **D**, GO cellular biological process of the genes with differential expression (p_{adj}<0.1) in human hearts from people with metabolic syndrome (MS) and died of heart failure (HF) compared to normal controls without MS and HF, suggested that these genes are within the prominent clusters of lipid metabolism regulation pathways and the ER pathways (n=3-5 hearts). Following Liquid chromatography-Mass spectrometry (LC-MS) of human heart lysates, pathway enrichment analyses of **E**, Reactome, **F**, KEGG, **G**, GO cellular component, and **H**, GO cellular biological process of the altered proteins (2382 proteins with absolute Log$_2$ fold change greater than 0.5 in human MS-HF hearts, and total raw abundances count greater than 6) (n=3 hearts). **I**, Immunoblot analyses of proteins indicating lipid overload (PLIN2, Perilipin 2) and cell death (Cleaved Caspase 9 and Cytochrome C) in metabolic syndrome-associated failing human hearts (MS-HF). Gβ is the loading control.
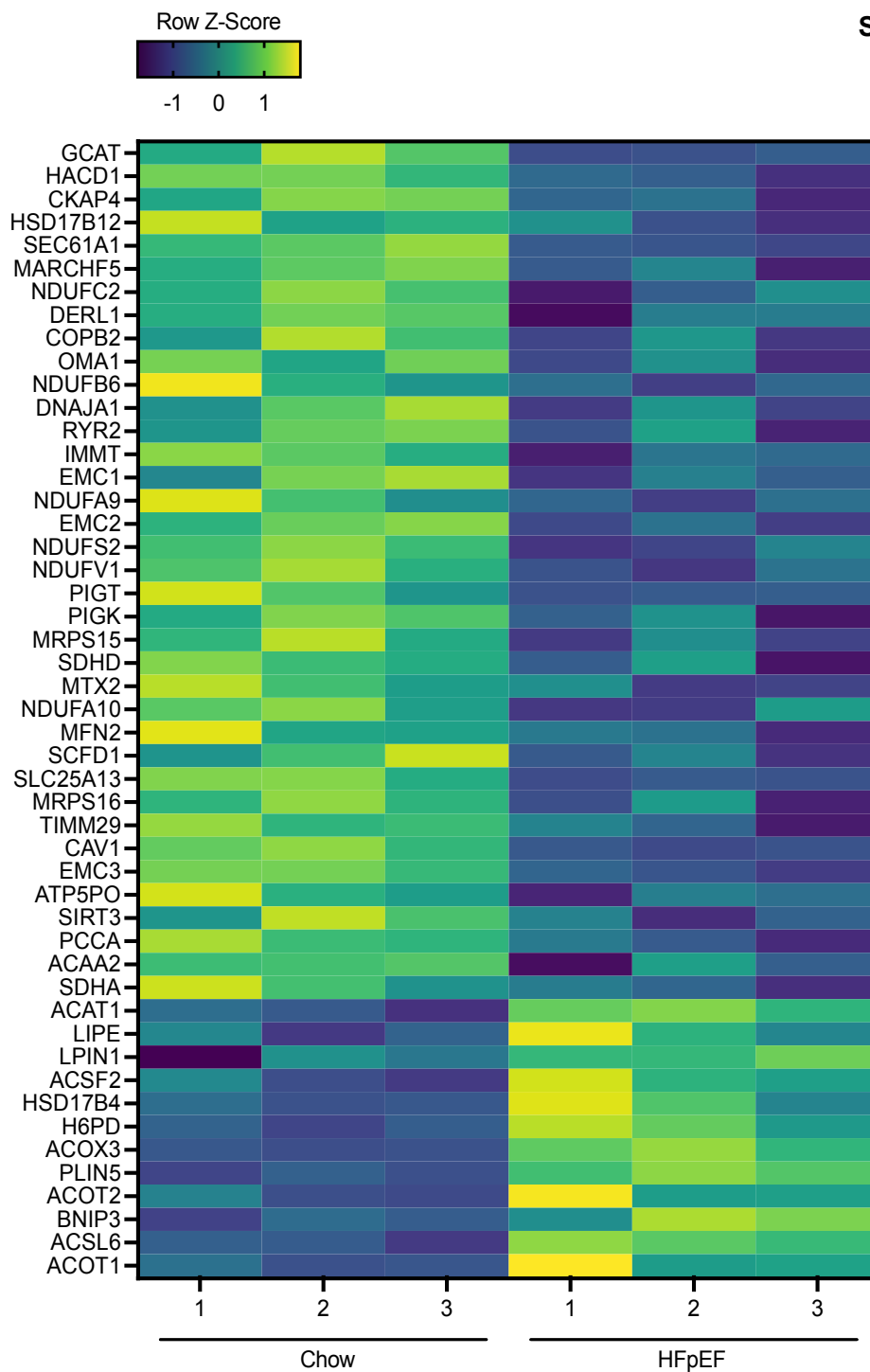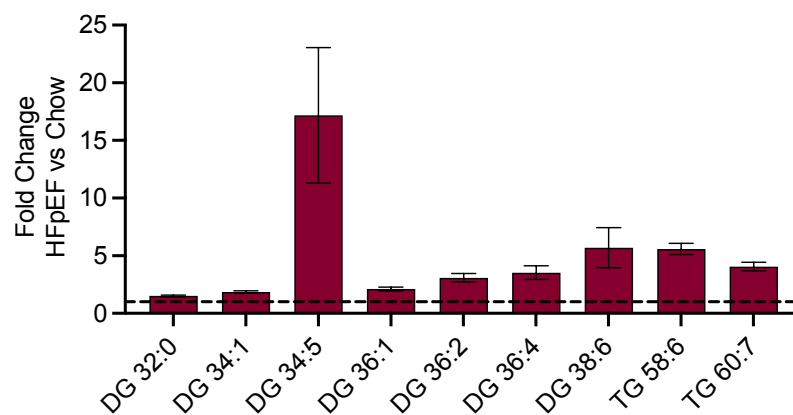
Supplemental Figure 2. Liquid chromatography-Mass spectrometry (LC-MS) and lipidomics of mice HFpEF hearts

A, Liquid chromatography-Mass spectrometry (LC-MS) heatmap analysis exhibiting differentially expressed proteins in mice normal hearts and HFpEF hearts induced by high-fat diet and L-NAME for 12 weeks (n=3 hearts, p_{adj}<0.05). **B**, Lipidomics displaying significantly increased diglycerides (DGs) and triglycerides (TGs) in mice HFpEF hearts compared to controls (n=3 hearts, p<0.05). Data are presented as mean ± S.E.M. p values were calculated using a Mann-Whitney test.
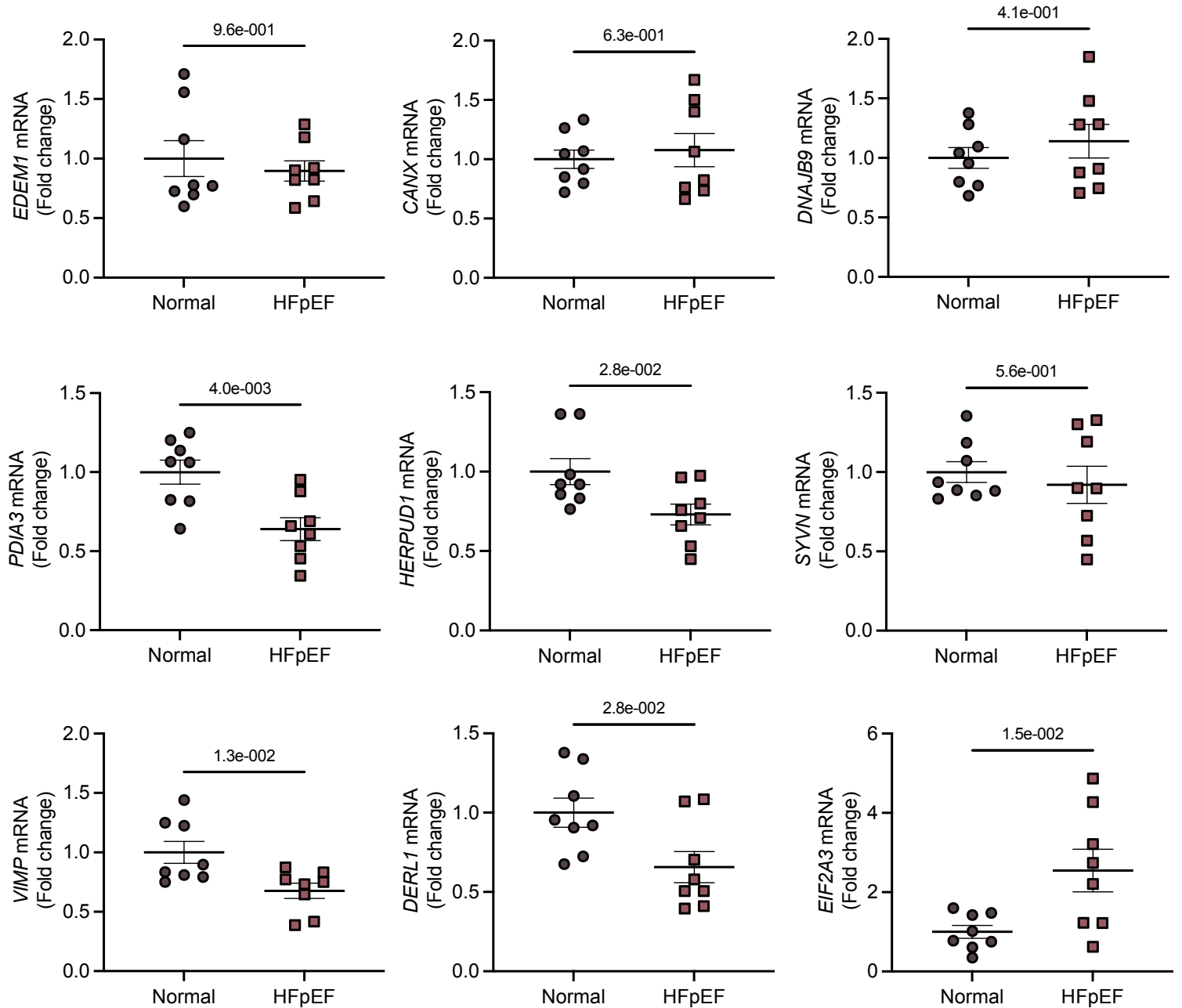
Supplemental Figure 3. The levels of genes putatively targeted by XBP1s in human HFpEF hearts

Quantitative PCR determining the transcripts of genes involved in ER function that are potential targets of XBP1s (n=8 hearts). Data are presented as mean ± S.E.M. *p* values were calculated using an unpaired Student's *t* test.
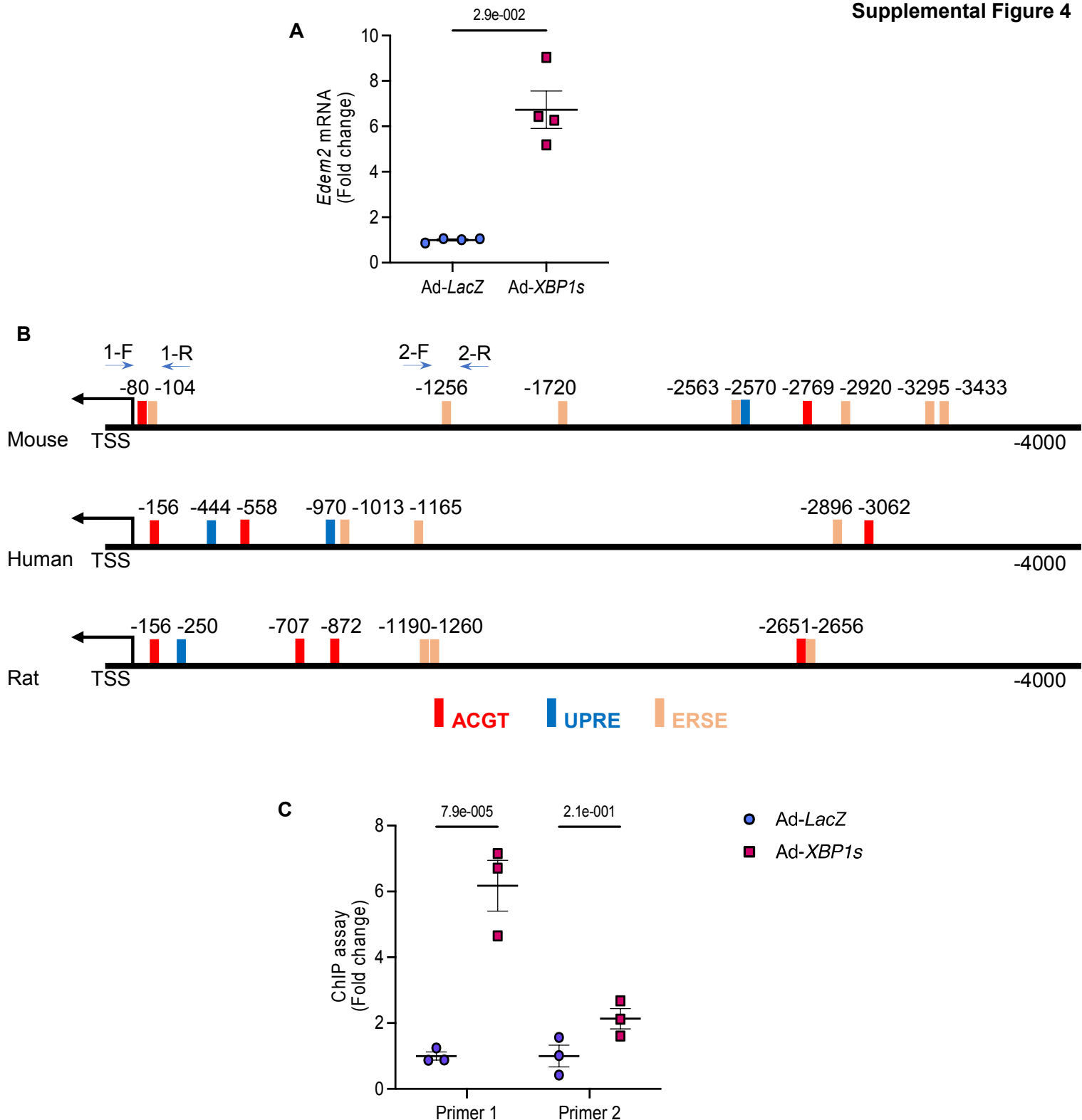
Supplemental Figure 4. XBP1s regulates EDEM2 at the transcriptional level

A, Quantitative PCR showing increased *Edem2* by overexpression of XBP1s (Ad-*XBP1s*, adenovirus expressing human *XBP1s*) (n=4 experiments). **B**, Schematic figure showing XBP1s-binding sites in the promoter region (−4,000bp from transcription start site, TSS) of mouse, human, and rat *Edem2*. ACGT enriched region, unfolded protein response element (UPRE), ER stress-response element (ERSE) are the putative binding sequences. **C**, Chromatin immunoprecipitation (ChIP) assay performed on mouse C2C12 myoblasts using anti-XBP1s antibody (normalized to the input chromatin, n=3 experiments). Primer pair 1 forward and reverse (1-F and 1-R) and primer pair 2 forward and reverse (2-F and 2-R) flanking the corresponding region are annotated in (**B**). Data are presented as mean ± S.E.M. *p* values were calculated using a Mann-Whitney test (**A**) or a Two-way ANOVA with Šidák post-hoc tests (**C**).
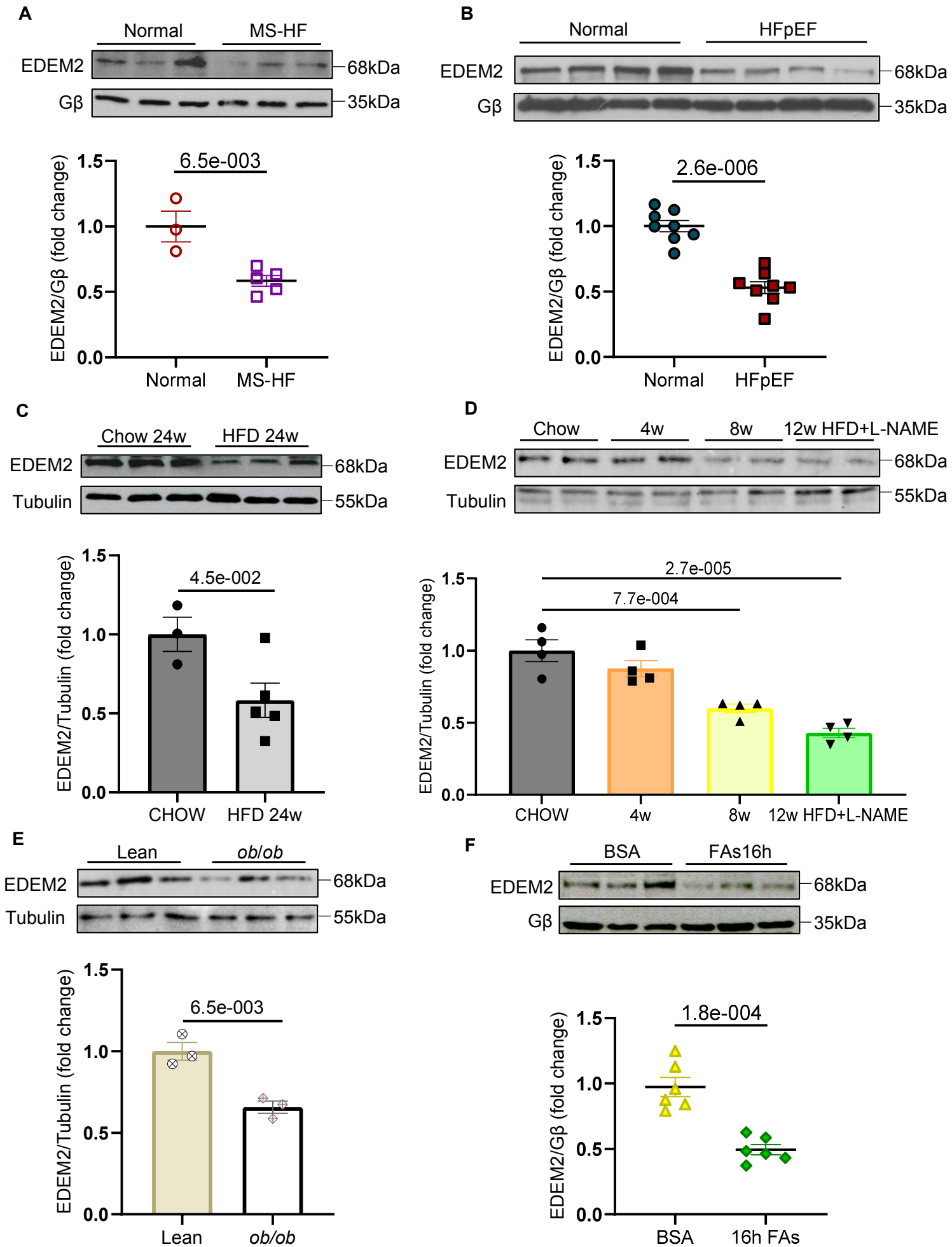
G
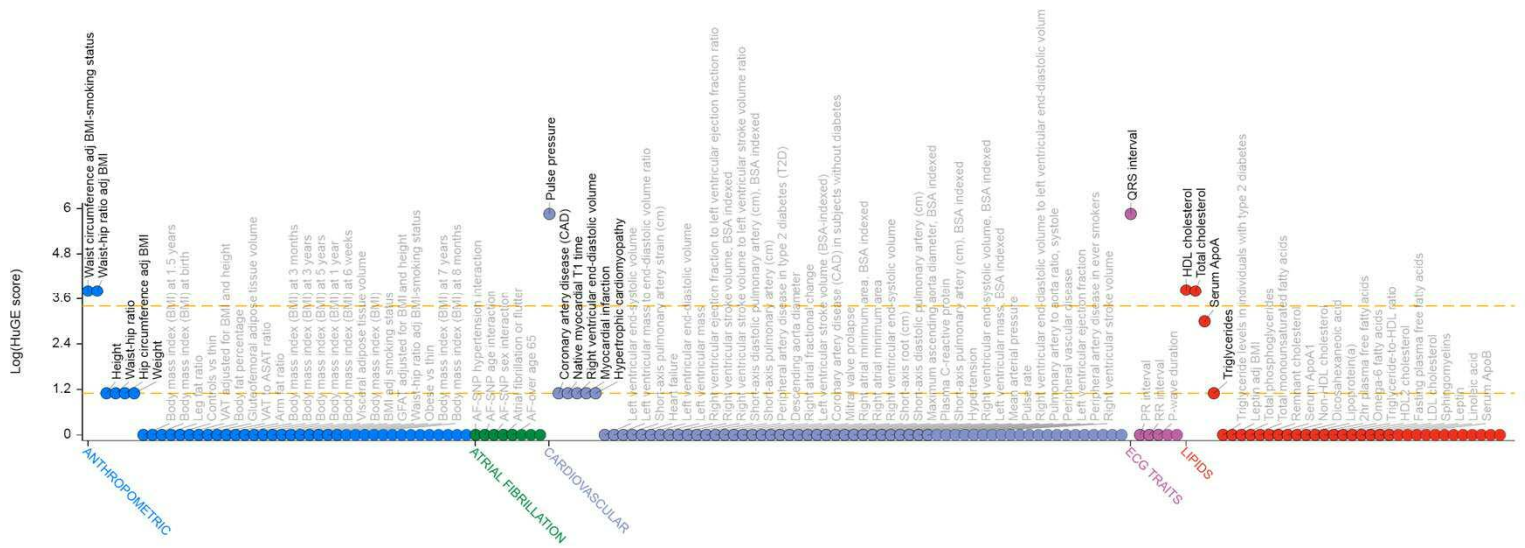
Supplemental Figure 5. EDEM2 is decreased in hearts from various metabolically stressed models

EDEM2 expression in **A**, human hearts with metabolic syndrome (MS) (n=5 hearts); **B**, human HFpEF hearts (n=7-8 hearts); **C**, hearts from mice fed with high-fat diet alone (HFD) (n=3-6 hearts per group); **D**, hearts from HFD and L-NAME induced HFpEF mice with different durations (n=4 hearts); **E**, hearts obtained from 14-week-old *ob/ob* mice (n=3 hearts); and **F**, cultured human heart slices stimulated with BSA-conjugated FAs (palmitic acid and oleic acid, 500µM) for 16 hours (n=6 experiments). Tubulin or Gβ is the loading control. **G**, Phenome-wide association (PheWAS) plot depicting significant cardiovascular traits associated with EDEM2. Data generated by bottom-line meta-analysis across all datasets in the Cardiovascular Disease Knowledge Portal. Data are presented as mean ± SEM. *p* values were calculated using an unpaired Student's *t* test (**A**, **B**, **F**), a Mann-Whitney test (**C** and **E**) or a One-way ANOVA with Šidák post-hoc tests (**D**).
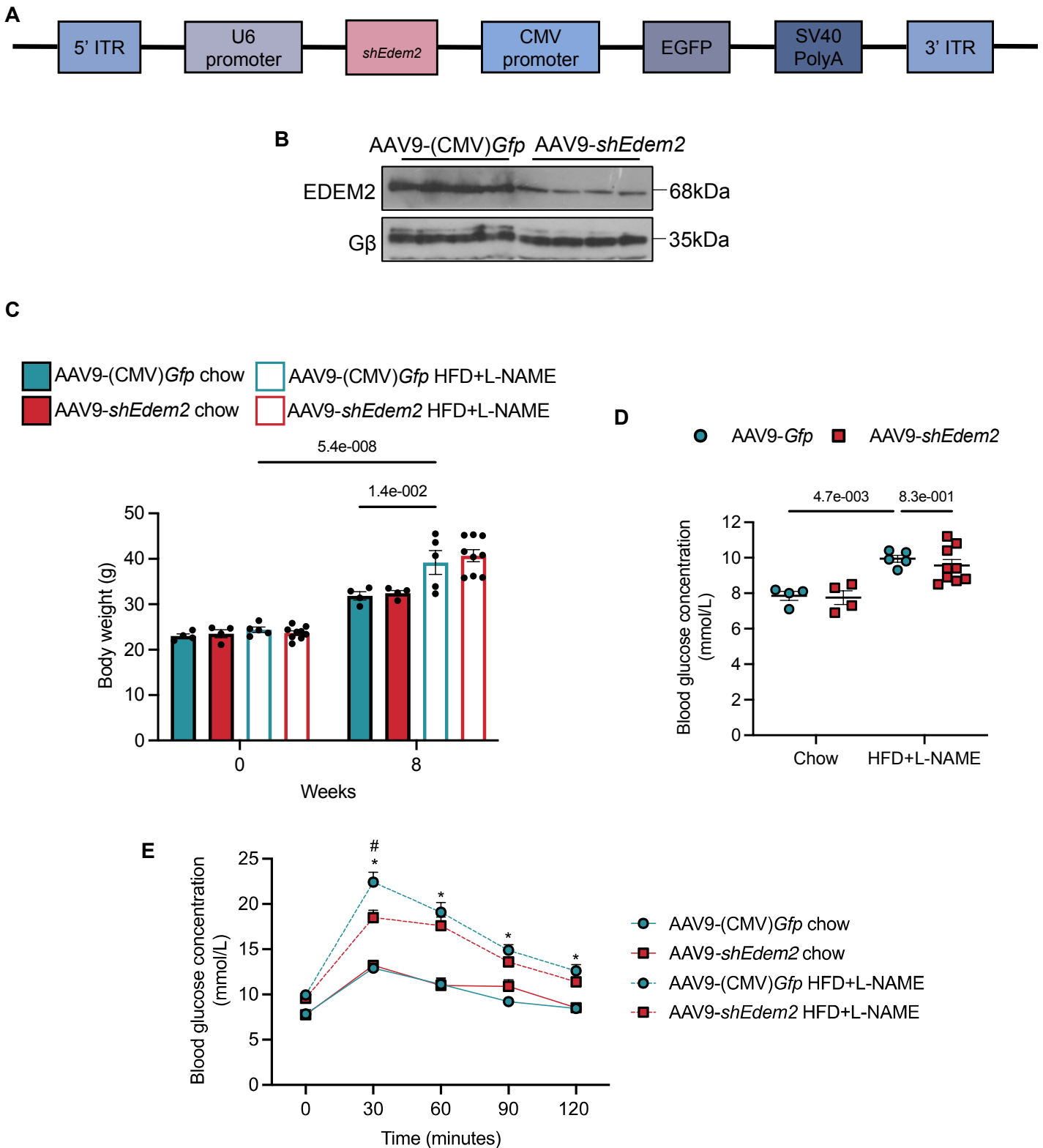
Supplemental Figure 6. EDEM2 deficiency does not affect systemic metabolism

A, AAV9 viral vector construct of AAV9-*shEdem2*. **B**, Immunoblots validating EDEM2 reduction in the heart using AAV9-*shEdem2*. Gβ is the loading control. **C**, Body weight before and after HFD+L-NAME for 8 weeks (n=4-9 mice). **D**, Fasting blood glucose concentration and **E**, Glucose tolerance tests after 8 weeks of HFD+L-NAME (n=4-9 mice). Data are presented as mean ± SEM. *p* values were calculated using a Two-way ANOVA with Tukey post-hoc tests (**C**, **D**) or Šidák post-hoc tests (**E**). Significant differences between chow vs HFD+L-NAME in AAV9-(CMV)*Gfp*, or AAV9-(CMV)*Gfp* HFD+L-NAME and AAV9-sh*Edem2* HFD+L-NAME at respective timepoints are indicated by * and #, respectively in (**E**).
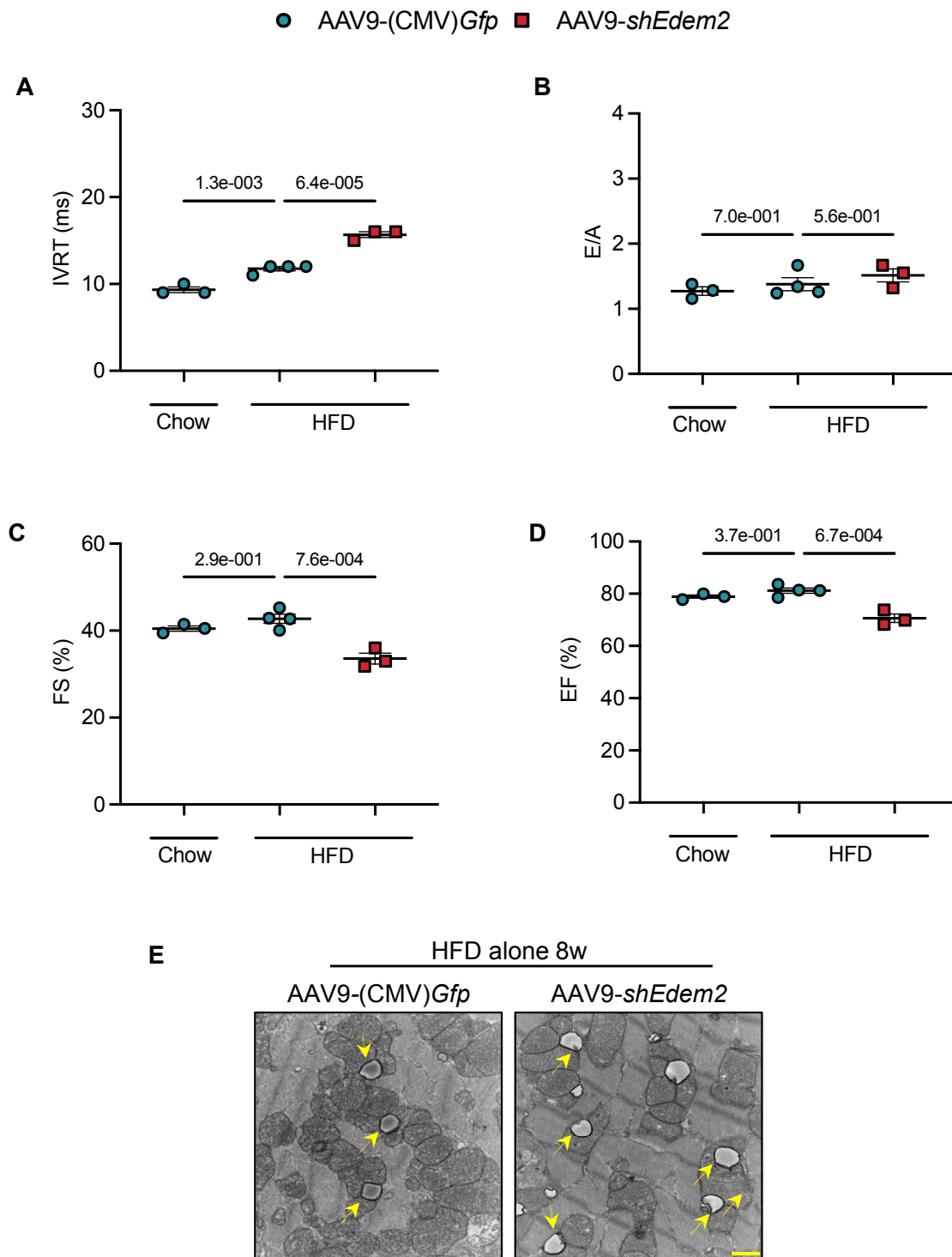
Supplemental Figure 7. EDEM2 deficiency impairs cardiac function under stress induced by HFD alone for 8 weeks

C57BL/6 mice were injected with AAV9-(CMV)*Gfp* or AAV9-*shEdem2* followed by receipt of either chow diet or HFD (60 kcal% fat) alone for 8 weeks. **A**, Isovolumic relaxation time (IVRT) and **B**, ratio of peak velocity blood flow in early diastole to late diastole (E/A) obtained from pulsed-wave Doppler imaging. **C**, Left ventricular fractional shortening (FS%) and **D**, ejection fraction (EF%) obtained from M-mode echocardiography (n=3-4 mice). Data are presented as mean ± SEM. *p* values were calculated using a Kruskal-Wallis test with Dunn's post-hoc tests. **E**, Representative transmission electron microscopy (TEM) images (arrows indicating lipid droplets, scalebar=1µm).

A

B

C

Chow 8w   HFD+L-NAME 8w

AAV9-(CMV)*Gfp*   *shEdem2*   (CMV)*Gfp*   *shEdem2*

XBP1s	60kDa
p50ATF6	50kDa
ATF4	45kDa
Gβ	35kDa

● AAV9-(CMV)*Gfp*   ■ AAV9-*shEdem2*

Supplemental Figure 8. EDEM2 knockdown triggers cardiac pathological remodeling in HFpEF hearts

A, Representative images and quantification of wheat germ agglutinin (WGA) staining for cardiomyocyte cross-sectional area (n=4-9 hearts, scalebar=20μm). **B**, Transcript levels of fibrotic and hypertrophic markers (n=4-7 hearts). **C**, Representative immunoblots and quantification of key factors involved in ER function in the myocardium (n=5 hearts). Data are presented as mean ± SEM. *p* values were calculated using a Two-way ANOVA with Tukey post-hoc tests (**A**) or Šidák post-hoc tests (**B**, **C**).
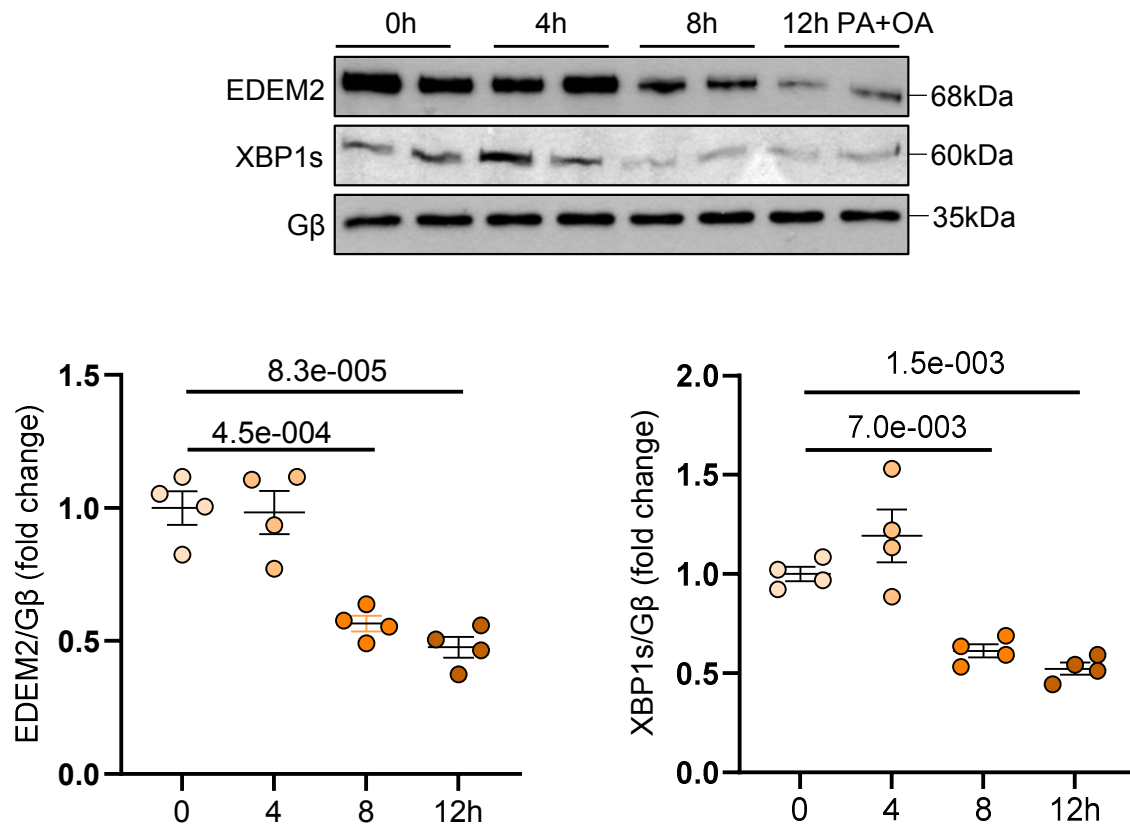
Supplemental Figure 9. Reduced EDEM2 in cardiomyocytes upon prolonged fatty acid stress

Immunoblots and quantification demonstrating a decrease in EDEM2 and XBP1s expression in neonatal rat cardiomyocytes (NRCMs) under longer durations (8 to 12 hours) of fatty acid stimulation (PA and OA, 300µM each, n=3 experiments). Gβ is the loading control. Data are presented as mean ± S.E.M. *p* values were determined using a One-way ANOVA with Tukey post-hoc tests.

BODIPY | DAPI

F GO cellular component pathway enrichment dotplot

G GO biological process pathway enrichment dotplot
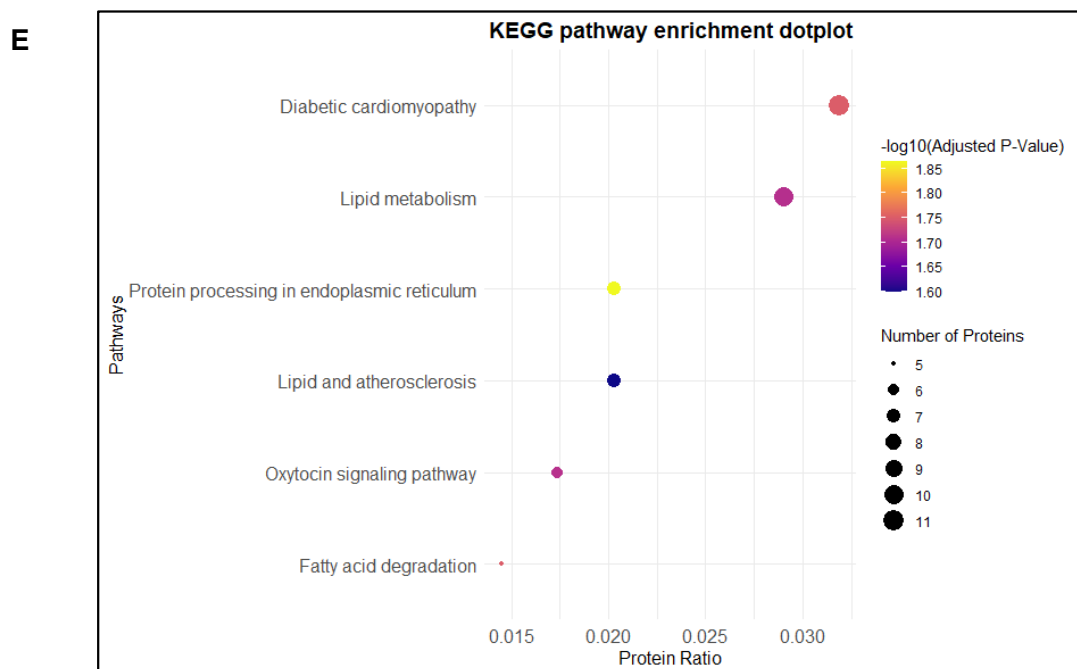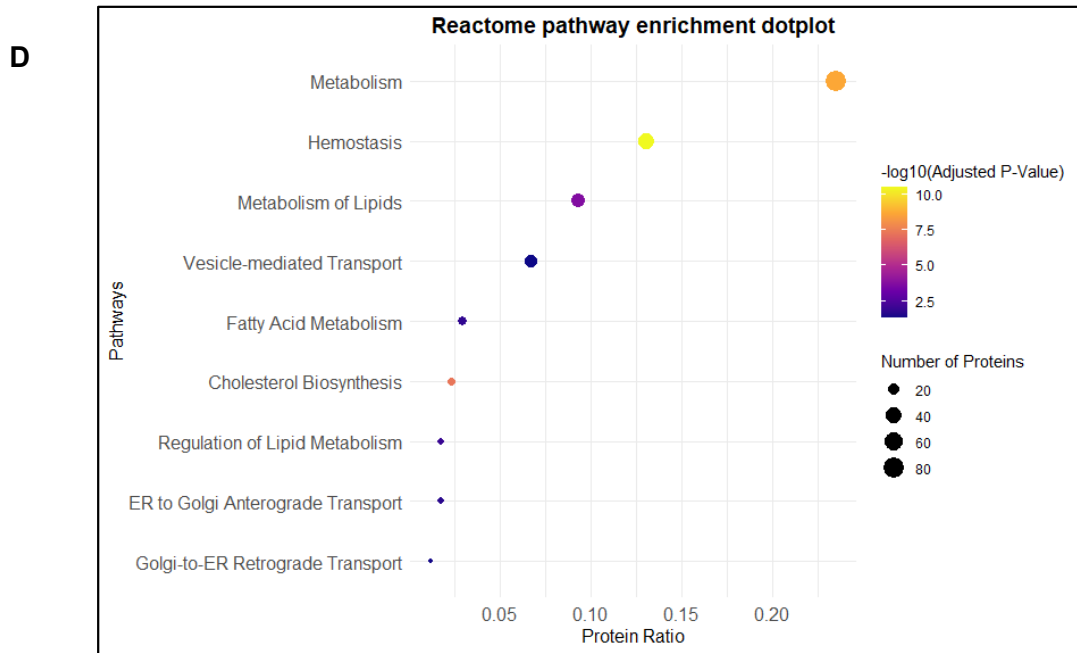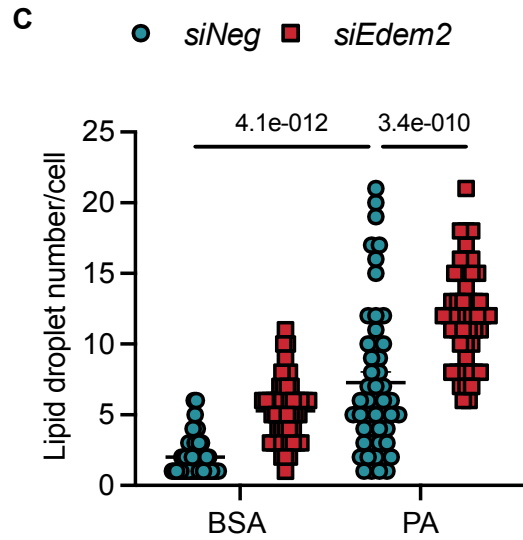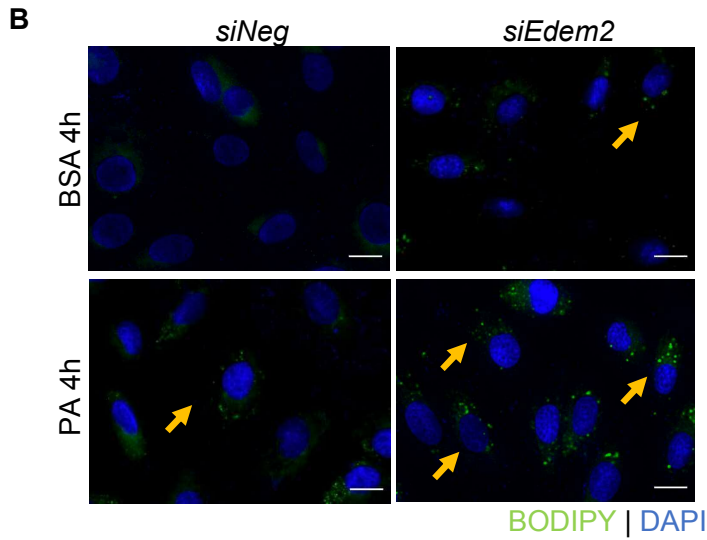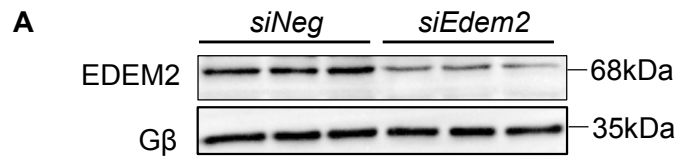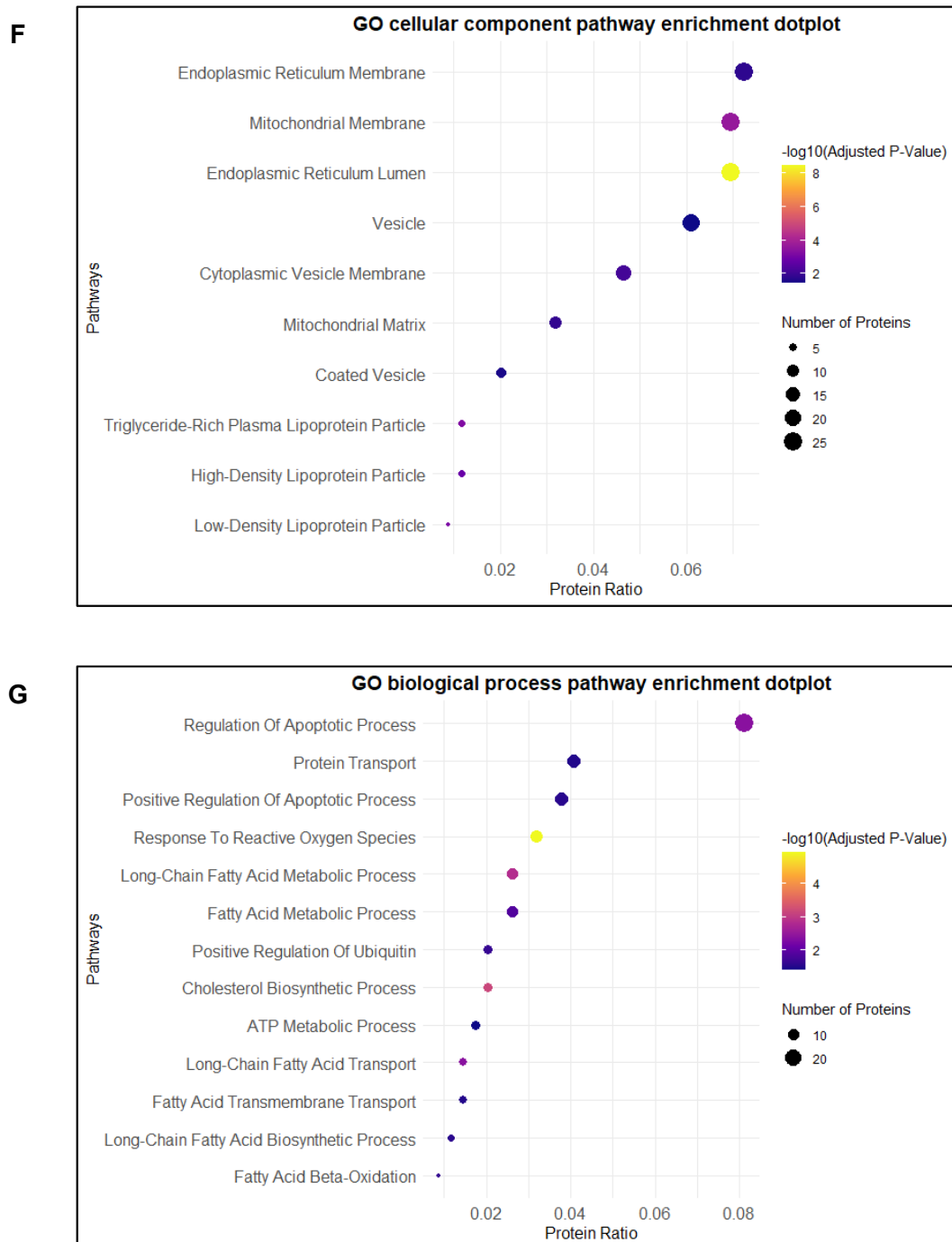
Supplemental Figure 10. Increased lipid droplets (LDs) associated with ER-retained ATGL in EDEM2-knockdown H9C2 cells upon fatty acid stress

A, Immunoblot confirming EDEM2 knockdown by its *siRNA* in H9C2 cells (*siNeg*: *siNegative* as control). Gβ is the loading control. **B**, BODIPY staining of LDs (arrows) and **C**, its quantification in EDEM2 knockdown cells under acute fatty acid stress (PA, 300μM, n=50 cells in 3 experiments; scalebar=20μm). DAPI (blue) stains nuclei. Data are presented as mean ± S.E.M. *p* values were determined using a Two-way ANOVA with Tukey post-hoc tests. Following Liquid chromatography-Mass spectrometry (LC-MS) in H9C2 cells, pathway enrichment analyses of **D**, Reactome, **E**, KEGG, **F**, GO cellular component, and **G**, GO cellular biological process of proteins (345 proteins with absolute Log_2 fold change greater than 0.5 in EDEM2-knockdown H9C2 cells compared to control cells upon 4 hours fatty acid stress, and total raw abundances count greater than 6, n=3 experiments).

C

D

E
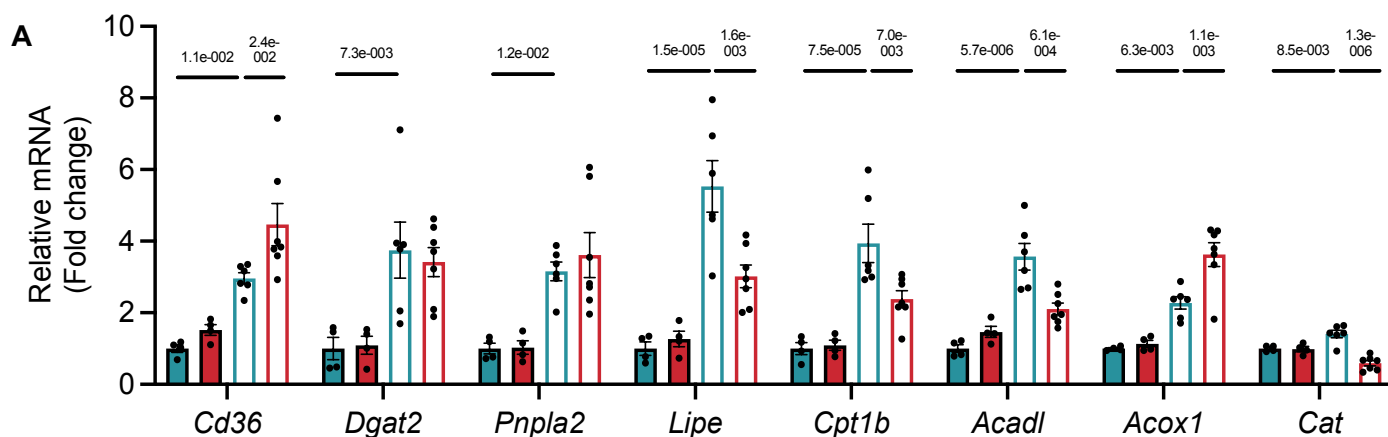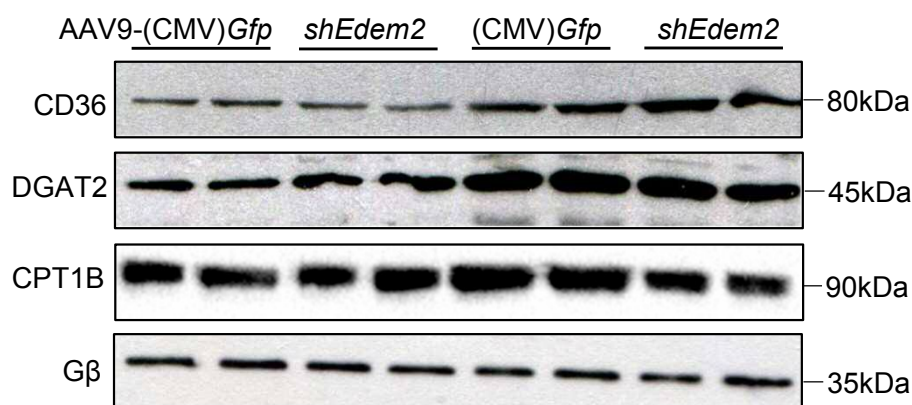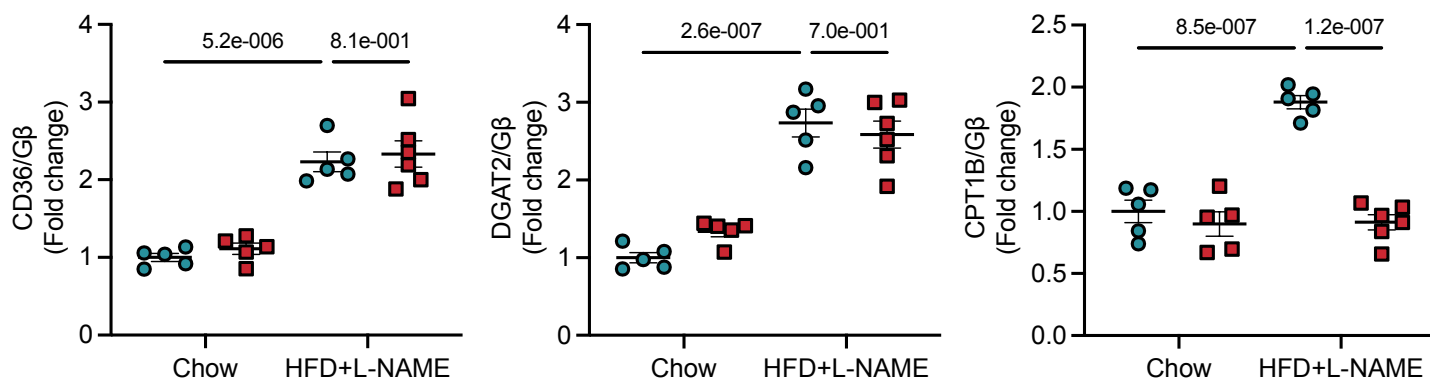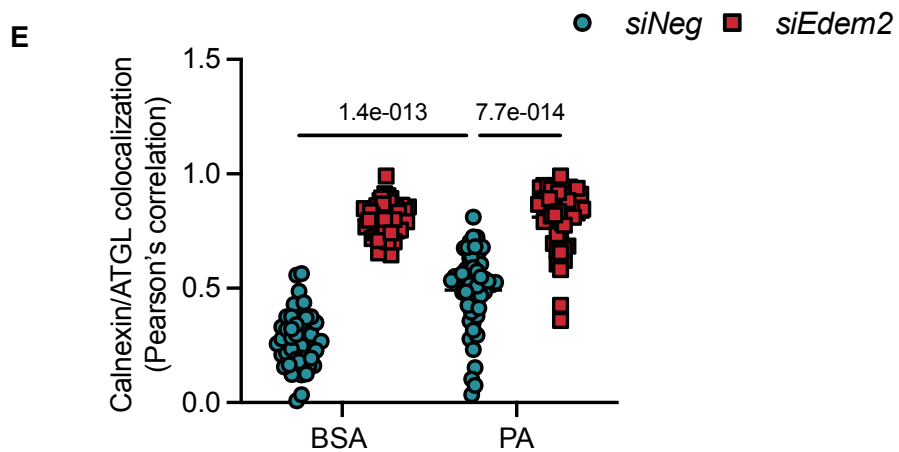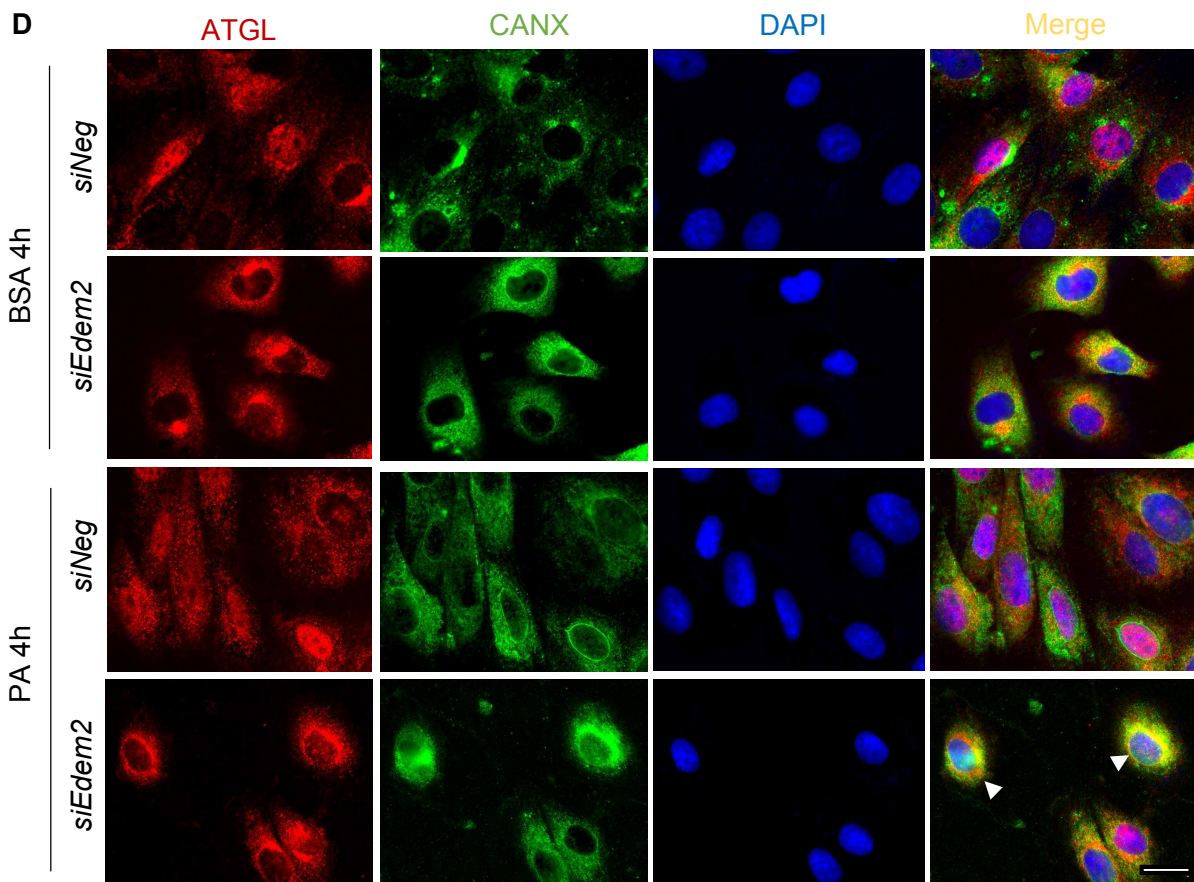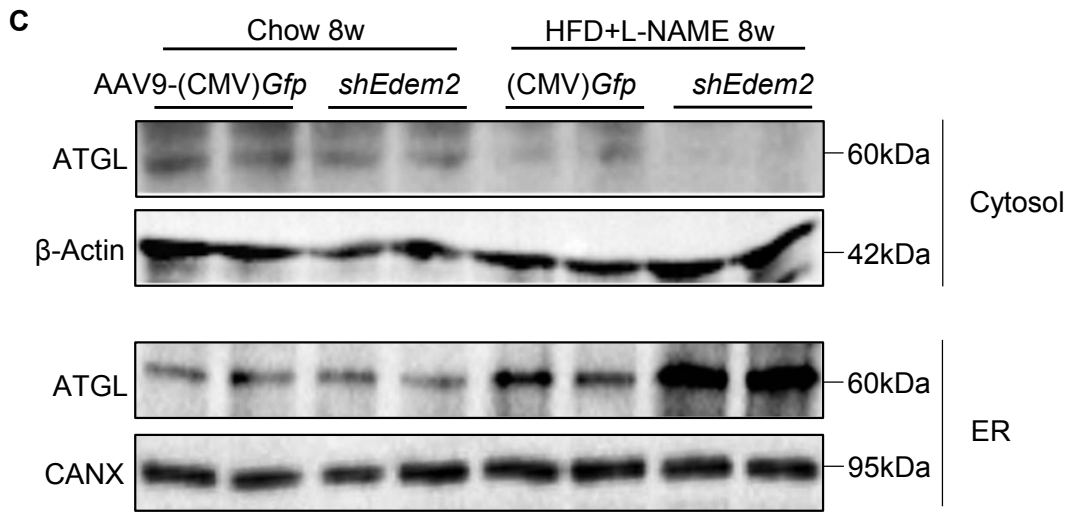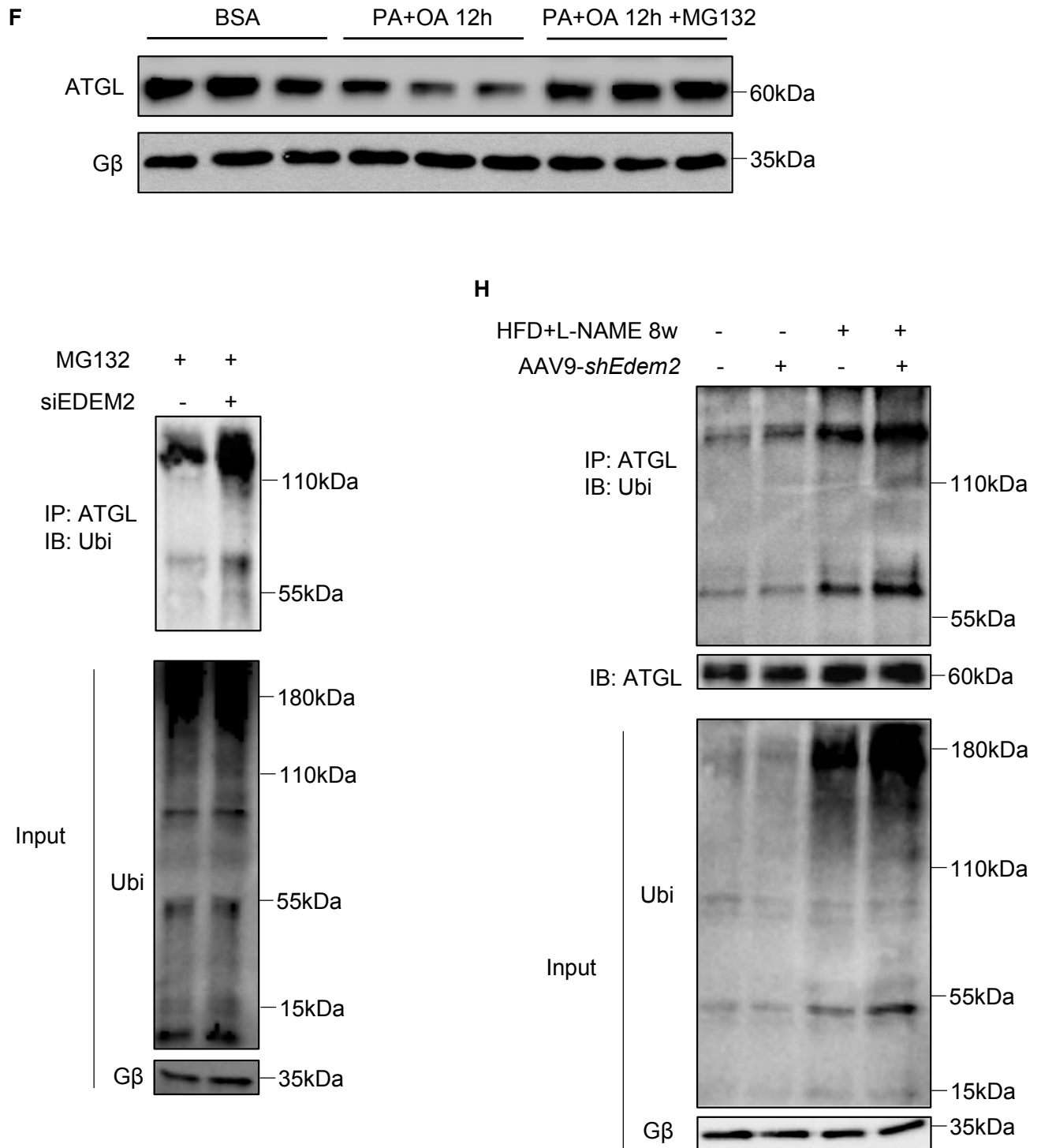
Supplemental Figure 11. EDEM2 loss induces ER retention of ATGL and its ubiquitination-mediated degradation

A, Quantitative PCR determining transcripts of genes involved in lipid metabolism in the myocardium (n=4-6 hearts). **B**, Representative immunoblots and quantification of lipid associated proteins in the myocardium (n=5-6 hearts). **C**, Representative immunoblots of ATGL in ER fraction and soluble cytosol in the myocardium (each sample represents the pooled extracts from 3 hearts), with CANX and β-Actin as controls, respectively. **D**, Representative images and **E**, quantification of colocalization of ATGL and CANX (an ER marker) in H9C2 cells under short-term stress of palmitic acid (PA, 300μM). Arrowheads indicates ER retention of ATGL. DAPI (blue) staining nuclei (n=50 in 3 experiments, scalebar=50μm). **F**, Reduction of ATGL in neonatal rat cardiomyocytes (NRCMs) was inhibited by proteosome degradation inhibitor, MG132 (10μM, 6-hour pre-treatment) under fatty acid stimulation (12 hours). **G**, Fatty acid stimulation for 4 hours stimulation increased endogenous ubiquitinated-ATGL in EDEM2 deficient cells. **H**, Endogenous ubiquitinated-ATGL was higher in EDEM2-depleted HFpEF hearts. Data are presented as mean ± S.E.M. p values were determined using a Two-way ANOVA with Šidák post-hoc tests (**A**, **B**, **E**).
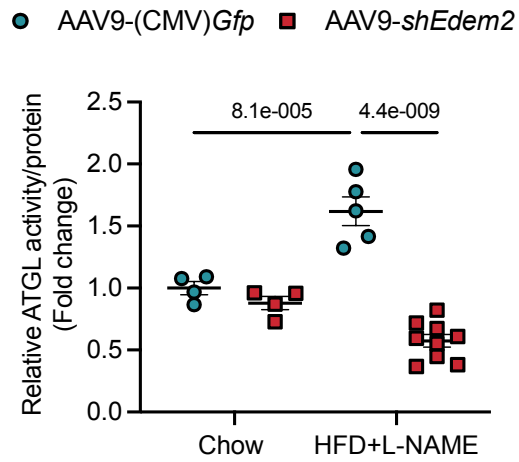
Supplemental Figure 12. ATGL lipase activity was reduced due to EDEM2 loss

ATGL lipase activity assay was conducted using whole extracts of the mouse myocardium (n=4-8 hearts). Data are presented as mean ± S.E.M. p values were determined using a Two-way ANOVA with Šidák post-hoc tests.

A

	Control	WT-ATGL	ATGL-KDEL	
ATGL				—60kDa
Gβ				—35kDa

B

PDI	ATGL	Merge

PA+OA 4h

WT-ATGL

ATGL-KDEL

C

	WT-ATGL		ATGL-KDEL	
MG132	−	+	−	+

IP: ATGL
IB: Ubi

—110kDa

—55kDa

IB: ATGL —60kDa

Input — Ubi

—180kDa

—110kDa

—55kDa

—25kDa

Gβ —35kDa
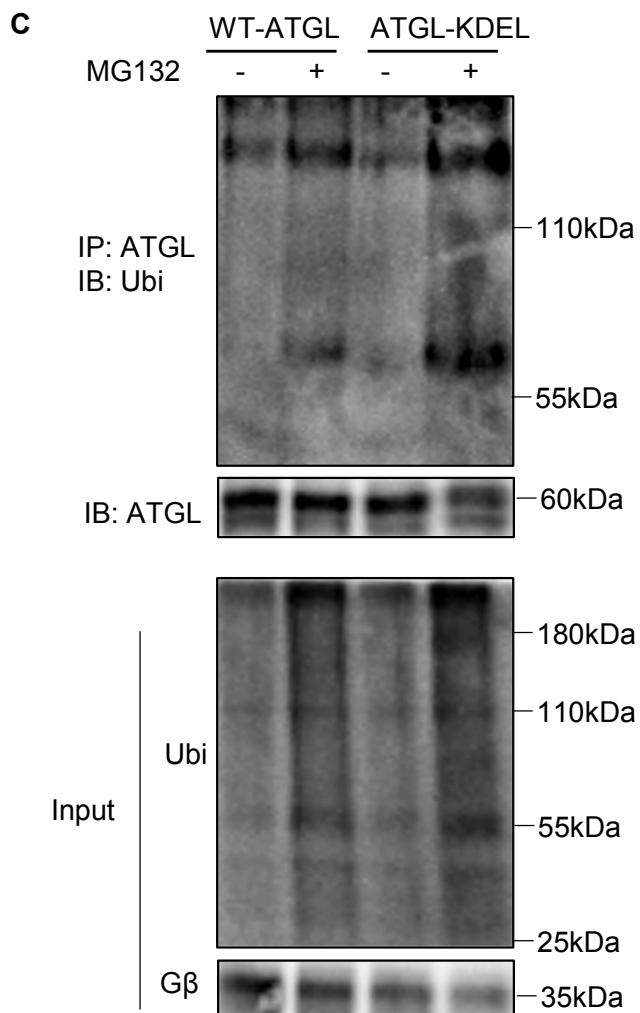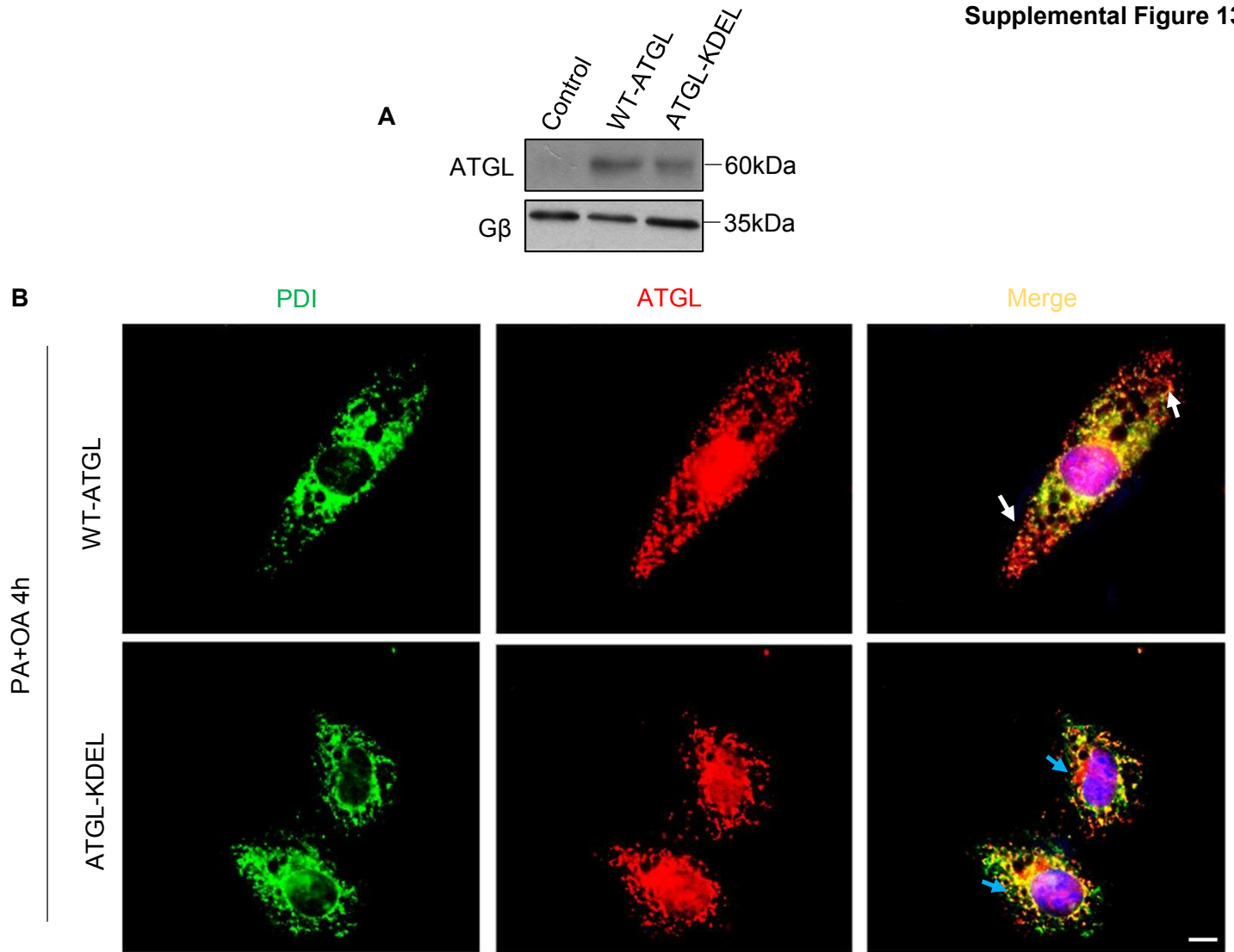
Supplemental Figure 13. ER-retained ATGL is susceptible to ubiquitination

A, ATGL overexpression in H9C2 cells transfected with WT-ATGL or ER-retained ATGL plasmid (ATGL-KDEL). **B**, Representative colocalization images of ATGL and PDI. ER retention (blue arrows) indicated by an ER marker PDI (green); white arrows indicating cytosol-diffused ATGL (red) (scalebar=20μm). **C**, H9C2 cells were transfected with WT-ATGL or ER-retained ATGL plasmid, followed by immunoprecipitation to enrich ATGL for ubiquitination analysis in the absence and presence of MG132 (10μM, 6-hour treatment).
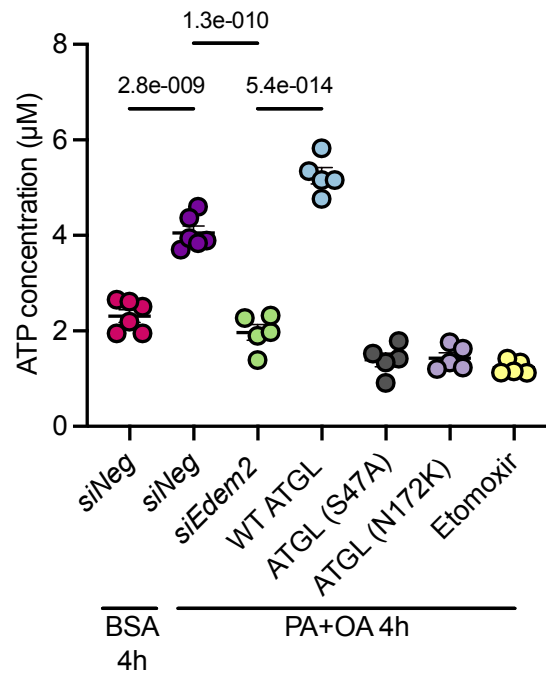
Supplemental Figure 14. ATP is reduced by either EDEM2 deficiency or ATGL functional mutations

Following fatty acid stress for 4 hours, ATP concentration in H9C2 cells with EDEM2 knockdown, overexpression of either WT-ATGL or mutant ATGL (ATGL-S47A and ATGL-N172K), or CPT1 inhibitor treatment (Etomoxir, 5µM) (n=5-6 experiments). Data are presented as mean ± S.E.M. *p* values were determined using a One-way ANOVA with Tukey post-hoc tests.

F
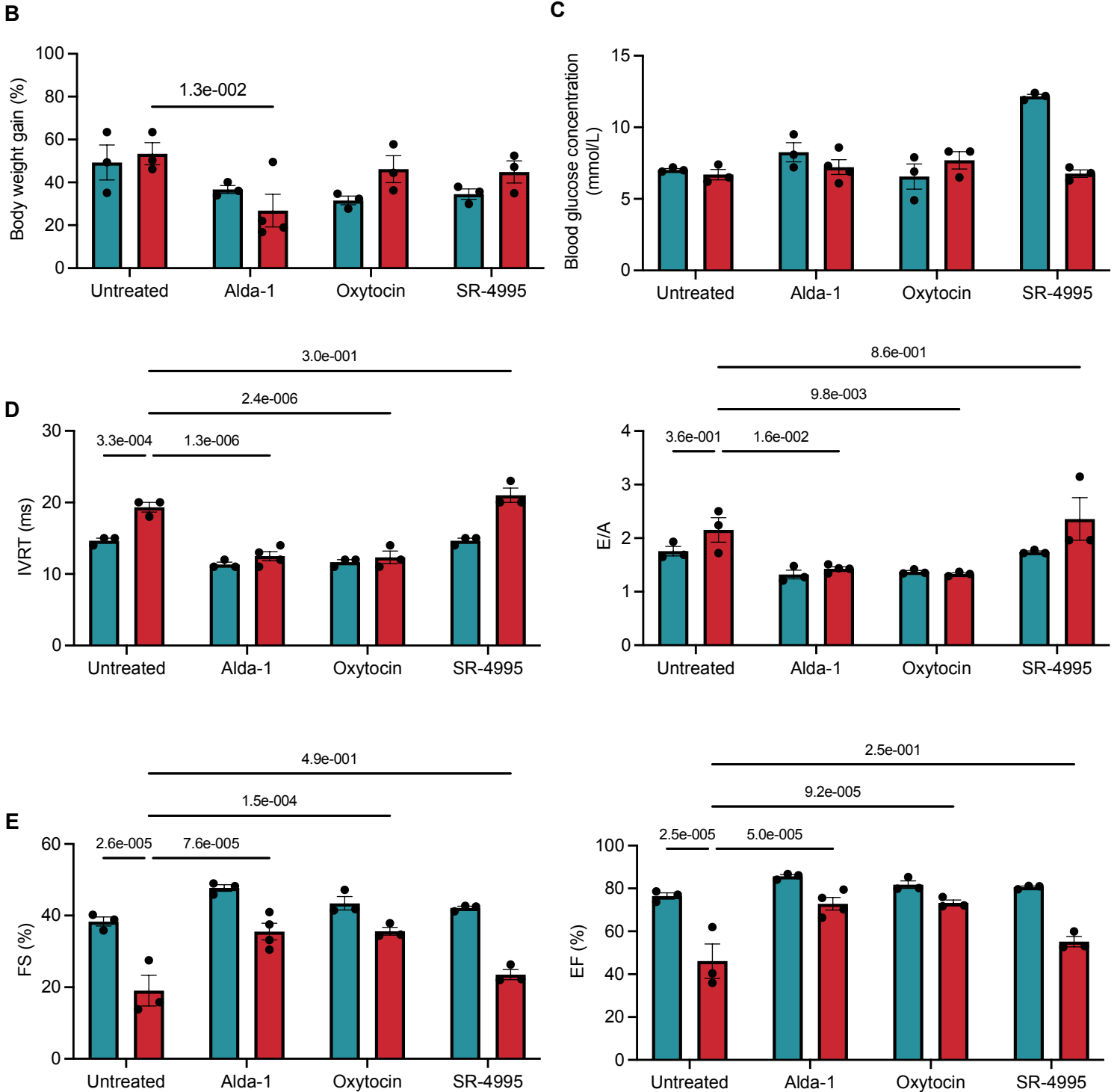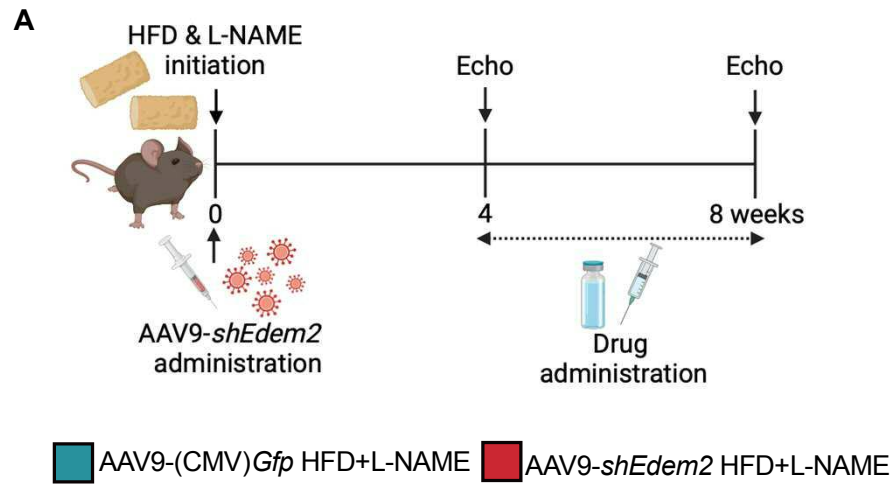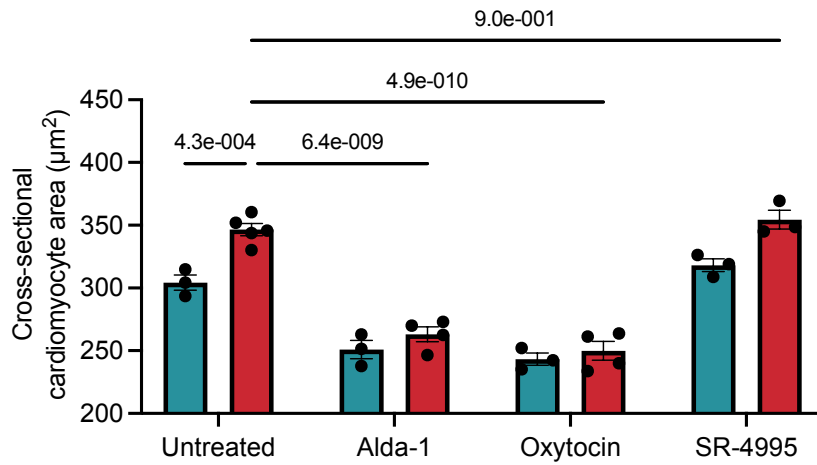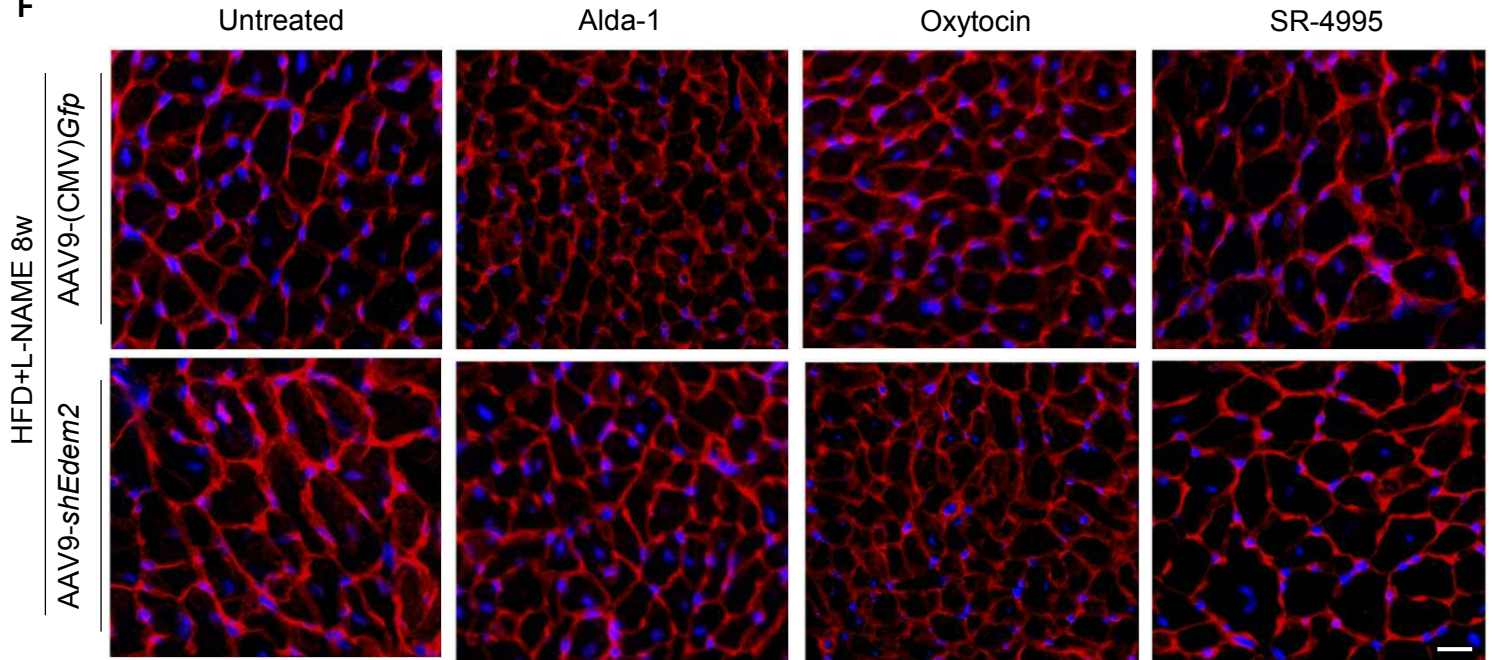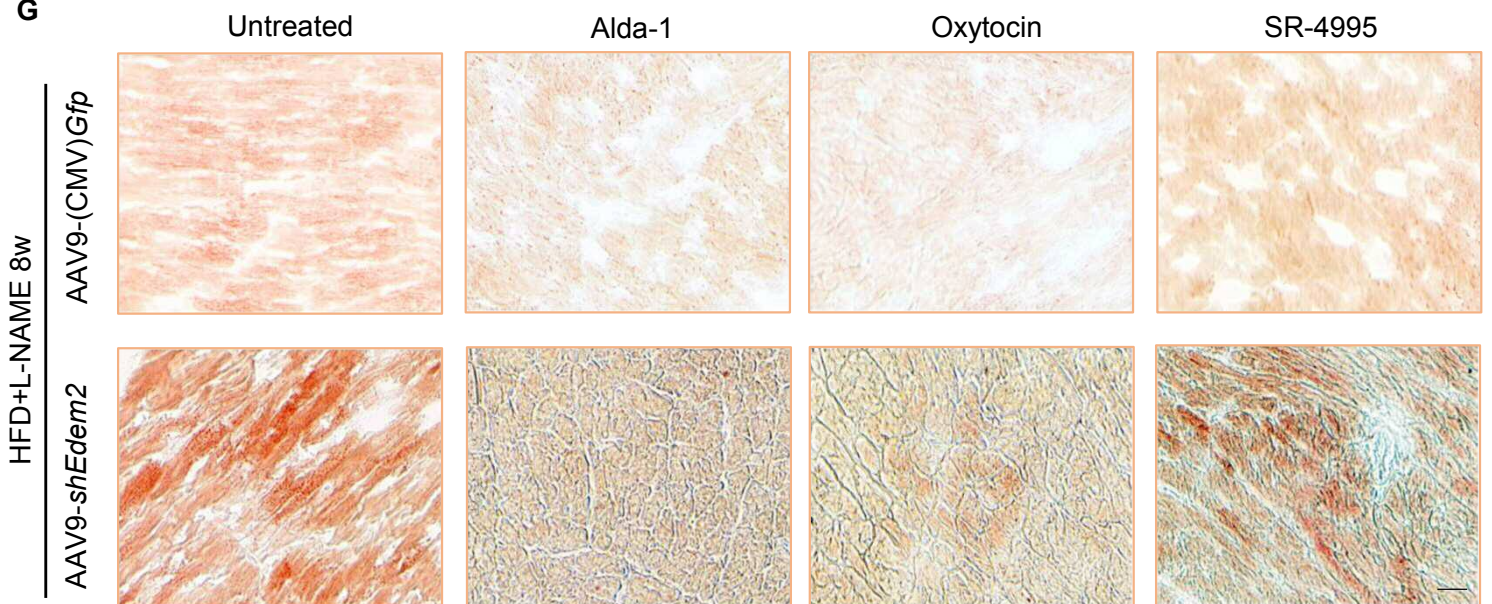
H
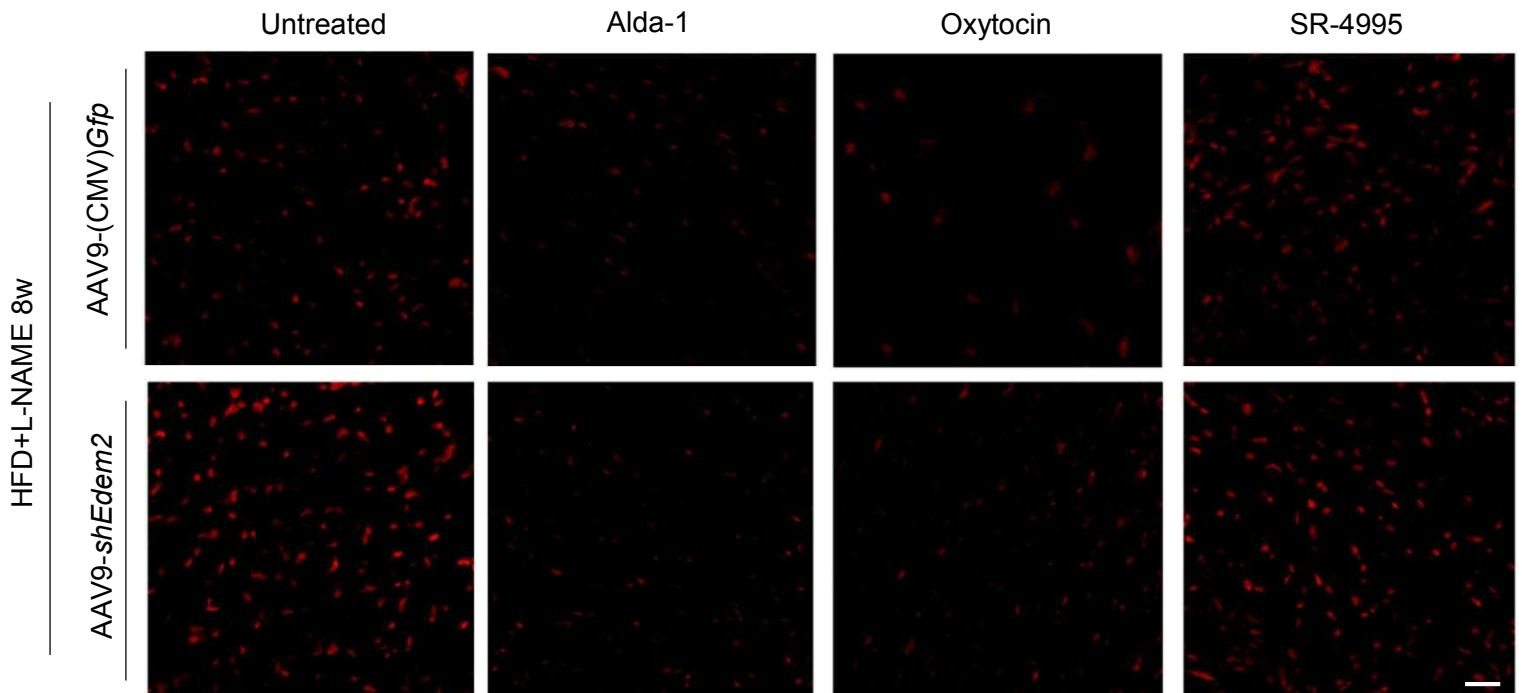
Supplemental Figure 15. Alda-1 and oxytocin, but not SR-4995, attenuates EDEM2 knockdown-induced cardiac lipotoxicity and dysfunction

A, Schematic of experimental design. Various treatments were administered to EDEM2-knockdown mice after 4 weeks of HFpEF stress, including Alda-1, oxytocin, and SR-4995. **B**, Percentage of body weight gain and **C**, Fasting blood glucose levels in mice after 8 weeks. **D**, Isovolumic relaxation time (IVRT) and Ratio of peak velocity blood flow in early diastole to late diastole (E/A) obtained from pulsed-wave Doppler imaging. **E**, Left ventricular fractional shortening (FS%) and ejection fraction (EF%) obtained from M-mode echocardiography. **F**, Representative images and quantification of wheat germ agglutinin (WGA) staining (scalebar=20μm). **G**, Representative images of Oil Red O staining for neutral lipids (scalebar=20μm). **H**, Representative images of DHE staining (scalebar=50μm). Data are presented as mean ± S.E.M (n=3-4 hearts). *p* values were calculated using a Two-way ANOVA with Šidák post-hoc tests (**B**, **C**, **D**, **E**, **F**).

A

attB1 | CMV promoter | *EDEM2-Myc-His* | HSV TK PolyA | attB2

B

	Ad-*LacZ*	Ad-*EDEM2*	
EDEM2			—68kDa
His			—68kDa
Gβ			—35kDa

C

Ad-*LacZ*　　Ad-*EDEM2*

BSA 12h

PA 12h

BODIPY | DAPI

D

● Ad-*LacZ*　■ Ad-*EDEM2*

2.4e-011　　1.6e-005

Lipid droplet number/cell

25
20
15
10
5
0

BSA　　PA

E

ATGL　　CANX　　DAPI　　Merge

BSA 12h — Ad-*LacZ*

Ad-*EDEM2*

PA 12h — Ad-*LacZ*

Ad-*EDEM2*

59
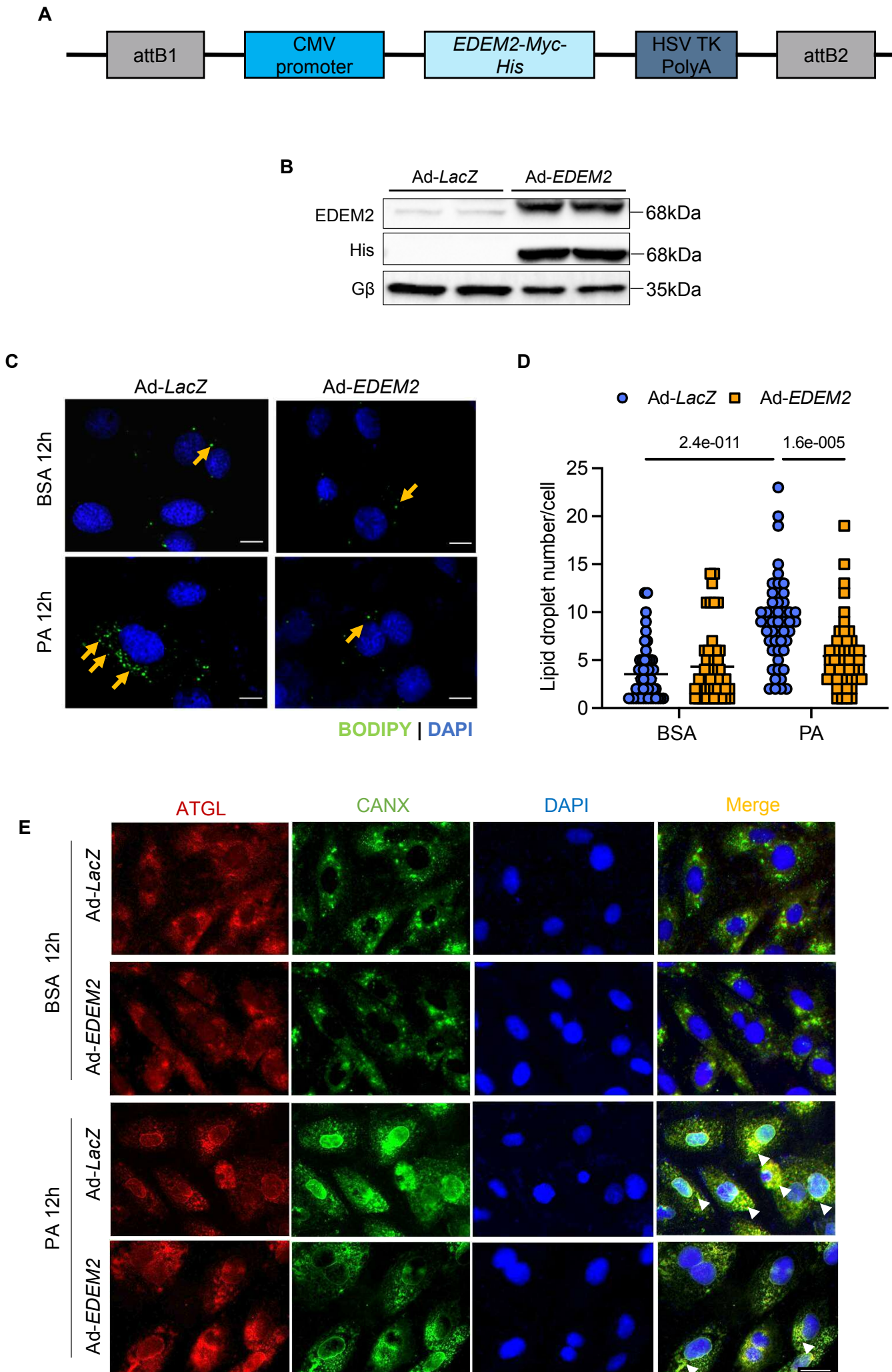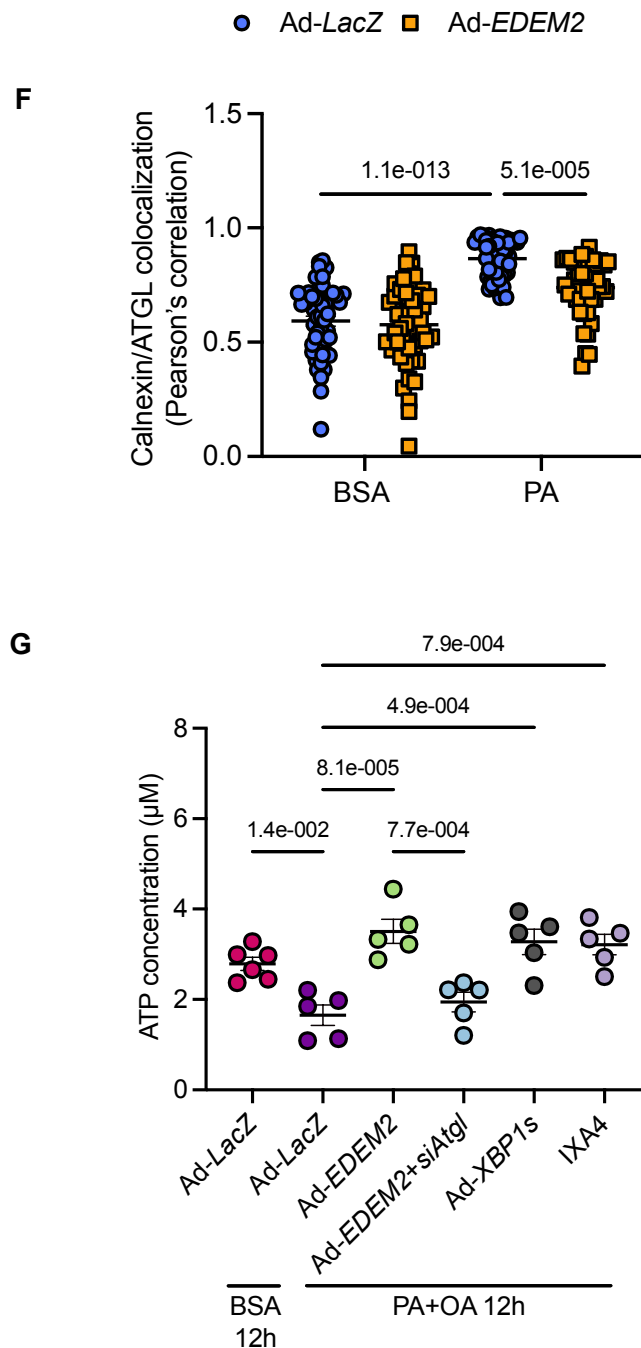
Supplemental Figure 16. EDEM2 overexpression decreased lipid droplets (LDs) in cells

A, Construct of adenovirus expressing human *EDEM2* (Ad-*EDEM2*). **B**, Immunoblot validating EDEM2 overexpression in H9C2. **C**, BODIPY staining of LDs (arrows) and **D**, Quantification in EDEM2-overexpressing cells under prolonged (12 hours) fatty acid stress (PA, 300μM, n=50 cells in 3 experiments, scalebar=20μm). DAPI (blue) stains nuclei. **E**, Representative images and **F**, Quantification of colocalization of ATGL and CANX (an ER marker) in EDEM2-overexpressing H9C2 cells under prolonged stress (n=50 cells in 3 experiments, scalebar=50μm). Arrowheads indicates ER retention of ATGL. **G**, ATP amount in H9C2 cells was preserved by EDEM2 overexpression, XBP1s overexpression, or pre-treatment of the XBP1s inducer (IXA4, 50μM) under prolonged stress of palmitic and oleic acid stress (PA and OA, 300μM), which was blocked by ATGL knockdown (n=5 experiments). Data are presented as mean ± S.E.M. *p* values were determined using a Two-way ANOVA (**D**, **F**) or One-way ANOVA (**G**) with post-hoc Tukey test.

A

B

C

Number of matching peptides
in immunoprecepitate
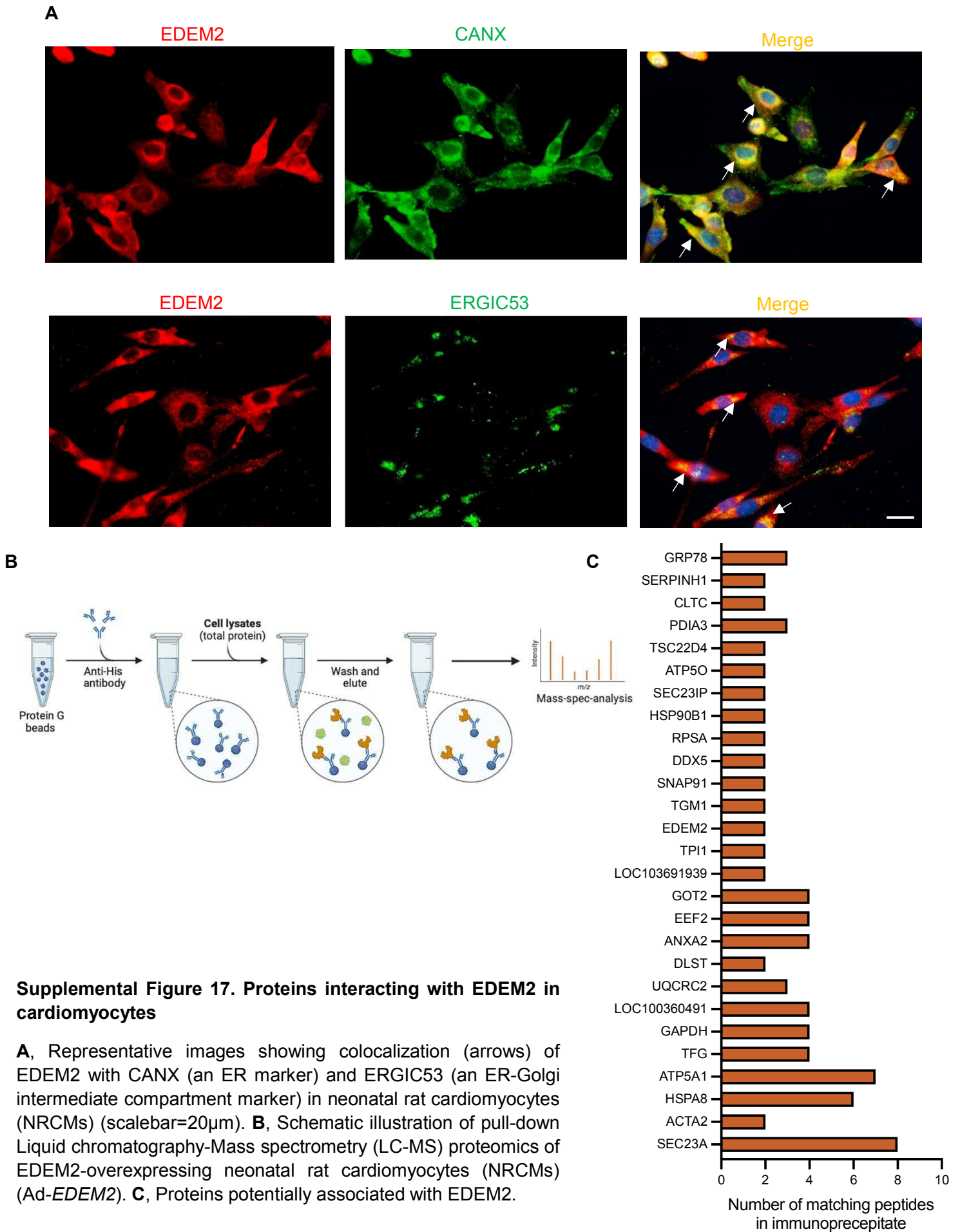
Supplemental Figure 17. Proteins interacting with EDEM2 in cardiomyocytes

A, Representative images showing colocalization (arrows) of EDEM2 with CANX (an ER marker) and ERGIC53 (an ER-Golgi intermediate compartment marker) in neonatal rat cardiomyocytes (NRCMs) (scalebar=20μm). **B**, Schematic illustration of pull-down Liquid chromatography-Mass spectrometry (LC-MS) proteomics of EDEM2-overexpressing neonatal rat cardiomyocytes (NRCMs) (Ad-*EDEM2*). **C**, Proteins potentially associated with EDEM2.

A

siNeg   siSec23a

SEC23A ——90kDa

Gβ ——35kDa

B

| PA+OA 4h | - | + | + |
| siSec23a | - | - | + |

ATGL ——60kDa

PLIN2 ——45kDa

C

siNeg   siSec23a

BSA 4h

PA+OA 4h

BODIPY | DAPI

D

PA+OA 4h

Ad-*EDEM2*	-	-	+
siSec23a	-	+	+

PLIN2 — 45kDa

Cleaved Caspase 9 — 35kDa

Cytochrome C — 15kDa

Gβ — 35kDa

E
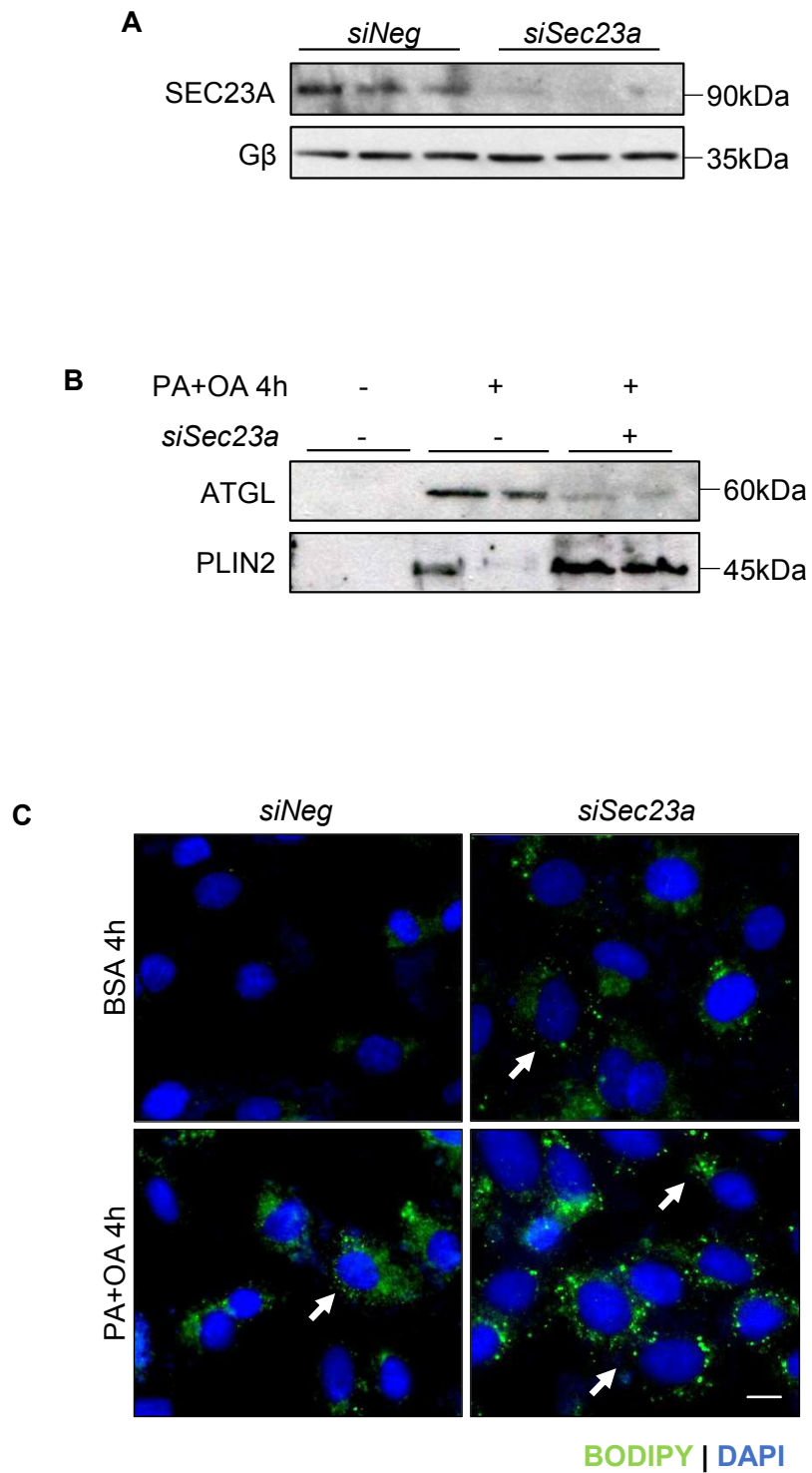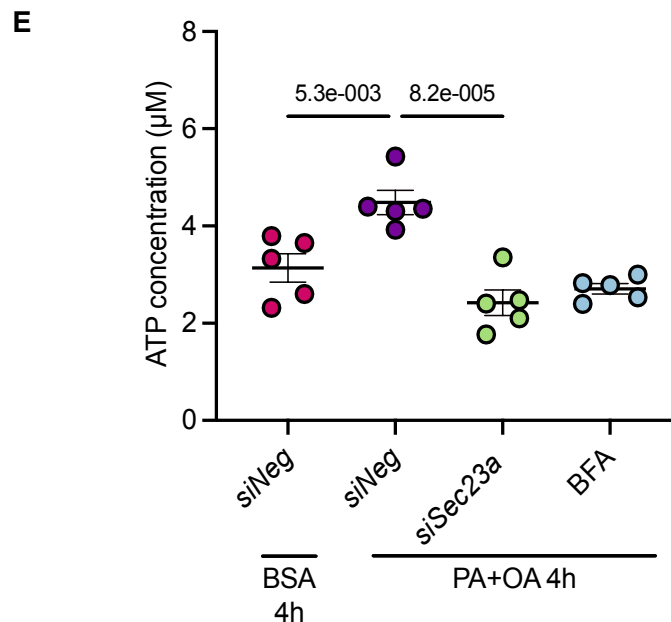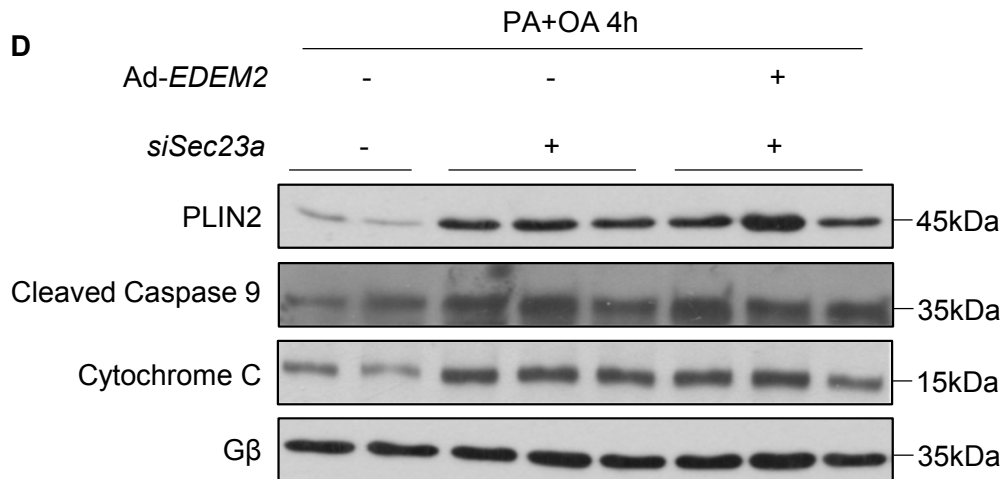
Supplemental Figure 18. SEC23A loss increases lipid droplets (LDs) in H9C2 cells

A, SEC23A knockdown in H9C2 by its *siRNA*. **B**, Levels of ATGL and PLIN2 on isolated LDs from 5×10^7 H9C2 cells upon stress of palmitic and oleic acid stress (PA and OA, 300µM) for 4 hours. **C**, Representative images of increased LD accumulation in SEC23A-knockdown H9C2 cells detected by BODIPY 493/503 (scalebar=20µm), DAPI (blue) stains nuclei. **D**, Immunoblots of proteins indicating LDs (PLIN2) and cell death in SEC23A-deficient neonatal rat cardiomyocytes (NRCMs). Gβ is the loading control. **E**, ATP amount in SEC23A-knockdown (*siSec23a*) cells (n=5 experiments). Data are presented as mean ± S.E.M. *p* values were calculated using a One-way ANOVA with post-hoc Tukey tests.
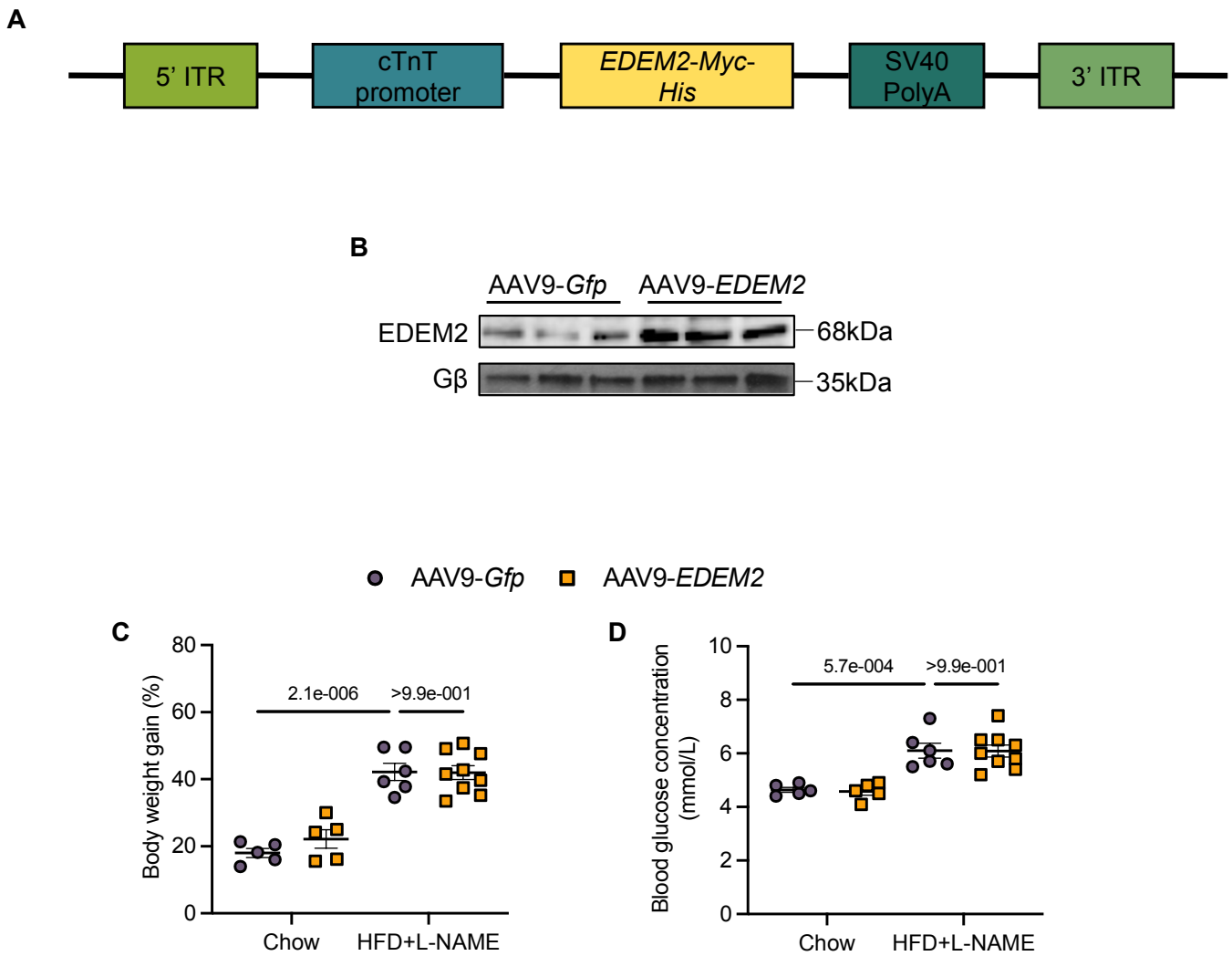
Supplemental Figure 19. Cardiac EDEM2 overexpression does not affect systemic metabolism following HFD+L-NAME stress for 8 weeks

A, Construct of viral vector AAV9-*EDEM2.* **B**, Immunoblots validating EDEM2 overexpression in the hearts from the mice injected with AAV9-*EDEM2*. Gβ is the loading control. **C**, Percentage body weight gain, and **D**, Fasting blood glucose levels 8 weeks post HFD+L-NAME (n=5-9 mice). Data are presented as mean ± SEM. *p* values were calculated using a Two-way ANOVA with Šidák post-hoc tests.
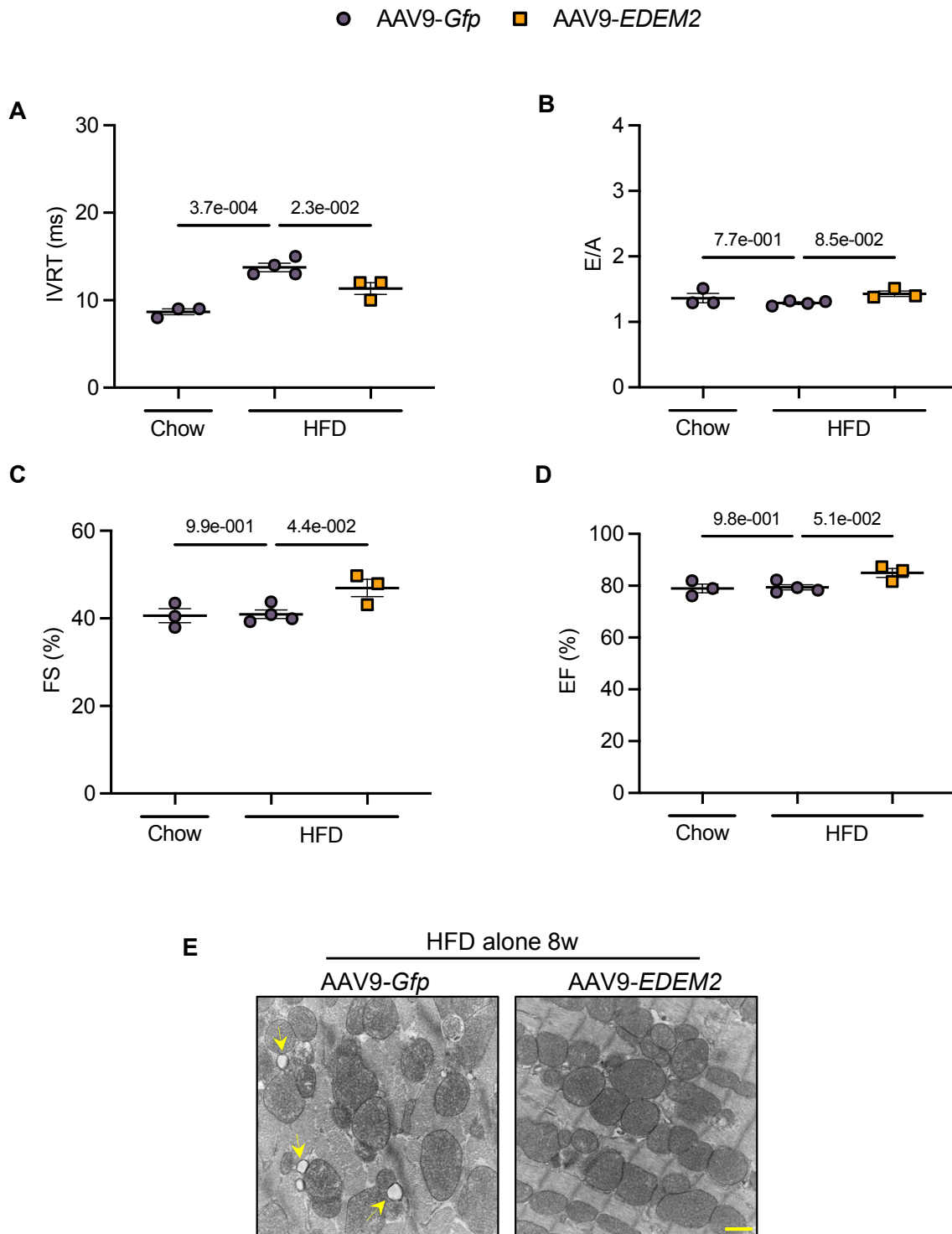
Supplemental Figure 20. EDEM2 overexpression preserves cardiac function under HFD alone for 8 weeks

C57BL/6 mice were injected with AAV9-*Gfp* or AAV9-*EDEM2* followed by receipt of either chow diet or HFD alone (60%) for 8 weeks. Echocardiographic analyses of **A**, Isovolumic relaxation time (IVRT), **B**, Ratio of peak velocity blood flow in early diastole to late diastole (E/A), **C**, fractional shortening (FS%), and **D**, ejection fraction (EF%). (n=3-4 mice). Data are presented as mean ± SEM. *p* values were calculated using a Kruskal-Wallis test with Dunn's post-hoc tests. **E**, Representative transmission electron microscopy (TEM) images (arrows indicating lipid droplets, scalebar=1µm).

A

B

C

D

E
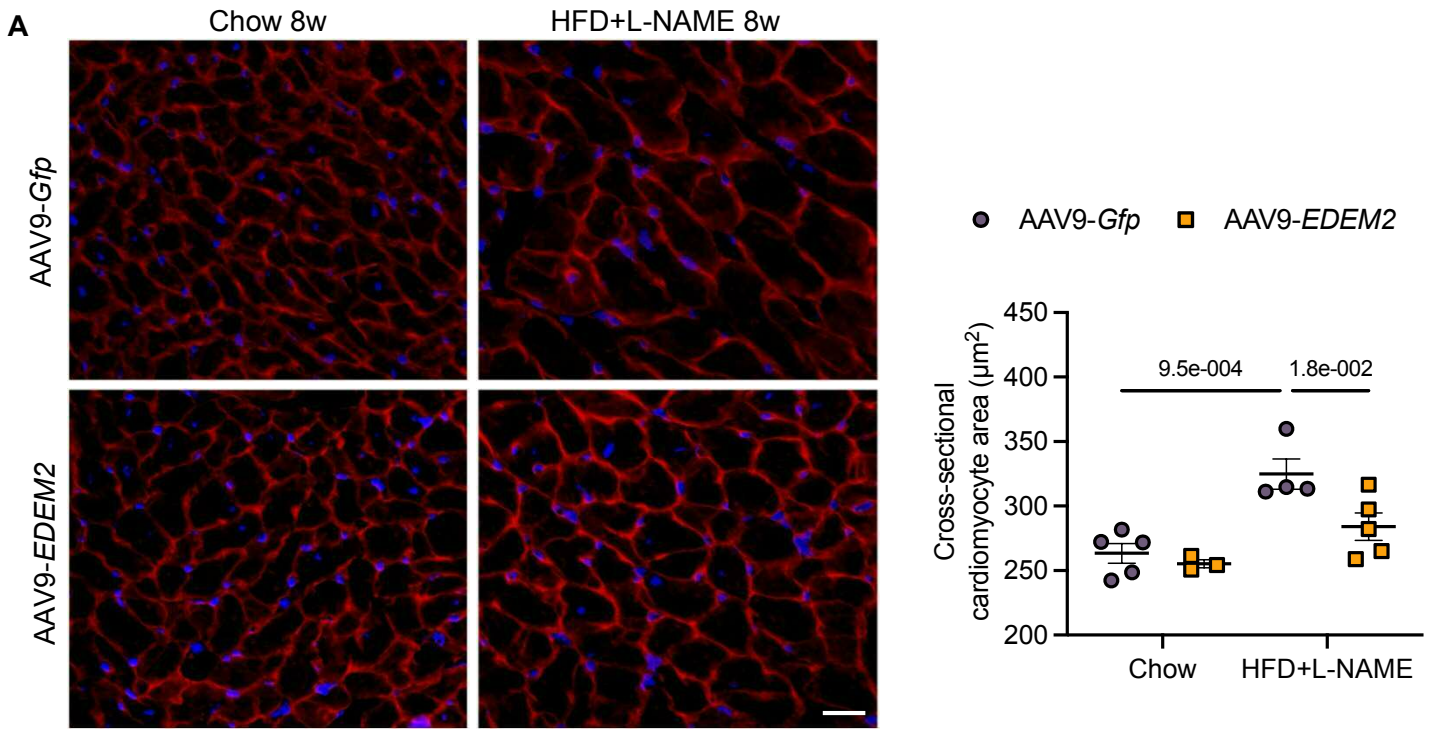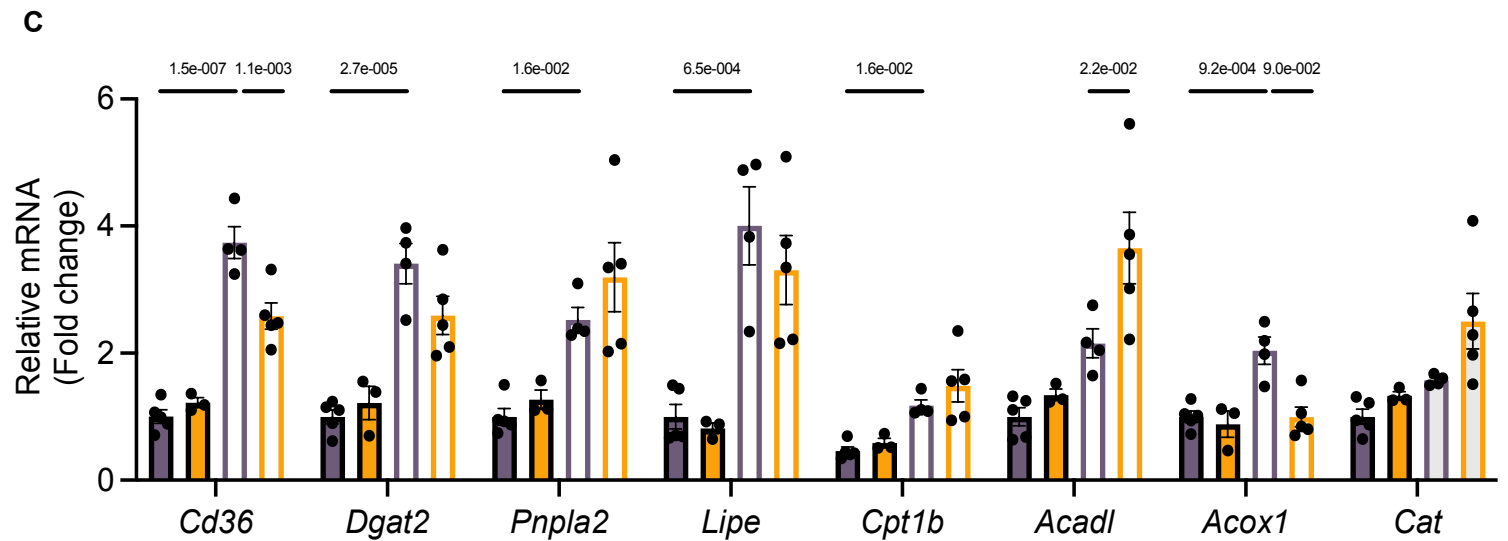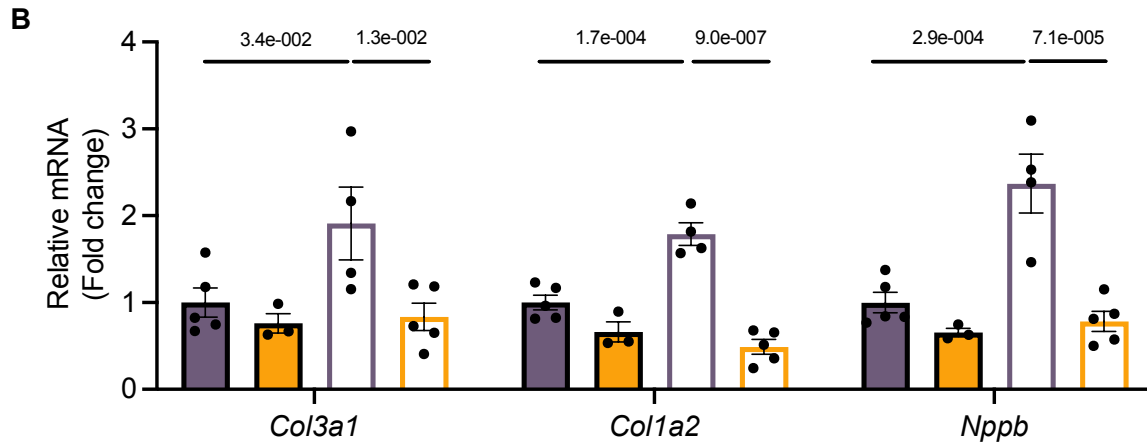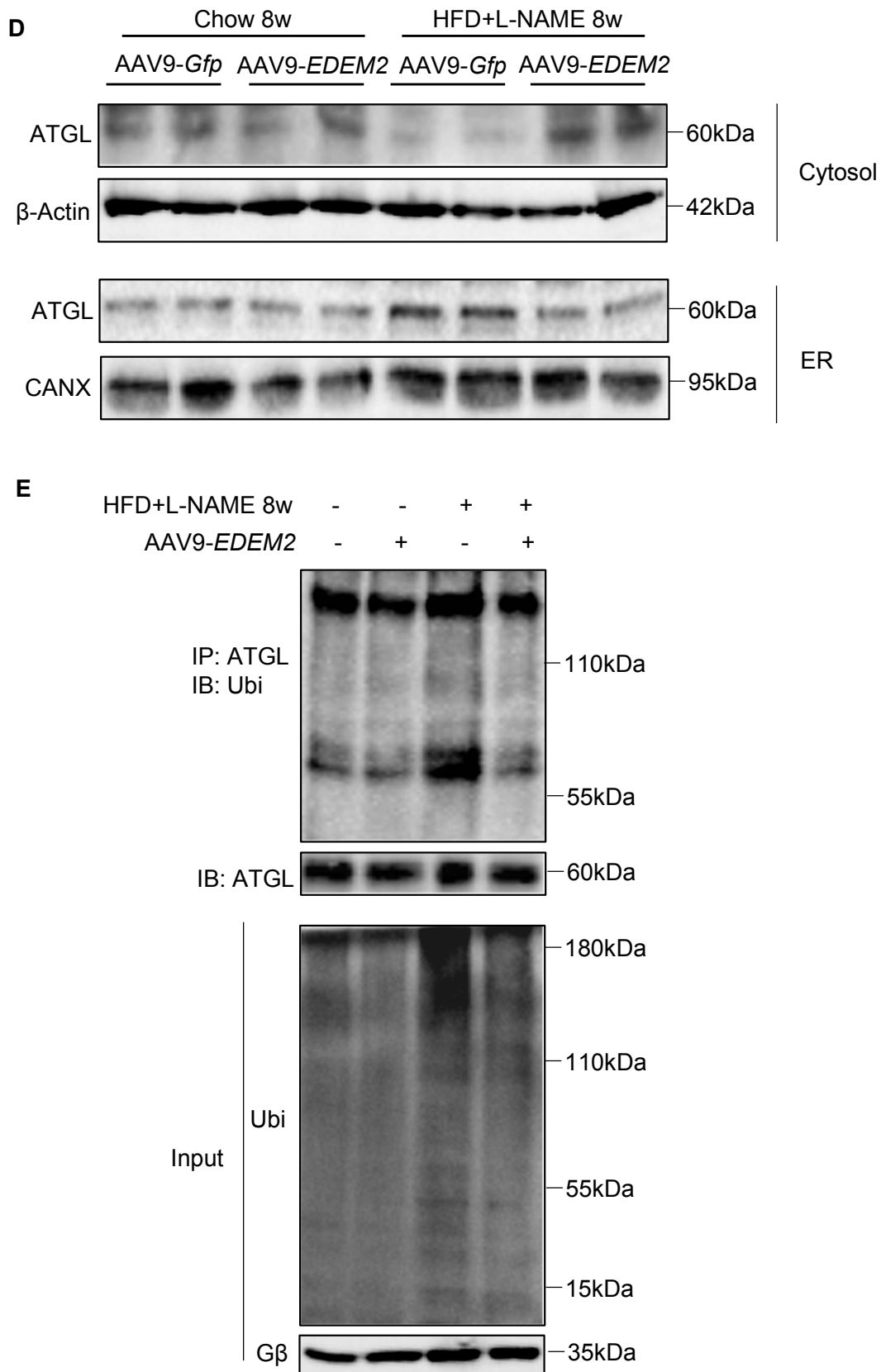
Supplemental Figure 21. Cardiac pathological remodeling is mitigated by EDEM2 overexpression following HFD+L-NAME stress for 8 weeks

A, Representative images and quantification of wheat germ agglutinin (WGA) staining for cross-sectional area (n=3-5 hearts, scalebar=20µm). **B**, Quantitative PCR determining *mRNA* levels of fibrotic and hypertrophic markers. **C**, Quantitative PCR determining transcripts of genes involved in lipid metabolism (n=3-5 hearts). **D**, Representative immunoblots of ATGL in ER fraction and soluble cytosol in the myocardium (each sample represents the pooled extracts from 3 hearts), with CANX and β-Actin as controls, respectively. **E**, Endogenous ubiquitinated-ATGL was less in EDEM2-overexpressing myocardium under HFD+L-NAME stress. Data are presented as mean ± SEM. *p* values were calculated using a Two-way ANOVA with Šidák post-hoc tests (**A**, **B**, and **C**).
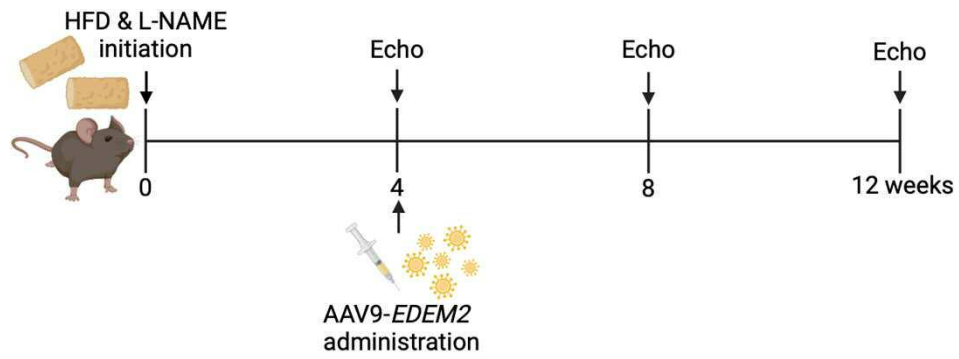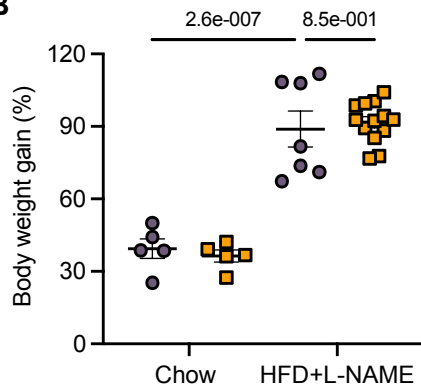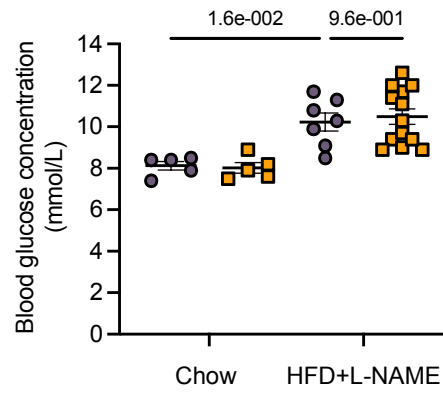
E

IVRT (ms) — Chow, HFD+L-NAME: 1.5e-008, 1.7e-006

E/A — Chow, HFD+L-NAME: 3.2e-004, 3.9e-005

F

FS (%) — Chow, HFD+L-NAME: 9.8e-001, 9.4e-001

EF (%) — Chow, HFD+L-NAME: 9.8e-001, 9.6e-001

AAV9-*Gfp*   AAV9-*EDEM2*

G

HFD+L-NAME 12w

AAV9-*Gfp*   AAV9-*EDEM2*

H

HFD+L-NAME 12w

AAV9-*Gfp*   AAV9-*EDEM2*

I

J

HFD+L-NAME 12w

AAV9-*Gfp*   AAV9-*EDEM2*

AAV9-*Gfp*   AAV9-*EDEM2*

1.8e-002

K

Chow 12w   HFD+L-NAME 12w

AAV9-*Gfp*

AAV9-*EDEM2*

1.7e-004   5.2e-005
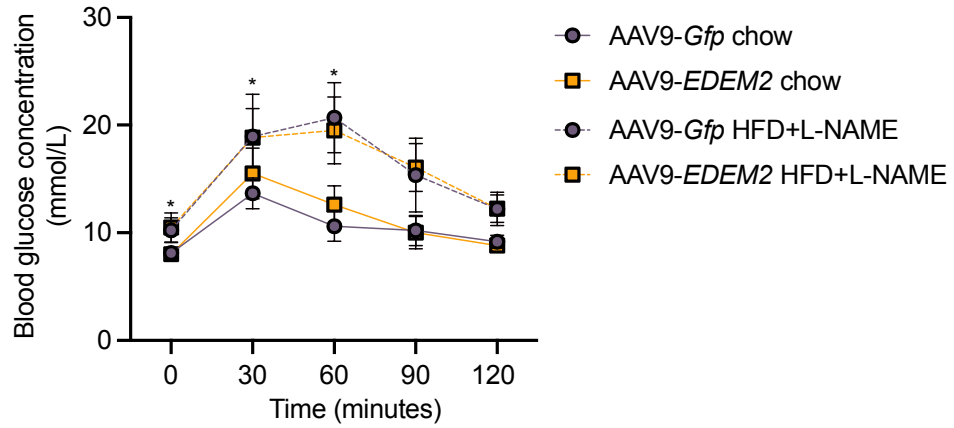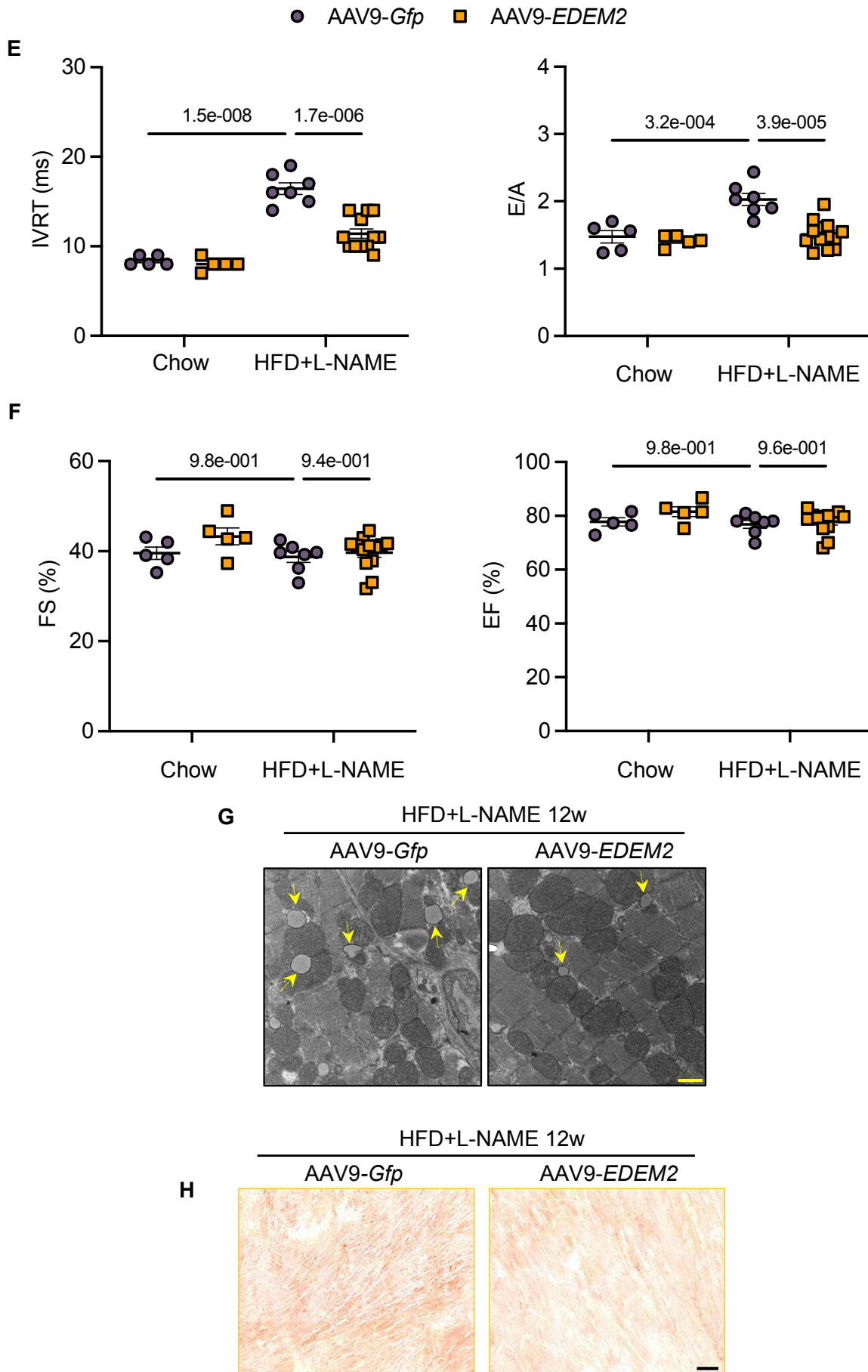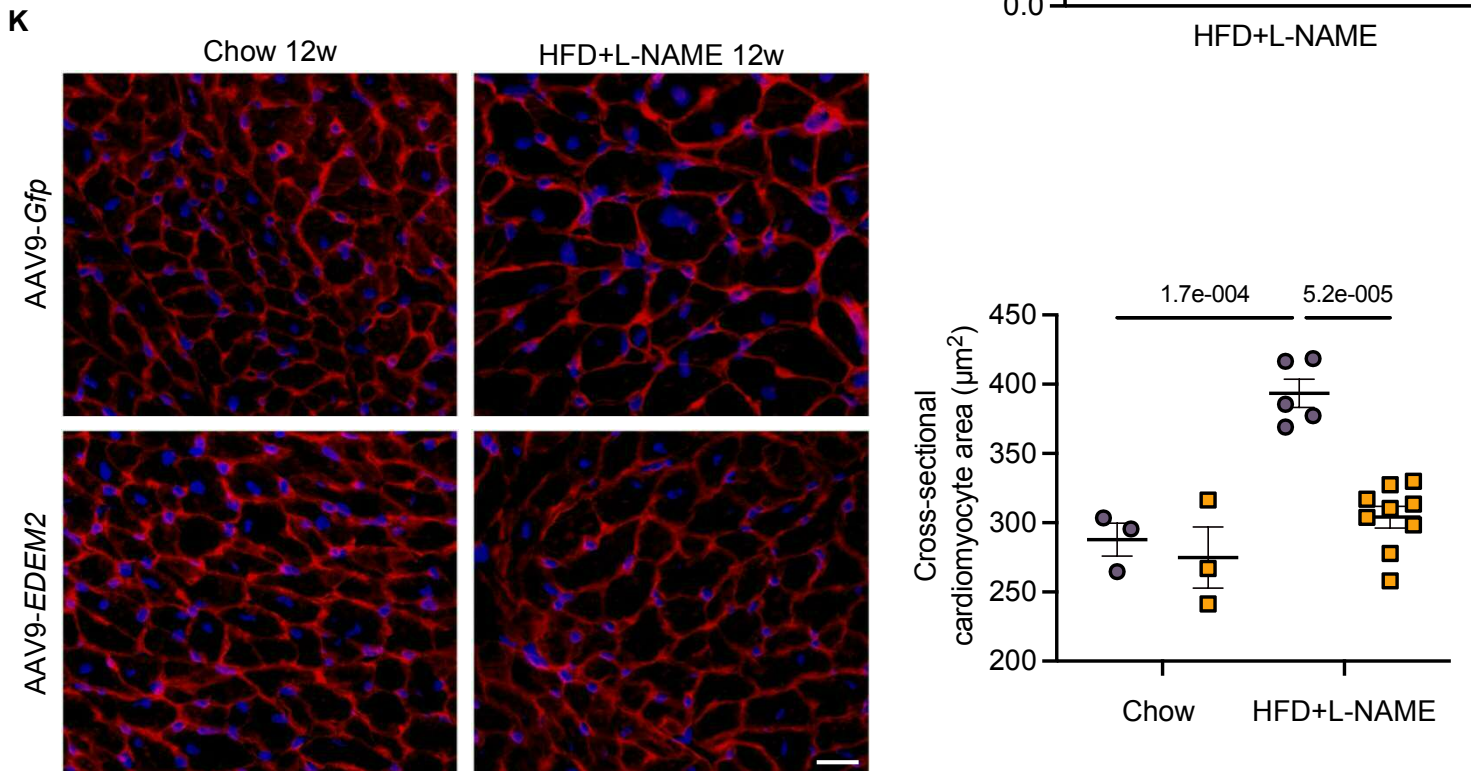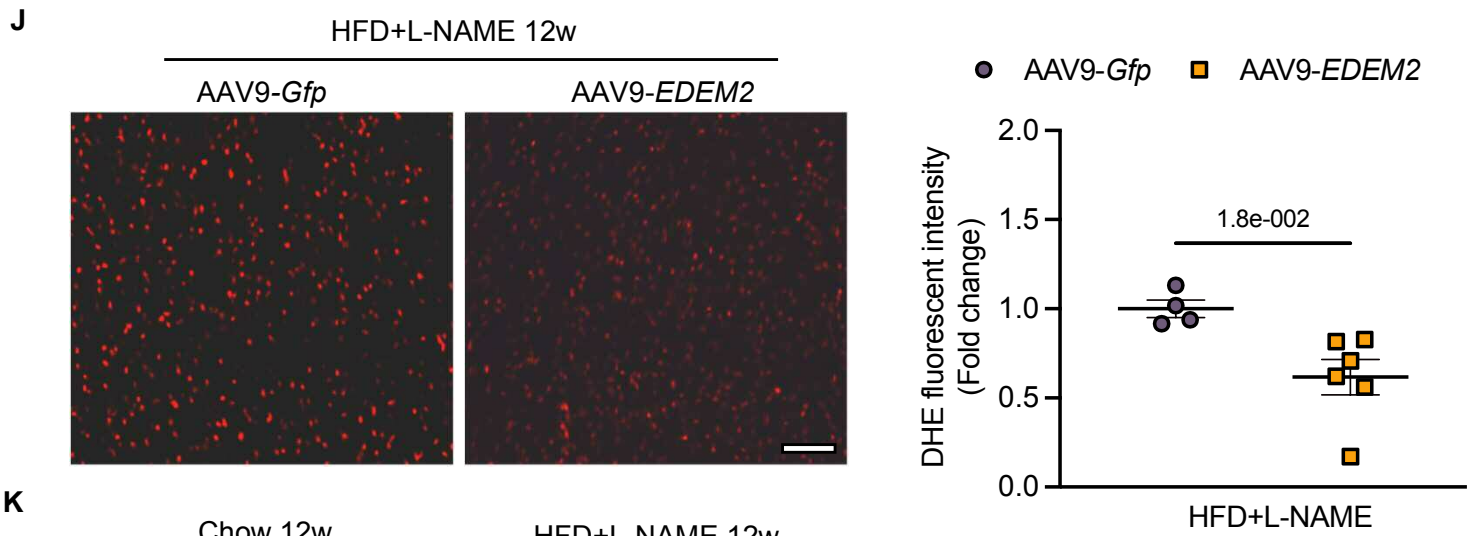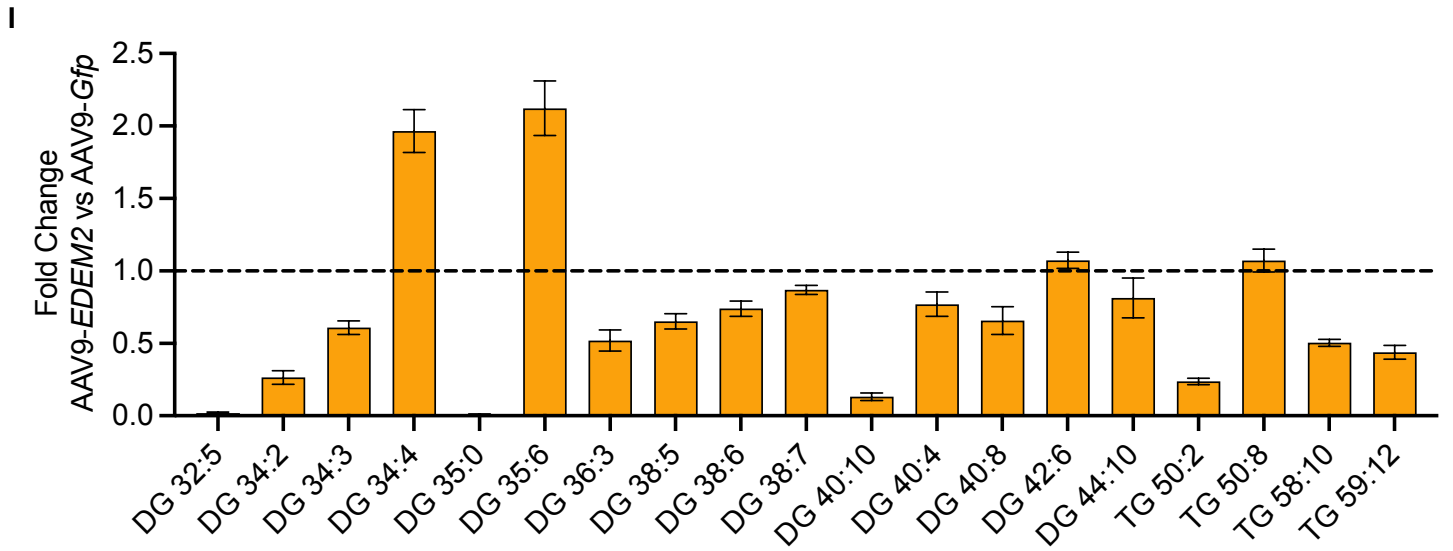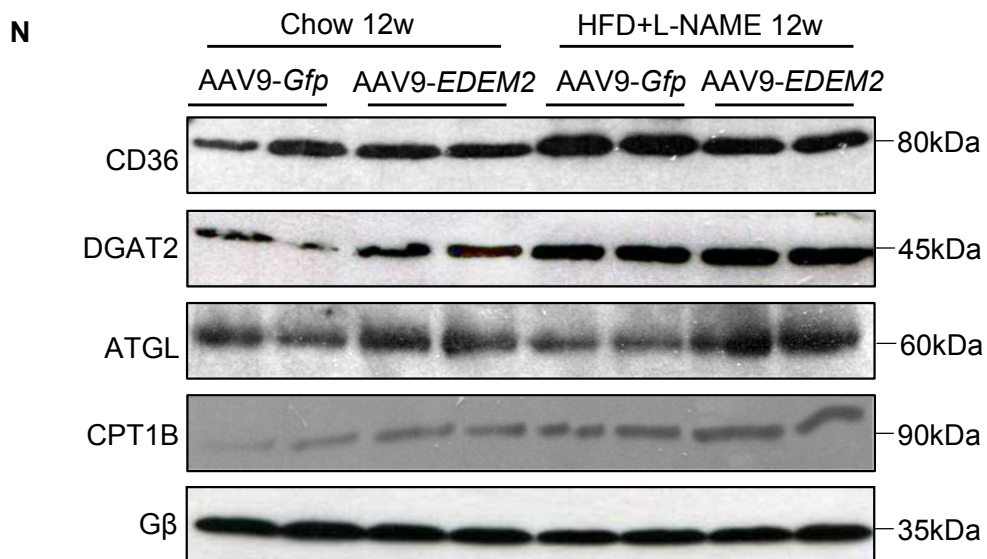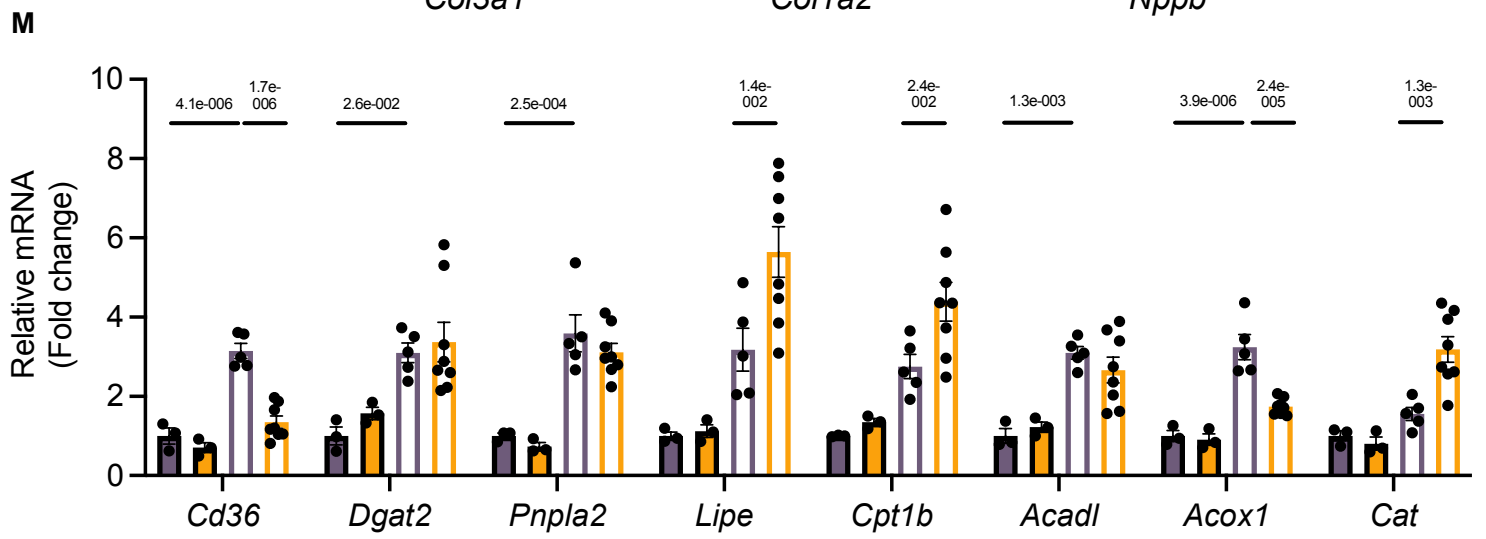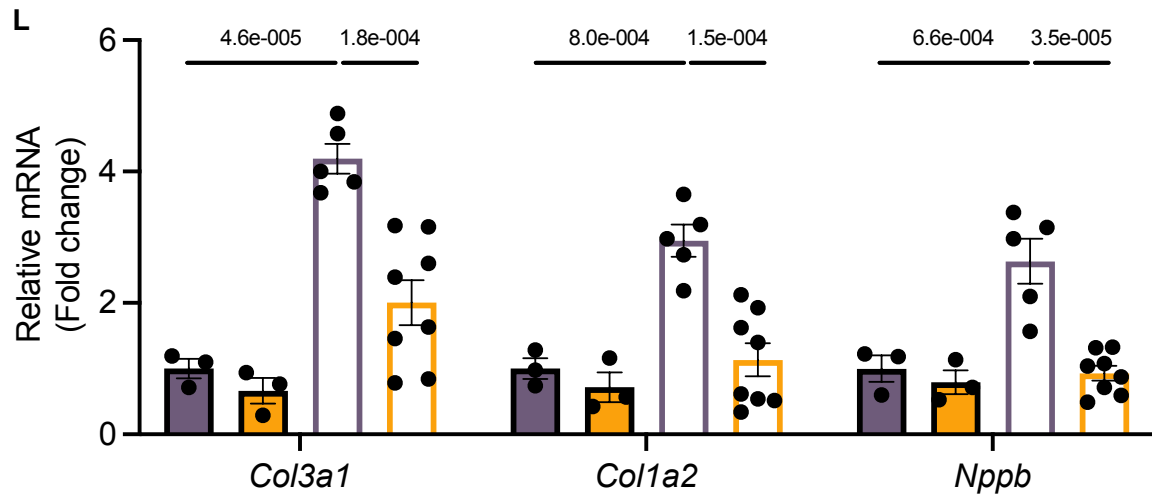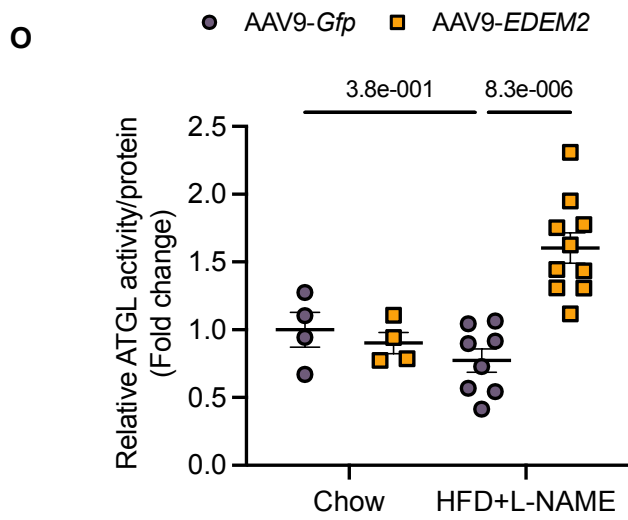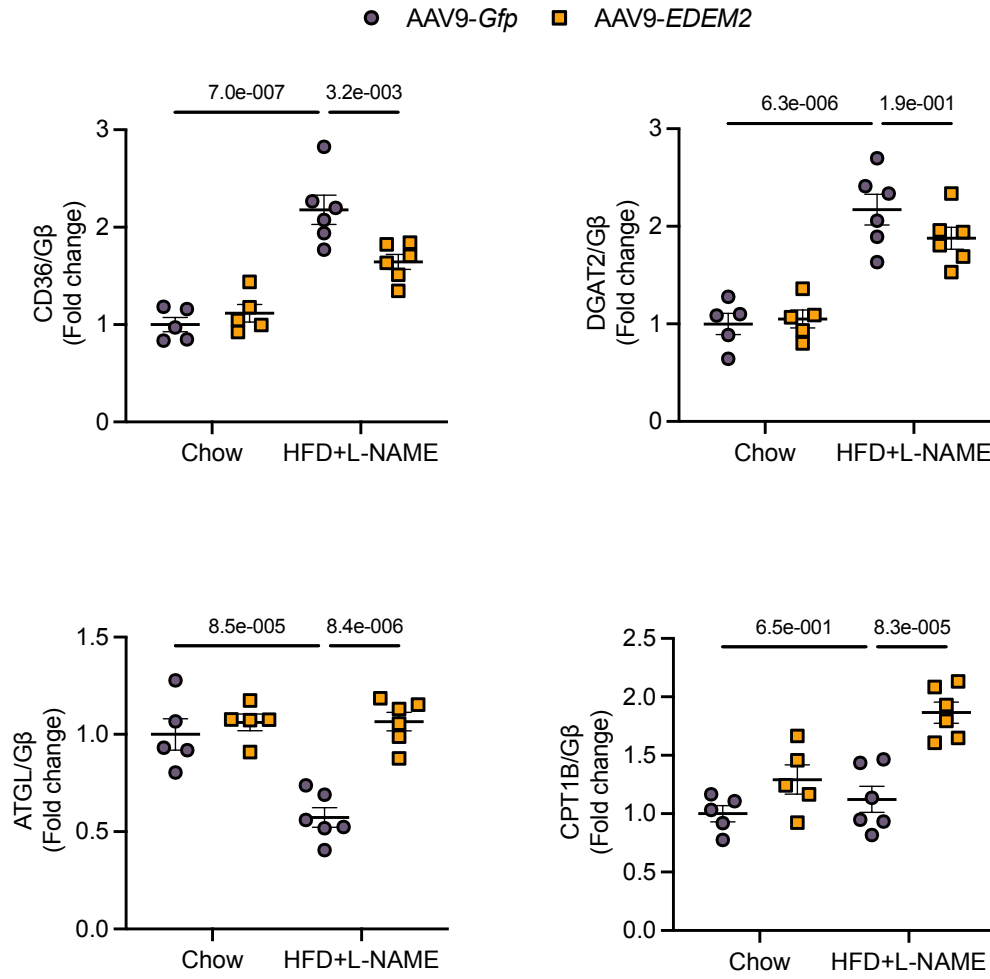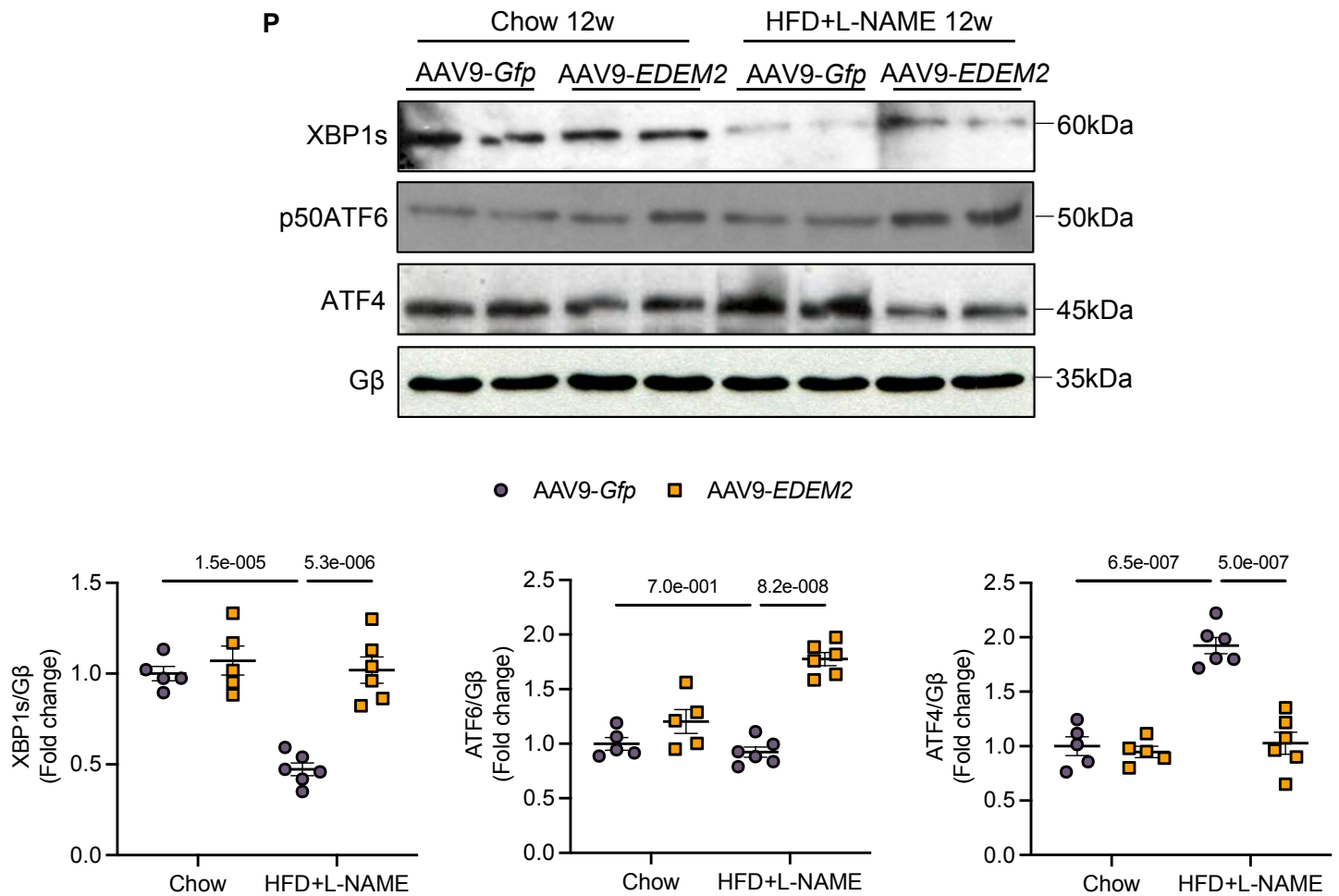
Supplemental Figure 22. EDEM2 restoration prevents cardiac lipotoxicity and HFpEF upon longer-term HFD+L-NAME stress

A, Schematic of the experimental design. **B**, Percentage body weight gain, **C**, Fasting blood glucose concentration, and **D**, Glucose tolerance tests after HFD+L-NAME for 12 weeks (n=5-13 mice). **E**, Pulsed-wave Doppler tracing, determining isovolumic relaxation time (IVRT) and Ratio of peak velocity blood flow in early diastole to late diastole (E/A). **F**, Left ventricular M-mode echocardiography assessing percentage of fractional shortening (FS%) and ejection fraction (EF%) (n=5-13 mice). **G**, Representative transmission electron microscopy (TEM) images (arrows indicating lipid droplets, scalebar=1µm). **H**, Oil Red O staining (scalebar=20µm). **I**, Lipidomic analysis of mice hearts exposed to metabolic stress for 12 weeks, showing significantly altered diglycerides (DGs) and triglycerides (TGs) (n=7-13 hearts, $p<0.05$). **J**, Representative images and quantification of DHE staining (scalebar=50µm, n=5-6 hearts). **K**, Representative images and quantification of wheat germ agglutinin (WGA) staining for cross-sectional area (n=3-9 hearts, scalebar=20µm). **L**, Quantitative PCR determining *mRNA* expression of fibrotic and hypertrophic markers (n=3-8 hearts). **M**, Quantitative PCR determining transcripts of genes involved in lipid metabolism (n=3-8 hearts). **N**, Representative immunoblots and quantification of lipid associated proteins in the myocardium with EDEM2 overexpression following prolonged HFD+L-NAME stress (n=4-7 hearts). Gβ is the loading control. **O**, ATGL lipase activity assay was conducted using the whole extracts of the myocardium (n=4-10 hearts). **P**, Representative immunoblots and quantification of key ER factors in the myocardium following prolonged HFD+L-NAME stress (n=5-6 hearts). Data are presented as mean ± S.E.M. *p* values were calculated using a Two-way ANOVA with Šidák post-hoc tests (**B**, **C**, **L** to **P**) or Tukey post-hoc tests (**D** to **F**, **K**), or an unpaired Student's *t* test (**I**, **J**). Significant difference between chow and HFD+L-NAME at respective timepoints is indicated by * in (**D**).
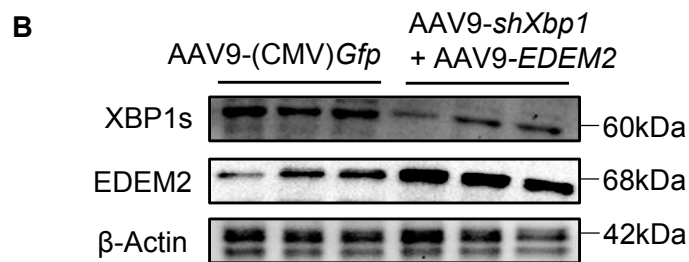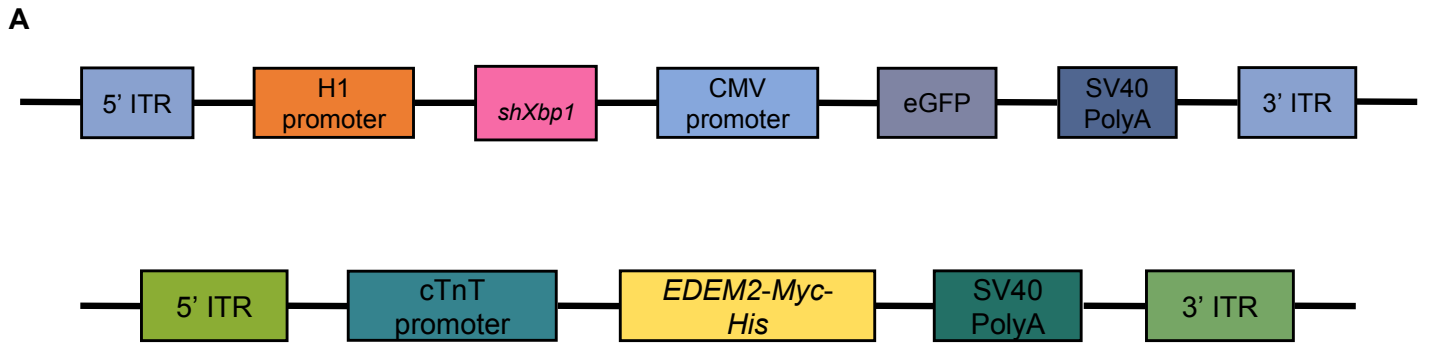
A

**B**

C

D

E
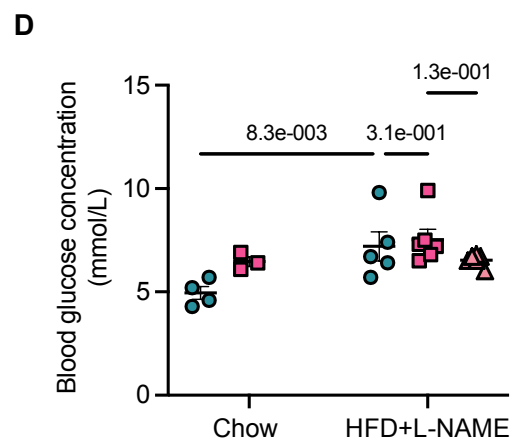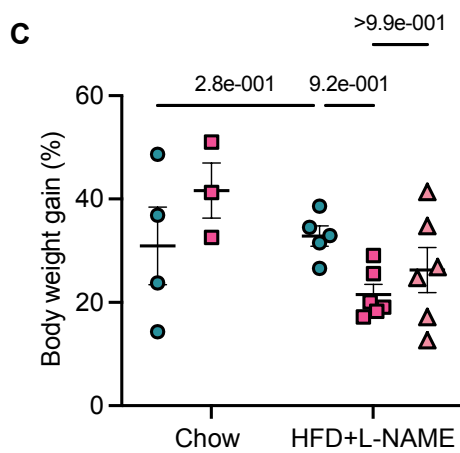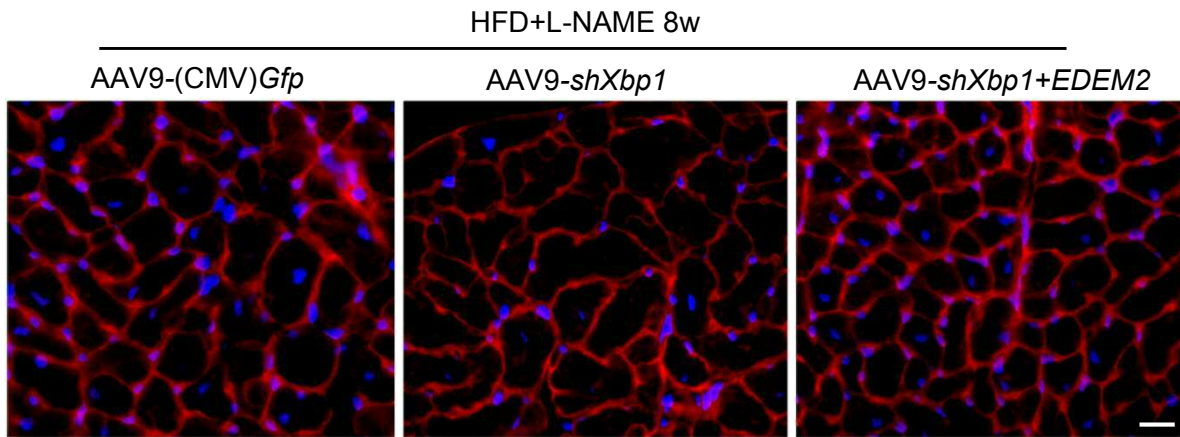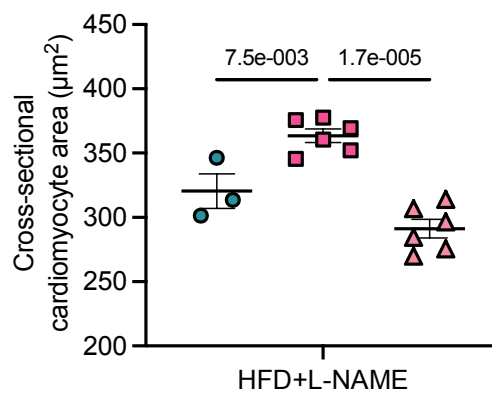
Supplemental Figure 23. XBP1s deficiency-induced cardiac hypertrophy is prohibited by EDEM2 overexpression under metabolic stress

A, AAV9 viral vector construct (AAV9-*shXbp1*). **B**, Validation immunoblots showing XBP1s reduction and EDEM2 overexpression in the heart. β-Actin is the loading control. **C**, Percentage body weight gain, and **D**, Fasting blood glucose levels after 8 weeks of HFD+L-NAME stress (n=4-6 mice). **E**, Representative images and quantification of wheat germ agglutinin (WGA) staining for cross-sectional area (n=4-6 hearts, scalebar=20μm). Data are presented as mean ± SEM. *p* values were calculated using a Two-way ANOVA with Šidák post-hoc tests (**C**, **D**) or a Kruskal-Wallis test with Dunn's post-hoc tests (**E**).
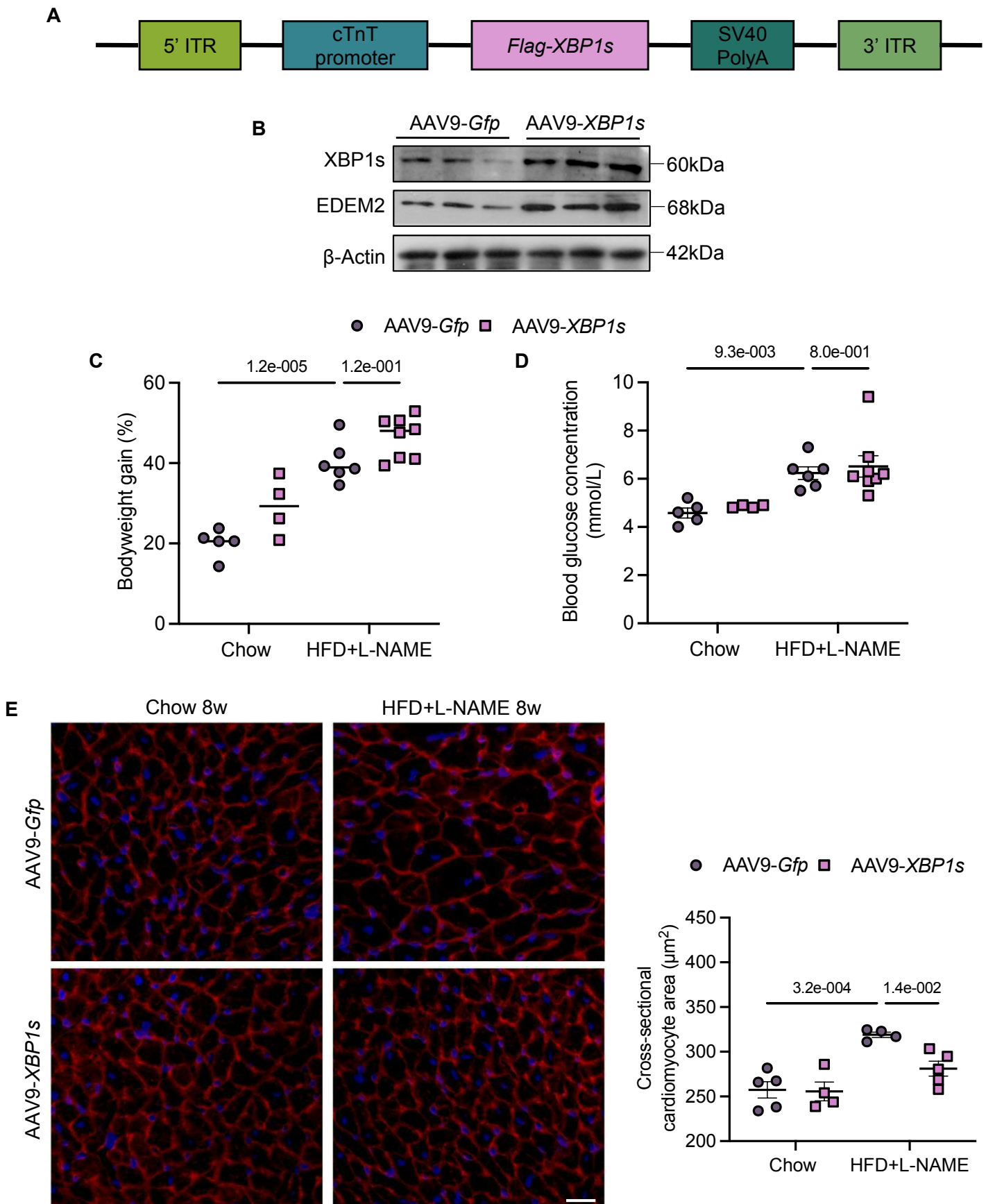
Supplemental Figure 24. XBP1s overexpression prevents cardiac hypertrophy upon metabolic stress

A, AAV9 viral vector construct (AAV9-*XBP1s*). **B**, Validation immunoblots showing XBP1s overexpression and increased EDEM2 levels in the heart. B-Actin is the loading control. **C**, Percentage body weight gain, and **D**, Fasting blood glucose concentration after 8 weeks of HFD+L-NAME (n=4-8 mice). **E**, Representative images and quantification of wheat germ agglutinin (WGA) staining for cardiomyocyte cross-sectional area (n=4-8 hearts, scalebar=20μm). Data are presented as mean ± SEM. *p* values were calculated using a Two-way ANOVA with Šidák post-hoc tests (**C** to **E**).